

RESIDUAL BREAST CANCER METABOLIC PHENOTYPE AFTER DOCETAXEL TREATMENT

by

TATIANA VOLPARI

A thesis submitted to the University of Birmingham for the degree of
DOCTOR OF PHILOSOPHY



**UNIVERSITY OF
BIRMINGHAM**

The Institute of Cancer and Genomic Sciences
College of Medical and Dental Sciences
University of Birmingham
November 2015

UNIVERSITY OF
BIRMINGHAM

University of Birmingham Research Archive

e-theses repository

This unpublished thesis/dissertation is copyright of the author and/or third parties. The intellectual property rights of the author or third parties in respect of this work are as defined by The Copyright Designs and Patents Act 1988 or as modified by any successor legislation.

Any use made of information contained in this thesis/dissertation must be in accordance with that legislation and must be properly acknowledged. Further distribution or reproduction in any format is prohibited without the permission of the copyright holder.

ABSTRACT

Despite improvements in early diagnosis and prevention, late stage breast cancer is often incurable due to metastasis, tumour relapse, resistance and incomplete response to treatments. Metabolic reprogramming has been recognised as a critical element for cancer cells to grow under hostile conditions and this is likely to contribute towards resistance against chemotherapeutics. This thesis therefore aimed at deciphering the metabolic phenotype of residual breast cancer which survived docetaxel treatment, *in vitro* and *in vivo*, quantifying polar metabolite levels and conducting pathway tracing and metabolic flux analysis using stable isotope (^{13}C) labelled tracers.

In vitro residual cells presented a hypermetabolic phenotype characterised by significant accumulation of essential and non-essential amino acids, together with an elicited Warburg effect and an increased antioxidant response based on glutathione production, while in growth arrest. A method to carry out *in vivo* tracer-based metabolic studies was successfully developed using a breast cancer mouse model. Although the metabolite accumulation outlined *in vitro* was not observed *in vivo*, a protective phenotype against oxidative stress was supported by increased flux through the oxidative branch of the pentose phosphate pathway.

In conclusion, this thesis demonstrated that metabolic phenotyping is a valid approach to uncover key metabolic alterations in residual tumours both *in vitro* and *in vivo*, and could be further exploited to design personalised treatments aimed at restoring sensitivity to therapies.

ACKNOWLEDGMENTS

I would firstly like to thank Professor Ulrich Günther and Doctor Daniel Tennant for their continued mentorship during the PhD. Thank you for the encouragement, and the opportunity to work in a vibrant and exciting research environment, as part of the Marie Curie ITN METAFLUX project. I would also like to thank two members of the METAFLUX network, Professor Marta Cascante and Anibal Miranda, for use of their GC-MS facility at The University of Barcelona.

A special thank you to a great scientist, Doctor Christian Ludwig, for the enormous patience demonstrated whilst teaching me theoretical and practical basics of NMR spectroscopy. Additional thanks to Chris for use of his multiplet analysis program during the *in vivo* data analysis.

I would like to show my gratitude to the staff of the School of Cancer Sciences, the Animal facility and the HWB-NMR, with a special reference to Sara, Sue and Karen, for making this work possible.

It has been a real pleasure working with my excellent colleagues in the Tennant lab. Debbie, you have been my English Mum, always there for me during up-and-down moments of the PhD experience. Thank you for this and for taking care of all the lab duties. Kate, I am deeply grateful for all your help and support in the lab and in private life, I am sure our friendship will go beyond this experience. You made my life in UK so much better. It was great to hang out, improve English from you, and sharing our different cultures. Giulio, it was great to have another Italian in the lab! You are a great scientist and should never give up. Des, I am so happy I met you! You have been fresh air in and outside the lab. Thank you for hosting me so many times, for our serious chats and being the party boy.

For my colleagues in the NMR facility, Mei, Sotiris and Kasia, a huge thank you for sharing such a strong and valuable experience in the METAFLUX project. Mei, your support with the NMR technology has been indispensable, thank you for sharing your knowledge, and collaborating on the mouse work. Also, thank you for introducing spicy Asian food to me! I will not forget that! Sot, thank you so so much for being a real friend more than anything. Your calm attitude is so reassuring even during difficult and

stressful times. I do not know how you do it, but I know I can count on you anytime I panic.

I cannot and will not forget to thank Doctor Gabriele Bertoni, without whom I probably would have never started this experience. Thank you for believing in me, supporting me and helping my decision to undertake this PhD.

I am deeply grateful to Andrea. Thank you for understanding and supporting my decision to undertake this important step of my career. Thank you for all your love and strength through good times and bad, and for boosting my motivation during those challenging days. Thank you for patiently staying by my side.

I cannot express the right words to thank my best friend Silvia. Without your lovely support, sweetness and belief in me, I would not have been able to continue through the challenging PhD experience. Thank you for sharing the pain and glory from afar. We both should not forget that:

“Once the storm is over you won’t remember how you made it through, how you managed to survive. [...] But one thing is certain. When you come out of the storm, you won’t be the same person who walked in.” (from Haruki Murakami, *Kafka on the Shore*).

Finally, I would like to thank my whole family, who always believed in me. Thank you to my Mum and Dad for their endless support and love, for being proud of me and backing my decisions, even though I was far from home.

DECLARATION

I confirm that this thesis is my own work, in which I have been involved in the experimental design, sample analysis, data analysis and preparing the manuscript.

Development of the *in vivo* [1,2-¹³C]glucose injection protocol (Chapter 4) has been carried out in collaboration with Doctor Geokmei Chong.

TABLE OF CONTENTS

CHAPTER 1 – GENERAL INTRODUCTION

1.1 CANCER AND METABOLISM	2
1.1.1 Hallmarks of tumours	2
1.1.2 Metabolic alterations in cancer	5
1.1.2.1 Tumour microenvironment and metabolic adaptations	14
1.2 BREAST CANCER	17
1.2.1 Epidemiology and subtypes	17
1.2.2 Breast cancer treatment	23
1.2.2.1 Docetaxel	29
1.2.3 Breast cancer resistance to treatments	30
1.2.3.1 Resistance to docetaxel and residual tumours	31
1.2.4 Breast cancer metabolism	32
1.2.5 Models of breast cancer	34
1.2.5.1 <i>In vitro</i> : MCF-7 breast cancer cell line	35
1.2.5.2 <i>In vivo</i> : MMTV-PyMT mouse model of breast cancer	35
1.3 APPROACHES TO DECIPHER CANCER METABOLISM	38
1.3.1 Tools for metabolic analyses	38
1.3.1.1 NMR spectroscopy	39
1.3.1.2 Mass spectrometry	40
1.3.2 Tools for metabolic flux analysis	40
1.3.2.1 ¹³ C-MFA in cancer cells	48
1.3.2.2 <i>In vivo</i> ¹³ C-MFA	48
1.4 AIM OF THE THESIS	51
2.1 BREAST CANCER CELL LINE MODEL	53

CHAPTER 2 – MATERIALS AND METHODS

2.2 <i>IN VITRO</i> DOCETAXEL TREATMENT OF MCF-7 BREAST CANCER CELLS ..	53
2.2.1 Determining the optimal concentration of docetaxel	53
2.2.2 Time-course of docetaxel effect on MCF-7 cell growth	54

2.2.3	Glutathione synthesis inhibition during docetaxel treatment	54
2.2.4	Sulforhodamine B colorimetric assay	55
2.3	RESIDUAL MCF-7 CELL CHARACTERISATION POST-DOCETAXEL TREATMENT	56
2.3.1	Metabolic analysis	56
2.3.2	Metabolic flux analysis	57
2.3.3	Establishment of residual clones	57
2.3.4	Growth curves	57
2.3.5	Western blotting	58
2.3.5.1	Sample preparation	58
2.3.5.2	Protein separation and transfer	59
2.3.5.3	Protein detection	59
2.4	MMTV-PYMT: TRANSGENIC MOUSE MODEL OF BREAST CANCER	60
2.4.1	Genotyping	61
2.4.1.1	DNA extraction	61
2.4.1.2	Amplification of the middle T antigen by PCR	62
2.4.1.3	Detection of the PCR product by agarose gel	63
2.5	<i>IN VIVO</i> DOCETAXEL TREATMENT OF MOUSE MAMMARY TUMOUR	63
2.5.1	Gene expression analysis	64
2.5.1.1	Extraction of total RNA	64
2.5.1.2	RNA sequencing	65
2.5.2	<i>In vivo</i> metabolic analysis	65
2.5.3	<i>In vivo</i> [1,2- ¹³ C]glucose flux	66
2.5.4	GC-MS analysis	67
2.6	NMR EXPERIMENTS	68
2.6.1	Sample preparation	68
2.6.2	NMR experiments	68
2.6.3	NMR data analysis	69
2.7	STATISTICAL ANALYSIS	72

CHAPTER 3 – *IN VITRO* CHARACTERISATION OF RESIDUAL BREAST CANCER CELLS AFTER DOCETAXEL TREATMENT

3.1 INTRODUCTION.....	75
3.2 MCF-7 RESPONSE TO DOCETAXEL TREATMENT	77
3.2.1 Determining the optimal concentration of docetaxel.....	77
3.2.2 Docetaxel time-course	78
3.3 RESIDUAL BREAST CANCER CELLS METABOLIC PHENOTYPE	80
3.3.1 Residual cells morphology	80
3.3.2 Residual cells metabolic analysis.....	82
3.3.3 Residual cell media metabolic analysis.....	85
3.3.4 Residual cell ¹³ C-MFA.....	87
3.3.5 Residual cell media ¹³ C-MFA	93
3.3.6 Glutathione role in residual cell survival	96
3.3.7 Residual cell regrowth.....	98
3.3.8 Clone 1 and 2 metabolic analysis.....	100
3.3.9 mTOR activity in MCF-7, residual cells and regrowth clones	103
3.3.10 Clone 2 ¹³ C-MFA.....	104
3.4 DISCUSSION	106

CHAPTER 4 - *IN VIVO* ¹³C-MFA: METHOD DEVELOPMENT

4.1 INTRODUCTION.....	119
4.2 INJECTION METHOD	121
4.3 LABELLING TIME POINT	123
4.4 DISCUSSION	125

CHAPTER 5 - RESIDUAL MAMMARY TUMOUR METABOLIC PHENOTYPE AFTER DOCETAXEL TREATMENT *IN VIVO*

5.1 INTRODUCTION.....	130
5.2 TUMOUR VOLUMES	132
5.3 GENE EXPRESSION ANALYSIS	133

5.4 RESIDUAL TUMOUR METABOLIC ANALYSIS.....	136
5.5 RESIDUAL TUMOUR ¹³ C-MFA BY NMR.....	138
5.5.1 Determining labelling time point	138
5.5.2 Comparing ¹³ C-MFA between residual and control tumours	139
5.6 MIDA by GC-MS.....	143
5.7 DISCUSSION	145

CHAPTER 6 - GENERAL DISCUSSION

6.1 DISCUSSION	156
6.2 CONCLUSIONS AND FUTURE WORKS.....	163
REFERENCES.....	165

LIST OF FIGURES

Figure 1.1. Glycolytic pathway in tumours.....	13
Figure 1.2. Mammary tumour development in the MMTV-PyMT mouse model of breast cancer.....	37
Figure 1.3. Multiplet patterns derived from adjacent ¹³ C atoms.....	45
Figure 1.4. ¹³ C isotopomer patterns following [1,2- ¹³ C]glucose catabolism.....	47
Figure 3.1. 10 nM is the Tax concentration able to kill 50% of the MCF-7 breast cancer cells in culture	78
Figure 3.2. Tax inhibits MCF-7 cells proliferation for several days.....	79
Figure 3.3. Tax induces changes in MCF-7 cells morphology.....	81
Figure 3.4. Metabolites more abundant in residual cells.....	84
Figure 3.5. Metabolites uptaken and secreted in the media.....	86
Figure 3.6. Relative ¹³ C isotope enrichment into glucose-derived metabolites.....	91
Figure 3.7. [2,3- ¹³ C]aspartate production via pyruvate carboxylase activity.....	92
Figure 3.8. Relative ¹³ C isotope enrichment into media-derived metabolites.....	95
Figure 3.9. Glutathione-synthesis inhibition.....	97
Figure 3.10. Additive effect of BSO and Tax on MCF-7 cells survival.....	97
Figure 3.11. Residual cell regrowth time-course.....	99
Figure 3.12. Residual cell regrowth staining.....	99
Figure 3.13. Growth curves.....	101
Figure 3.14. Clone 1 and clone 2 metabolic analysis.....	102
Figure 3.15. mTOR activity.....	103
Figure 3.16. Clone 2 ¹³ C-MFA.....	105

Figure 3.17. <i>In vitro</i> metabolic phenotype of residual breast cancer cells.....	116
Figure 4.1. Comparison of injection sites.....	122
Figure 4.2. ¹³ C-glucose time-course in the mouse mammary tumour.....	124
Figure 5.1. Tumour shrinkage after docetaxel treatment.....	132
Figure 5.2. Residual mammary tumour differential gene expression.....	135
Figure 5.3. Mammary tumour-derived metabolite quantification.....	137
Figure 5.4. [1,2- ¹³ C]glucose enrichment in the mouse mammary tumour.....	139
Figure 5.5. Isotopomers derived from [1,2- ¹³ C]glucose metabolism by the mouse mammary tumour.....	142
Figure 5.6. MIDA of [1,2- ¹³ C]glucose-derived mammary tumour metabolites.....	144
Figure 5.7. <i>In vivo</i> metabolic phenotype of residual mammary tumours.....	153

LIST OF TABLES

Table 2.1. List of primary antibodies used in this thesis.....	60
Table 3.1. Metabolites more abundant in residual cells.....	83
Table 4.1. Metabolite concentration variability across replicates.....	122
Table 5.1. Residual tumour gene expression analysis.....	134

ABBREVIATIONS

1D	One-dimensional
2D	Two-dimensional
2-HG	2-hydroxyglutarate
3D	Three-dimensional
3-PG	3-phosphoglycerate
6PGDH	6-phosphogluconate dehydrogenase
α -KG	α -ketoglutarate
AAT	Alanine aminotransferase
ACL	ATP citrate lyase
AML	Acute myeloid leukaemia
AMPK	AMP-activated protein kinase
Arg	Arginine
Asp	Aspartate
AST	Aspartate transaminase
ATP	Adenosine triphosphate
BCA	Bicinchoninic acid
BCS	Breast conserving surgery
BRCA	Breast Cancer, early onset
BSA	Bovine Serum Albumine
BSO	L-Buthionine-sulfoximine
CAFs	Cancer associated fibroblasts
CDKs	Cyclin D kinases
CE	Capillary electrophoresis

Cf	Final number of cells
Ci	Initial number of cells
CNAs	Copy number aberrations
CTRL	control
D ₂ O	Deuterium oxide
DARP	Diabetes-related ankyrin repeat protein
DCIS	Ductal carcinoma <i>in situ</i>
DHAP	Dihydroxyacetone phosphate
DMEM	Dulbecco's Modified Eagle Medium
DMSO	Dimethyl sulphoxide
Dt	Doubling time
EGFR	Epithelial Growth Factor Receptor
EI	Electron Impact
EIPA	5-(N-ethyl-Nisopropyl) amiloride
EMT	Epithelial-to-mesenchymal transition
EMU	Elementary metabolite units
ER	Oestrogen Receptor
F1,6BP	Fructose-1,6-bisphosphate
F6P	Fructose-6-phosphate
FBC	Familial breast cancers
FBP	Fructose-1,6-bisphosphate
FDG-PET	¹⁸ F-deoxyglucose positron emission tomography
FGF	Fibroblast growth factor
FH	Fumarate hydratase

FID	Free induction decay
G1P	Glucose-1-phosphate
G3P	Glycerol-3-phosphate
G6P	Glucose-6-phosphate
G6PD	Glucose-6-phosphate dehydrogenase
GAP	Glyceraldehyde-3-phosphate
GC-MS	Gas Chromatography-Mass Spectrometry
GF	Growth factor
GLS2	Glutaminase 2
GLUT	Glucose transporter
Gln	Glutamine
Glu	Glutamate
Gly	Glycine
GPC	Glycerophosphocholine
GSH	Glutathione
GWAS	Genome wide association studies
HDAC	Histone deacetylase
H&E	Haematoxylin and eosine
HER2	Human Epidermal Growth Factor Receptor 2
HIF1	Hypoxia-inducible factor 1
HILIC	Hydrophilic interaction liquid chromatography
HLRCC	Hereditary Leiomyomatosis and Renal Cell Cancer
HR+	Hormone receptor positive
HRMS	High-resolution mass spectrometry

HRP	Horseradish peroxidase
HSQC	Heteronuclear Single Quantum Correlation
IDH2	Isocitrate dehydrogenase 2
ILC	Invasive lobular cancer
Ile	Isoleucine
I.p.	Intraperitoneal
I.v.	Intravenous
JRES	<i>J</i> -resolved
LCIS	Lobular carcinoma <i>in situ</i>
LC-MS	Liquid chromatography-mass spectrometry
LDH	Lactate dehydrogenase
Leu	Leucine
LTR	Long terminal repeat
MARPs	Muscle ankyrin repeat proteins
MBTSTFA	<i>N</i> -Methyl- <i>N</i> - <i>tert</i> -butyldimethylsilyltrifluoroacetamide
MCF-7	Michigan Cancer Foundation-7
MCT	Monocarboxylate transporter
Met	Methionine
MFA	Metabolic flux analysis
MIDA	Mass Isotopomer Distribution Analysis
MINDACT	Microarray In Node negative Disease may Avoid ChemoTherapy
MMPs	Matrix metalloproteinases
MMTV-PyMT	Mouse mammary tumour virus–polyoma middle T antigen
MRI	Magnetic resonance imaging

MS	Mass spectrometry
mTOR	Mechanistic Target of Rapamycin
mTORC1	Mechanistic target of rapamycin complex 1
Muc4	Mucin 4
NADP ⁺	Nicotinamide adenine dinucleotide phosphate
ni	non injected
nmol _f	final nmols
nmol _i	initial nmols
NMR	Nuclear Magnetic Resonance
NST	No special type
NUS	Non-uniform sampling
OXPPOS	Oxidative phosphorylation
oxPPP	Oxidative branch of the pentose phosphate pathway
PAGE	Polyacrylamide gel electrophoresis
PARP	Poly(ADP-ribose) polymerase
PBS	Phosphate buffered saline
PBST	PBS with Tween-20
PC	Pyruvate carboxylase
PCho	Phosphorylcholine
PDH	Pyruvate dehydrogenase
PDK1	Pyruvate dehydrogenase kinase-1
PEP	Phosphoenolpyruvate
PFK	Phosphofructokinase
PGAM1	Phosphoglycerate mutase 1

Phe	Phenylalanine
PHGDH	Phosphoglycerate dehydrogenase
PK	Pyruvate kinase
PPP	Pentose phosphate pathway
PR	Progesterone Receptor
R5P	Ribose-5-phosphate
RIPA	Radioimmunoprecipitation assay
ROS	Reactive oxygen species
RP	Reversed-phase
Ru5P	Ribulose-5-phosphate
S6K	S6 kinase
SD	Standard deviation
SDS	Sodium dodecyl sulphate
SDH	Succinate dehydrogenase
SEM	Standard error of the mean
Ser	Serine
SERMs	Selective oestrogen response modulators
SIM	Selected-ion monitoring
SIRM	Stable Isotope-Resolved Metabolomics
SNPs	Single nucleotide polymorphisms
SOFT	Suppression of Ovarian Function Trial
SRB	Sulforhodamine B
TAE	Tris-acetate-EDTA
TAILORX	Trial Assigning Individualized Options for Treatment [Rx]

TAMs	Tumour-associated macrophages
Tax	Docetaxel
TAX	Tax-treated residual tumours/cells
TBDMCS	Tert-Butyldimethylchlorosilane
TCA	Trichloroacetic acid
TCA cycle	Tricarboxylic acid cycle
TEXT	Tamoxifen and Exemestane Trial
Thr	Threonine
TIGAR	TP53-induced glycolysis and apoptosis regulator
TKIs	Tyrosine kinase inhibitors
TMSP	Trimethylsilyl propanoic acid
TNM	Tumour size, Nodal involvement, presence of Metastasis
TOCSY	Total Correlation Spectroscopy
TOF	Time-of-flight
TRAIL	Tumour necrosis factor-related apoptosis inducing ligand
Try	Tryptophan
Tyr	Tyrosine
UPLC	Ultra-performance liquid chromatography
Val	Valine
VEGF	Vascular endothelial growth factor
Xu5P	Xilulose-5-phosphate

CHAPTER 1

GENERAL INTRODUCTION

1.1 CANCER AND METABOLISM

1.1.1 Hallmarks of tumours

At the beginning of the 21st century cancer remains a significant threat to human life, with 161,823 deaths for cancer in UK in 2012 (Cancer Research UK).

In 2000, *Hanahan and Weinberg* identified common traits in all types of human cancers that can be grouped into six hallmarks. They further reviewed and expanded this in 2011, and postulated the following hallmarks of cancer: “self-sufficiency in growth signals, insensitivity to antigrowth signals, resisting cell death, limitless replicative potential, sustained angiogenesis, tissue invasion and metastasis, reprogramming energy metabolism and avoiding immune destruction” (Hanahan and Weinberg, 2000, Hanahan and Weinberg, 2011). Despite the high heterogeneity of human cancer progression, these hallmarks represent a common end-point arising through different steps from predisposing characteristics such as genomic instability, due to mutations in tumour suppressors (caretakers) and oncogenes (gatekeepers) (Hanahan and Weinberg, 2000), and inflammatory state (Hanahan and Weinberg, 2011). The eight hallmarks of tumour are described below:

1. **“Self-sufficiency in growth signals”**. While normal cells require stimulation from exogenous growth and survival factors in order to grow, tumour cells are able of autocrine growth factor (GF) stimulation by producing their own growth factors, or carry somatic mutations that result in permanent signalling even in the absence of these factors, accompanied by GF receptors overexpression, or hyper-activated downstream signalling molecules (Hanahan and Weinberg, 2011). In recent years, a new mechanism emerged where the tumour

microenvironment participates in providing growth factors to stimulate cancer cell growth (Cheng et al., 2008).

2. **“Insensitivity to antigrowth signals”**. In order to maintain normal tissue homeostasis, cells are kept in a quiescent state if needed, via antiproliferative signals that block the progression of the cell cycle. The control over cancer cell proliferation is mainly operated by tumour suppressors. These proteins are inactivated or lost in many cancers allowing them to hyper-proliferate and form the malignant mass. When cells are cultured *in vitro*, another proliferation inhibition signal is provided through cell-cell contact, which triggers various receptors and adhesion molecules signalling. Again, this “contact inhibition” effect is lost in cancer cells.
3. **“Resisting cell death”**. Apoptosis and autophagy are programmed cell death processes that act to counterbalance cell growth inducing cell death when abnormalities are sensed. These processes therefore represent important obstacles for uncontrolled cellular proliferation, requiring cancer cells to acquire the ability to avoid them as part of their development.
4. **“Limitless replicative potential”**. The presence of the three hallmarks described above would not be useful if malignant cells were able to replicate for a limited number of doublings, as occurs in normal cells. In fact, tumour cells are able to avoid telomeres (the ends of chromosomes) shortening via enhanced telomerase activity, acquiring replicative immortality.
5. **“Sustained angiogenesis”**. Blood vessels are important carriers of oxygen and nutrients. For this reason cells cannot survive further than 100-200 μm from this blood supply (Helmlinger et al., 1997). To try to avoid this, cancer cells

undergo a so called “angiogenic switch” starting from the early stages of tumour mass formation (1-2 mm³), where new vessels are produced to allow tumour progression. However, these vessels are often dysfunctional, which results in the microenvironments of low oxygen (hypoxia) forming, which further drives malignant progression.

6. **“Tissue invasion and metastasis”**. Almost all types of cancer are characterised by the ability to invade adjacent tissues and to metastasise to distant sites, often undergoing an epithelial-to-mesenchymal transition (EMT) process, following signalling from the tumour microenvironment. Once it reaches a distal site, malignant cells need to colonize and adapt to the new environment in order to form the metastatic tumour. This ability is the main cause of human cancer deaths.
7. **“Reprogramming energy metabolism”**. In order to sustain the need for continuous proliferation and growth, cancer cells need to adjust their metabolism accordingly. This hallmark will be discussed in detail in the following sections.
8. **“Evading immune destruction”**. The immune system, cytotoxic T Lymphocytes and natural killer cells in particular, is responsible of an antitumour response that recognises and eliminates cancer cells. However, some cancer cells are able to evade the immune surveillance and killing capacity by suppressing immune system activity (Yang et al., 2010). Moreover, leukocytes (macrophages, mast cells, neutrophils, T and B lymphocytes in particular) can also be tumour-promoters, producing various growth factors, chemokines and cytokines.

1.1.2 Metabolic alterations in cancer

One of the emerging cancer hallmarks presented by *Hanahan and Weinberg* in their 2011 review was the reprogramming of energy metabolism. This apparently new concept has its foundation in studies conducted by Otto Warburg in the 1920s, during which he observed that tumour cells produce lactate from glucose even in the presence of O₂ (normoxic conditions), a phenotype termed “aerobic glycolysis” (Warburg, 1923). This phenotype is now called the Warburg effect, and it is considered a major feature of the metabolic adaptation of cancer cells. The aerobic glycolysis by itself is not a mechanism specific for cancer cells, in fact all eukaryotic cells are able to produce adenosine triphosphate (ATP) by glycolysis as well as by oxidative phosphorylation (OXPHOS) in mitochondria. What is unique is the consequent production of high level of lactate, that create an acidic microenvironment (Tennant et al., 2009). Considering that glycolysis is a more inefficient energy production pathway compared with OXPHOS (2 mole of ATP versus 36 mole of ATP per mole of glucose), tumour cells need to considerably increase the rate of glycolysis, in order to sustain rapid proliferation (Tennant et al., 2009). This requires an increased glucose uptake, which has been also exploited as a clinical marker for tumour detection through the use of ¹⁸F-deoxyglucose positron emission tomography (FDG-PET) (Strauss, 1997).

Therefore, the choice of tumour cells of glycolysis over OXPHOS cannot be explained in terms of ATP production, but in terms of production of glycolytic intermediates. These are then employed as substrates for many important biosynthetic pathways involved in the production of macromolecules (e.g. the pentose phosphate pathway (PPP), lipids and nucleotide synthesis) (Vander Heiden et al., 2009) aimed at biomass accumulation, and maintenance of the redox state (Cantor and Sabatini, 2012).

Warburg originally hypothesised that mitochondrial dysfunction was at the centre of the aerobic glycolytic phenotype (Warburg et al., 1927). Consistent with this, some inherited mutations in the mitochondrial metabolic machinery have more recently been shown to drive the Warburg effect in specific cancer syndromes, providing a basis for Warburg's original hypothesis, albeit in rare tumours. Loss-of-function germline mutations in two tricarboxylic acid (TCA) cycle enzymes have been shown to lead to cancer - succinate dehydrogenase (SDH) mutations, which lead to pheochromocytomas, paragangliomas and renal cell cancers (Baysal et al., 2000, Gimm et al., 2000), and fumarate hydratase (FH) mutations, which lead to Hereditary Leiomyomatosis and Renal Cell Cancer (HLRCC) (Koppenol WH, 2011, Tomlinson et al., 2002). These two enzymes were therefore the first described 'metabolic' tumour suppressors, and directly result in the Warburg effect through mitochondrial dysfunction (Gottlieb and Tomlinson, 2005). In addition, a further TCA cycle enzyme, the nicotinamide adenine dinucleotide phosphate (NADP⁺)-dependent isocitrate dehydrogenase 2 (IDH2) as well as its cytosolic isozyme, IDH1 (Bayley and Devilee, 2010) was shown to be an early mutation in some cases of acute myeloid leukaemia (AML) (Green and Beer, 2010) and glioblastomas (Yan et al., 2009). It has been demonstrated that mutated IDH is not able to oxidise and decarboxylate the TCA cycle intermediate isocitrate to produce α -ketoglutarate (α -KG) (Yan et al., 2009). In these cells α -KG levels are therefore lower, resulting in the stabilisation of the hypoxia-induced transcription factor, hypoxia-inducible factor 1 (HIF1), and promotion of "pseudo-hypoxia" (Bayley and Devilee, 2010). *Dang et al.* demonstrated that IDH1 mutations confer a new enzymatic activity, that is the ability to convert α -KG in 2-hydroxyglutarate (2-HG) via NADPH-dependent reduction. Interestingly, 2-HG levels

have been found elevated in tumour samples, correlating with reactive oxygen species (ROS) levels and favouring tumourigenesis (Dang et al., 2009), identifying IDH1 as an oncogene. However, it has been noted that mitochondrial dysfunction is not generally apparent in most tumours exhibiting the Warburg effect, suggesting that other mechanisms are generally at work (Koppenol et al., 2011). In this case, it has been shown that activation of proto-oncogenes can directly lead to an aerobic glycolytic phenotype.

c-MYC

The most direct link between an overexpressed oncogene and altered glucose metabolism is illustrated by the oncogenic transcription factor c-MYC which regulates cell proliferation, differentiation and apoptosis (Evan and Littlewood, 1993, Packham and Cleveland, 1995) and in particular, it activates most glycolytic genes and glucose transporters, supporting the glycolytic phenotype. Among all the c-MYC targets, one in particular plays an important role: lactate dehydrogenase A (LDH-A), an enzyme which converts pyruvate to lactate (Figure 1.1) and is therefore highly involved in the regulation of the Warburg effect in cancer cells (Shim et al., 1997). MYC also favours the alternative splicing of the ATP-producing pyruvate kinase (PK) enzyme, favouring the expression of the PKM2 isoform (David et al., 2010), which is normally expressed in embryonic development and it has been found to be upregulated in tumour tissues (Eigenbrodt et al., 1992, Christofk et al., 2008a). The switch from the PKM1 (isoform expressed in adult, non-proliferating tissues) to the embryonic (and proliferating cell) isoform M2, could be explained by the ultimate goal of cancer cells: proliferation and growth (Christofk et al., 2008a, Mazurek et al., 1997, Ye et al., 2012). A possible mechanism of regulation of PKM2 activity has been proposed, which involves binding

of peptidyl phospho-tyrosine residues to PKM2, linking its activity directly with oncogenic activity of signalling pathways such as AKT. The binding of phosphorylated residues to PKM2 catalyses the release of its allosteric activator, fructose-1,6-bisphosphate (FBP), and the consequent inhibition of the enzymatic activity (Christofk et al., 2008b). Reduced PKM2 activity in tumour cells leads to the accumulation of the upstream glycolytic intermediates, which will be channelled to anabolic processes, providing tumour cells with the precursors necessary to sustain cell growth and proliferation (Figure 1.1) (Ye et al., 2012). A further mechanism of regulation involves ROS, which inactivates PKM2, contributing to anabolic mechanisms and anti-oxidant production through diversion of glucose carbons into the PPP. The consequent NADPH production is responsible for boosting the cellular antioxidant activity via glutathione activation (Figure 1.1) (Dang, 2012). Finally, c-MYC is also involved in glutamine metabolism (favouring glutaminolysis) (Wise et al., 2008), fatty acid synthesis (Morrish et al., 2009) and serine/glycine metabolism, underlining the involvement of this oncogene in controlling cell growth and proliferation (Dang, 2012).

AKT

Another oncogene able to sustain the Warburg effect in tumour cells, is AKT, which is activated by PI3K as part of the PI3K/AKT pathway, triggered by tyrosine kinase receptors bound to growth factors when nutrients are available. PTEN is a tumour suppressor that antagonises PI3K through the de-phosphorylation of the membrane-bound phosphoinositol-3,4,5-trisphosphate required for AKT activity. AKT activates two glycolytic enzymes - hexokinase-2 and phosphofructokinase (PFK1 and PFK2) - and recruits glucose transporters to the cell surface (GLUT1), enhancing glycolysis (Elstrom et al., 2004). Moreover, this oncogene makes a broader contribution to cancer

metabolic reprogramming, stimulating *de novo* fatty acids synthesis through ATP citrate lyase (ACL) phosphorylation (Berwick et al., 2002), and increasing protein synthesis activating the mechanistic (previously known as mammalian) target of rapamycin complex 1 (mTORC1) (Laplante and Sabatini, 2012).

mTOR

The serine/threonine kinase mTOR is the catalytic domain of two complexes – mTORC1 and mTORC2. The former in particular plays a pivotal role in controlling cell growth based on nutrient availability (Efeyan et al., 2012). The availability of free amino acids in the cytosol is particularly important for maintaining cellular homeostasis: their requirement for *de novo* protein synthesis means that a cell cannot alter its phenotype without investing in new protein synthesis. Their abundance is sensed by the mTORC1: a number of amino acids – especially glutamine - activates this kinase, which shuts down autophagy and drives cellular growth (Efeyan et al., 2012), also inducing initiation of translation via S6K1 and eIF4E-BP1 phosphorylation and activation (Wu et al., 2005). While in starvation conditions, where concentrations of amino acids in the cytosol drop, mTORC1 is inhibited, cell growth arrested and autophagy activated to replenish missing nutrients (Kroemer et al., 2010).

AMPK

One of the pivotal tumour-associated driver of metabolic transformation during metabolic stresses, such as nutrient deprivation and hypoxia, is AMP-activated protein kinase (AMPK). It responds to changes in the ATP:ADP:AMP ratio by shutting down energy-consuming pathways such as fatty acids synthesis (Carling et al., 1987), and mTORC-mediated protein synthesis (Gwinn et al., 2008) while increasing energy-producing processes.

P53

P53 is a transcription factor that acts as a tumour suppressor and in some cases an oncogene, and its importance in counteracting tumour development is also highlighted by the fact that around 50% of all human cancer present a mutated or deleted p53 gene (Liu et al., 2015). Besides its well-known pro-apoptotic and cell-cycle arrest role, p53 has recently been discovered to participate in metabolic control (Shen et al., 2012), decreasing glycolytic metabolism through the activation of the TP53-induced glycolysis and apoptosis regulator (TIGAR) (Lee et al., 2014). Blocking PFK-1 activity, TIGAR causes an accumulation of the upstream fructose-6-phosphate which is consequently channelled into the PPP, supporting a proliferative and antioxidant cellular response (Lee et al., 2014). However, when p53 activity is lost, cellular proliferation can still be promoted, this time through control over another glycolytic enzyme – the phosphoglycerate mutase 1 (PGAM1). In the absence of p53, PGAM1 increases the conversion of 3-phosphoglycerate (3-PG) to 2-phosphoglycerate, reducing the availability of the PPP-inhibitor 3-PG. Moreover, this metabolite also participates in serine biosynthesis further supporting nucleotide production (Hitosugi et al., 2012). P53 control over glycolysis is also exerted directly on glucose transporters (GLUT1 and GLUT4) decreasing the entry of glucose into the cell (Schwartzberg-Bar-Yoseph et al., 2004). P53 metabolic control is not limited to glycolysis, but there are evidences showing its control over OXPHOS through cytochrome c oxidase 2 activation (Matoba et al., 2006) and glutaminase 2 (GLS2) activation (Hu et al., 2010). Interestingly, p53 and AMPK exert positive stimulation between each other, favouring mTORC1 inhibition following DNA damage detection and *de novo* fatty acids synthesis inhibition (Feng et al., 2007).

Other examples of oncogenes supporting the Warburg effect are K-RAS, which stimulates glucose uptake, and SRC, which upregulates glycolytic enzymes (Flier et al., 1987) and can stabilise HIF1 α (Jiang et al., 1997).

Mutations in metabolic enzymes can result in the acquisition of oncogenic features as described above for SDH, FH, IDH1 and IDH2, creating a strong link between metabolic alterations and tumourigenesis (Dang, 2012). Another example is given by the enzyme phosphoglycerate dehydrogenase (PHGDH) whose elevated expression mediates diversion of glucose carbons from glycolysis to increased serine biosynthesis (Locasale et al., 2011), permitting increased rates of proliferation.

Even though the Warburg effect is now commonly seen as a major metabolic phenotype in cancer cells, this mechanism alone is not sufficient to sustain cell growth (Koppenol et al., 2011), considering for example the central role of lipid synthesis for cancer cell growth. Moreover, given that most of the glucose is consumed upstream of the TCA cycle, the functional mitochondria of most proliferating tumour cells need to be fuelled by nutrients other than glucose, e.g. through so-called anaplerotic pathways that allow the continuous production of TCA cycle intermediates used for anabolic reactions. Glutamine, the most abundant amino acid in the plasma, represents an important anaplerotic nutrient for the Krebs cycle in cancer cells. Through oxidation in the TCA cycle (glutaminolysis), it provides cancer cells with ATP, NADPH, anabolic carbons and nitrogen for redox maintenance, nucleotide and lipid synthesis, therefore supplying the building blocks for cell replication (DeBerardinis et al., 2007, Gaglio et al., 2011). However, cancer cells with defective mitochondria are unable to use this oxidative pathway. *Mullen at al.* recently showed that these cells support their growth via an alternative pathway: known as reductive carboxylation. In this reaction, α -

ketoglutarate derived from glutamine is reductively carboxylated through isocitrate to form citrate, providing the substrates for lipid synthesis. This reductive pathway is mediated by IDH1 or 2 (although IDH1 is a cytosolic enzyme, therefore removing the pathway from this organelle), acting in a reverse reaction compared to the oxidative pathway (Mullen et al., 2012).

Glutamine is also essential for glutathione (GSH) production, hence it plays an important role in helping tumour cells to resist the oxidative stress produced in the hostile environment of the tumour (DeBerardinis and Cheng, 2010). Moreover, the role of glutamine in directly regulating cell signalling has been demonstrated, such as through its involvement in controlling cell growth via the mTOR described above (DeBerardinis and Cheng, 2010).

The TCA cycle can also be fuelled by glucose-dependent anaplerosis involving pyruvate carboxylase (PC) activity, which converts glycolysis-derived pyruvate directly into oxaloacetate (Cheng et al., 2011), thus avoiding entry of nutrients via pyruvate dehydrogenase (PDH) which is regulated by many factors (e.g. pyruvate dehydrogenase kinases, PDKs). PC activity has recently been shown to be fundamental in SDHB-deficient tumours, where a blocked TCA cycle does not allow intermediates and ATP production via the classical route. Therefore, in these cells PC supports a positive regulation of glycolytic flux, and consequently an increased glycolysis-derived ATP production through decreasing pyruvate availability (Cardaci et al., 2015).

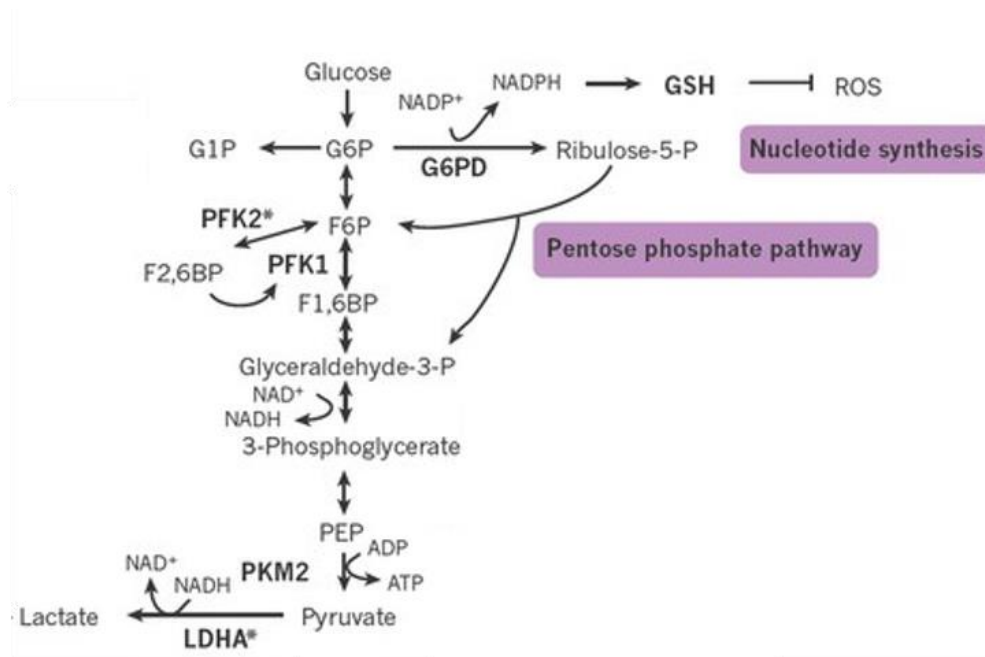


Figure 1.1. Glycolytic pathway in tumours.

Glucose is catabolised in tumours through aerobic glycolysis (the Warburg effect) leading to the production of lactate via lactate dehydrogenase A (LDHA) activity. However, the expression of the M2 isoform of pyruvate kinase (PKM2) can decrease the conversion of phosphoenolpyruvate (PEP) to pyruvate, favouring the channelling of the upstream glycolytic intermediates into proliferation-prone pathways, such as the pentose phosphate pathway. Abbreviations: F1,6BP, fructose-1,6-bisphosphate; F6P, fructose-6-phosphate; G1P, glucose-1-phosphate; G6P, glucose-6-phosphate; G6PD, glucose-6-phosphate dehydrogenase; GSH, glutathione; PEP, phosphoenolpyruvate; PFK, phosphofructokinase; ROS, reactive oxygen species. Adapted from (Schulze and Harris, 2012).

1.1.2.1 Tumour microenvironment and metabolic adaptations

Tumours cannot be fully understood if one does not consider that they are complex tissues, composed not only of cancer cells forming the parenchyma, but also by non-mutated cells organised into the stroma, immune cells and tumour vasculature, altogether creating the so-called tumour microenvironment (Hanahan and Weinberg, 2000, Hanahan and Weinberg, 2011). The interaction between the tumour cells and the stroma contributes to the multistep progression of cancer, characterised by an initial stage of normal stromal cells recruitment by cancer cells, which then stimulate the development of the malignant phenotype, eventually supporting invasion and metastasis (Hanahan and Weinberg, 2011). In most solid tumours, the microenvironment is 'hostile', characterised by a number of stresses such as low oxygen levels (hypoxia), increased ROS (Fiaschi and Chiarugi, 2012), nutrient depletion and build-up of toxic cellular waste products due to their rapid and uncontrolled growth surrounded by an aberrant neovasculature (Bergers and Benjamin, 2003). Cancer cells need to adapt to this environment through reprogramming of their energy metabolism, in order to be able to survive and proliferate in such an environment. In particular, the presence of hypoxia renders cells more invasive and resistant to therapies (Harris, 2002). The metabolic adaptation to hypoxia is mainly driven by HIF1, a heterodimeric transcription factor that upregulates the expression of most glycolytic enzymes (e.g. hexokinase 1/2, LDH-A, GLUT1/3) in order to support increased glycolytic metabolism (Semenza, 2009). HIF1 also regulates a key enzyme that inhibits oxidation of pyruvate, PDK1, which phosphorylates and inactivates PDH, decreasing the oxidative decarboxylation of pyruvate to acetyl CoA (Kim et al., 2006). This happens in parallel with the upregulation of LDH-A, therefore

favouring the conversion of pyruvate into lactate. As a consequence, production of high levels of lactate creates an acidic environment promoting tumour invasion (Semenza, 2013). The presence of acidosis also applies a selective pressure, given that cells that are not able to adapt to these unfavourable conditions will undergo apoptosis (Justus et al., 2015). HIF1-dependent inhibition of pyruvate oxidation consequently results in inhibition of glucose-derived fatty acid synthesis, making cells more dependent on glutamine metabolism, specifically reductive carboxylation of this amino acid, for their synthesis (Metallo et al., 2012, Wise et al., 2011). Moreover, decreased pyruvate oxidation in hypoxia also ensures decreased ROS production, although the full process is not yet understood (Justus et al., 2015). Another member of the HIF family – HIF2 – has shown involvement in the adaptation process to hypoxia, mainly controlling VEGF expression (Krieg et al., 2000), particularly *in vivo* (Wiesener et al., 2003). However, HIF2 predominantly drives changes in response to prolonged (chronic) hypoxia, while HIF1 is responsible for adaptations to acute hypoxia (Loboda et al., 2012, Holmquist-Mengelbier et al., 2006). While HIF1 is ubiquitously expressed, HIF2 shows a non-ubiquitous, cell-specific localisation, being expressed in endothelial cells, in tumour-associated macrophages (Talks et al., 2000), and in the cytoplasm of mouse embryo fibroblasts even in normoxic conditions (Park et al., 2003). Moreover, HIF2 expression has been correlated with decreased breast cancer patient survival and increased distant recurrence (Helczynska et al., 2008), supporting its contribution to tumour development and malignancy. There are also a number of HIF-independent mechanisms of adaptation to hypoxia, an example being the activation of AMPK in these conditions, which stimulates macroautophagy (Papandreou et al., 2008), and inhibits mTOR activity, in order to reduce energy consumption (Liu et al., 2006).

Nutrient abundance and oxygen availability are not homogenous throughout the whole tumour mass, but constitute a gradient based on the proximity of the region to a functional blood vessel. As a consequence, the tumour is composed of cells with different metabolic profiles based on their localisation within the same environment. In particular, it was recently shown that glycolytic cells that produce and secrete lactate via the Warburg effect maintain a symbiotic relationship with aerobic cells that uptake and utilise that lactate as the main energy substrate for their oxidative metabolism (Sonveaux et al., 2008). This relationship is therefore glucose sparing, permitting a larger tumour size than would be possible in its absence. Lactate, and the monocarboxylate transporters, MCT1 and 4, have a central role in this symbiotic metabolism (Sonveaux et al., 2008, De Saedeleer et al., 2014, Draoui et al., 2014). The idea evolved into the “two-compartment tumour metabolism” model more recently, which describes how cancer-associated fibroblasts (CAFs) perform glycolytic metabolism to fuel the neighbouring epithelial cancer cells oxidative metabolism (Salem et al., 2012). Therefore, the catabolic tumour microenvironment provides autophagy/mitophagy-derived nutrients to the anabolic epithelial component of cancers to offer metabolic support to tumour growth (Carito et al., 2012, Salem et al., 2012).

Despite the perception of many common traits in cancer cell metabolic reprogramming, one has to bear in mind that cancers are highly heterogeneous (Cantor and Sabatini, 2012), making patient stratification and personalised treatments necessary (Kalia, 2015). However, the discovery of the metabolic intra-tumour heterogeneity described above, on top of the longer-known genetic and protein expression heterogeneity (Marusyk and Polyak, 2010), has the potential to radically influence diagnostic

procedures and therapeutic approaches (Sun and Yu, 2015), given that different regions of the same tumour could lead to opposite metabolic profiles, and therefore to the choice of unsuccessful therapies.

1.2 BREAST CANCER

1.2.1 Epidemiology and subtypes

Breast cancer is the most common cancer in the UK, accounting for 49,900 cases in women in 2011, while more than 1.68 million women were diagnosed worldwide in 2012 (Cancer Research UK).

There are two types of risk factors: those that can be controlled, and those that cannot. The former includes being overweight, lack of physical activity, alcohol consumption, nulliparity, high age at first birth, and use of exogenous hormones (like oestrogen and progesterone), while uncontrolled risk factors include age (increased incidence after 40), younger age at menarche, race (higher incidence in White women), family history, genetic factors, medical history, duration of breastfeeding and late menopause (Mahoney et al., 2008, Barnard et al., 2015). Interestingly, the incidence rate of breast cancer is higher in developed countries (71.7/100,000) compared to poorer countries (29.3/100,000) (Ferlay et al., 2010). This underlines the influence of lifestyle, and in particular of specific aspects of western world lifestyle, such as having fewer children, higher obesity, and use of oral contraceptives (Porter, 2008). Recently, it has been pointed out that the above described risk factors can have different associations with each breast cancer subtype, while family history is the only factor affecting all subtypes

(luminal A, luminal B, HER2-overexpressing, triple negative, all described later) (Barnard et al., 2015).

Considering the strong link between stage at diagnosis and survival (Elmore et al., 2005), enhancements in early stage detection are of vital importance to decrease the morbidity and overall mortality (Youlden et al., 2012). To reach this aim, improvements in diagnostic imaging and in screening approaches are required (Moulder and Hortobagyi, 2008). National screening programmes exist in different countries; for example in the UK women between the ages of 47-73 are subjected to mammography-based screening every 3 years (Health & Social Care Information Centre). However, the high heterogeneity of breast cancer needs to be considered in order to achieve personalised screening tailored to individual risk factors. In particular, breast density (determined by the proportion of fat and fibroglandular tissue), emerged to be a risk factor that should be used to discriminate between the use of mammography or alternative screening approaches such as magnetic resonance imaging (MRI) and sonography. This is because high-density breast tissue, such as found in younger women, does not allow good visibility through mammography decreasing its sensitivity as an early detection approach (Gucalp et al., 2014). As a result of the improvement of screening approaches, the percentage of breast cancer detected at an early stage has increased in developed countries. This early diagnosis has led to an increase in breast cancer survivors over the last decade, favouring a relative survival rate of 88% at five years after diagnosis (Soerjomataram et al., 2008, Youlden et al., 2012). However, it has also resulted in the significant issue of overdiagnosis: specifically the detection of tumours that could have remained benign throughout the whole lifetime (Gunsoy et al., 2014). For this reason, the effectiveness of mammographic screening

is still controversial (Gunsoy et al., 2014). In contrast to the above-described situation, developing countries do not show the same survival rate. Many aspects of healthcare in these countries contribute to this challenge, such as reduced availability of screening programmes (therefore presentation at a more advanced stage at diagnosis), low levels of awareness, poor infrastructure and inadequate expertise (Agarwal et al., 2009).

Breast cancer can be classified into two subtypes based on the anatomical localisation of the rising tumour: ductal, which is the most common, arising from the cells lining the ducts of the breast, and forming glandular structures (Korkola et al., 2003); and lobular, that originates in the cells lining the lobules or lobes of the breast. Both can be invasive or *in situ*. In the case of ductal origin, when these abnormal cells have not started to invade the basal membrane of the ducts, it is defined ductal carcinoma *in situ* (DCIS) (Wellings and Jensen, 1973): this accounts for about 20% of breast cancers and results in a good prognosis (Van Cleef et al., 2014). However, it can evolve into the invasive subtype, previously known as ductal carcinoma, and now called No Special Type (NST), which accounts for about 80% of all invasive breast tumours (Korkola et al., 2003). The lobular subtype instead, is defined lobular carcinoma *in situ* (LCIS) when not invasive, and it is less common than the ductal subtype (around 11% of cases). However, it can be the precursor of the invasive lobular cancer (ILC) which represents the 15% of all invasive cancers (Korkola et al., 2003). This subtype consists of small atypical cells, able to rapidly invade the adjacent stroma following loss of E-cadherin (Mastracci et al., 2005). In this way, this type of tumour will not form an easily detectable mass (by physical exam or mammography). Thus, it is usually detected when the tumour is already at a more advanced stage (Wasif et al., 2010). At the

molecular level, most of the lobular tumours are hormone receptor-positive: Oestrogen Receptor (ER, 70-92%) and Progesterone Receptor (PR, 63-67%) positive (Zhao et al., 2004), while fewer ductal tumours are hormone receptor-positive (Korhonen et al., 2004).

The use of immunohistochemistry first, of gene expression arrays later, and of genomic approaches most recently (Sonnenblick et al., 2014), has made it clear that breast cancer is a highly heterogeneous disease, both inter-tumour and intra-tumour (Skibinski and Kuperwasser, 2015), that therefore needs a wider classification for a more precise diagnosis, and more specific treatment approaches.

Based on tumour histology and molecular pattern, five different biological subtypes of breast cancer can be identified: luminal A, luminal B, Human Epidermal Growth Factor Receptor 2 (HER2) overexpressing, basal-like, and claudin-low (Perou et al., 2000, Sorlie et al., 2001, Herschkowitz et al., 2007). The majority are luminal subtype (luminal A and B), accounting for 75-80% of breast cancer cases (Perou et al., 2000). The subtype A can be distinguished from the subtype B accordingly to the ER expression: the highly expressing subtype A with good prognosis, and the lower expressing subtype B with poorer prognosis (Sorlie et al., 2001). Moreover, they can be separated accordingly to Ki67 (a marker of cell proliferation) expression levels (Murase et al., 2014). Recently, a clinical study has proposed another marker to distinguish these two subtypes: the PR expression level. Indeed, luminal subtype B exhibits a significantly lower PR expression level than subtype A, probably due to a lack of intratumoural estradiol, which is known to upregulate PR (Murase et al., 2014). Recently, a further subtype defined as “triple positive” has been identified for cancers positive for ER, PR and HER2 expression (Vici et al., 2015). The luminal subtypes present a lobular origin

in most cases (Korhonen et al., 2004), and they are characterised by a much better prognosis, compared to non-luminal tumours (Phipps et al., 2008). The HER2 (also called NEU, ERBB2 and p185) overexpressing subtype represents 15-20% of all breast cancer tumours (Musolino et al., 2012), and are usually ER- and PR- (Perou et al., 2000). HER2 is a member of cell-surface epidermal growth factor receptors, the overexpression of which is related to a more aggressive, highly proliferative phenotype of breast cancer, with decreased disease-free survival (Musolino et al., 2012, Slamon et al., 1987). In most cases, this subtype is detected in invasive ductal carcinomas and very infrequently in benign breast hyperplasia (Allred et al., 1992).

The basal-like tumours, also known as triple-negative tumours, are the rarest subtype accounting for 10-15% of all cases (Cleator et al., 2007). They are characterised by the absence of all the three most common markers, such as ER, PR, and HER2 (Perou et al., 2000, Lin et al., 2012b). This subset arises especially in young and premenopausal women, and it is predominant in African American and Hispanic White women (Phipps et al., 2008). It is also associated with a more advanced cancer, showing characteristics like high proliferative rate and central necrosis, contributing to worse survival outcome and poorer prognosis due to high rate of distant relapses, especially in brain or lung (Lin et al., 2012b), with a median survival of only one year among these patients (Lin et al., 2008). The triple-negative subtype is linked to family history and in particular to Breast Cancer, early onset 1 (BRCA1) mutations (Foulkes et al., 2003). Interestingly, it is not associated with increased risk of lymph node positivity, which represents the most important prognostic indicator, the lymph nodes being the most common site of metastasis in patients with invasive breast cancer (Lin et al., 2012a).

The more recently-discovered claudin-low subtype shows high expression of mesenchymal markers (i.e. vimentin), together with low expression of luminal, cell-cell adhesion and junctions genes (i.e. Claudin 3, 4, 7, Occludin and E-cadherin) (Herschkowitz et al., 2007). It accounts for a small fraction of breast tumours (12-14%), and shares similarities with the basal-like subtype given the absence of the three hormone receptors expression. Patients with this tumour type generally have a poor prognosis (Prat and Perou, 2011).

Breast cancer tumourigenesis arises from a multistep acquisition of different genetic or genomic alterations, including changes in copy number, acquisition of single nucleotide polymorphisms (SNPs), as well as loss and gain of function mutations (Dankort and Muller, 2000, Curtis et al., 2012). The order in which the alterations are acquired varies among tumours, and this determines the different tumour phenotypes (Skibinski and Kuperwasser, 2015). All three of these mutational types are found in breast tumours: e.g. amplification of both the Epithelial Growth Factor Receptor (EGFR) and HER2 as well as mutations (SNPs) in BRCA1&2 tumour suppressor genes being regularly observed (Venkitaraman, 2002). Moreover, *Curtis et al.* showed the association between copy number aberrations (CNAs) in the genome, and expression of genes leading to breast cancer, with the identification of ten novel subgroups (Curtis et al., 2012).

While most of breast cancers derive from somatic mutations (so called “sporadic” cancers), five to seven percent are early onset and arise from germline mutations, being therefore defined as hereditary breast cancer (Melchor and Benitez, 2013). BRCA1 and 2 are the most frequently found mutations in familial breast cancers (FBC), responsible for 25% cases (Melchor and Benitez, 2013). These two tumour

suppressors are involved in different functions, such as DNA repair and recombination, cell cycle control and transcription (Venkitaraman, 2002). Their mutation in human cells leads to altered chromosomal structure, therefore predisposing to carcinogenesis (Tirkkonen et al., 1997). 5% of FBC are the result of mutations in high susceptibility genes such as TP53, PTEN, STK11, and CDH1, and another 5% by moderate susceptibility genes among which there are ATM, CHEK2, RAD50, RAD51B/C/D. Low susceptibility genes explain a further 14%, while 51% cases are still caused by unknown mutations (Melchor and Benitez, 2013). Recently, genome wide association studies (GWAS) allowed the identification of around 90 genomic loci associated with the risk of familial breast cancer, accounting for a further 14% of these tumours (Fachal and Dunning, 2015).

1.2.2 Breast cancer treatment

After diagnosis of breast cancer, the treatment protocol is carefully chosen based on several tumour characteristics including disease TNM stage (Tumour size, Nodal involvement, presence of Metastasis), receptor status (mainly determined by immunohistochemistry), molecular subtype and tumour grade (Bossuyt et al., 2015).

The first approach for early stage diagnosed breast cancer usually consists of surgical resection of the primary mass, followed by radiotherapy or systemic adjuvant therapy, to reduce the risk of local recurrence or distant metastasis respectively (Gucalp et al., 2014, Hassan et al., 2010). The adjuvant chemotherapy mainly consists of anthracycline-based treatment, moreover in recent years, the addition of taxanes demonstrated a higher recurrence-free survival (Alken and Kelly, 2013). Until few years ago, surgical treatment consisted of radical mastectomy, while more recently this

approach is being most often replaced with breast conserving surgery (BCS). Many trials demonstrated that BCS does not decrease the overall survival, compared to total mastectomy (Clarke et al., 2005). Furthermore, it provides a better cosmetic outcome, which is important for the acceptance of the disease among women (Margenthaler, 2011). The main risk with BCS is the presence of positive margins, that require further surgical intervention in order to avoid local recurrence (Gucalp et al., 2014).

Locally advanced breast cancer is instead treated with neoadjuvant systemic chemotherapy, which includes anthracyclines (i.e. doxorubicin) and taxanes (i.e. docetaxel) (Yalcin, 2013), a strategy which reduces the risk of recurrence by 30-50% (Moulder and Hortobagyi, 2008). This approach is often used prior to surgery in order to reduce tumour dimensions and render it more easily operable (Zardavas and Piccart, 2015). To date, the combination of these two classes of drugs offers the best clinical outcome, not further improved by addition of other compounds (Zardavas and Piccart, 2015), and showing the highest responses for basal-like and HER2-enriched breast cancer subtypes (Prat and Perou, 2011).

Anthracyclines and taxanes are also used to treat metastatic breast cancer, although their use in this way is mainly palliative, as advanced disease is still incurable and has low survival rates (2-years median survival) (Moulder and Hortobagyi, 2008, Hassan et al., 2010).

Given the interconnection between increased risk of cancer in diabetic patients (Tsilidis et al., 2015) and the elevated insulin levels as a breast cancer risk factor (Ferroni et al., 2015), the efficacy of the antidiabetic drug metformin in systemic breast cancer treatment and prevention has been recently investigated (Vona-Davis and Rose, 2012, Hatoum and McGowan, 2015, Luo et al., 2014). *In vitro* studies showed great efficacy

in treating breast cancer cell lines of various subtypes with metformin, either as monotherapy or in combination with other established breast cancer treatment drugs (Ma et al., 2014, Liu et al., 2012). However, results *in vivo* are still contradictory. Most of the clinical studies are retrospective and while some of them demonstrated a decreased breast cancer risk and mortality in diabetic patients using metformin, others did not. This drug has also shown capacity to decrease androgen and oestrogen circulating levels. Consequently its diabetes-independent activity against breast cancer is now being investigated (Hatoum and McGowan, 2015).

In order to overcome the high heterogeneity of breast cancers, to improve outcomes and patient survival, it is necessary to move toward a more personalised medicine, that could help to predict response to therapy, frequently based on molecular profiles (Gucalp et al., 2014, Perou et al., 2000). Patient tailored therapies could be achieved through the discovery of biomarkers in order to predict individual response or resistance to treatment (Di Leo et al., 2015). Biomarkers can be classified in diagnostic, prognostic, treatment and prevention (Kalia, 2015). Two ongoing trials will probably determine the guidelines for more personalised treatment in the near future: TAILORX (Trial Assigning Individualized Options for Treatment [Rx]) and MINDACT (Microarray In Node negative Disease may Avoid ChemoTherapy) (Di Leo et al., 2015).

Two of the most important biomarkers for breast cancer are ER and PR. Hormonal therapies (also known as selective oestrogen response modulators –SERMs-) such as tamoxifen and raloxifene are aimed at blocking specific hormones' signalling. They are suggested for luminal breast cancers (in particular subtype A, ER+ in premenopausal women) as first-line treatments, showing great efficacy (Abdulkareem and Zurmi, 2012), while for postmenopausal women the preferred treatment involves an

aromatase inhibitor (i.e. letrozole) (Di Leo et al., 2015). Recently, the SOFT (Suppression of Ovarian Function Trial) phase III trial demonstrated that young premenopausal women with hormone receptor positive (HR+) early breast cancer could take advantage of co-treatment with tamoxifen and ovarian suppression, resulting in reduced risk of recurrence, and secondary invasive cancer (Francis et al., 2015). The same type of patients were included in another phase III trial, the TEXT (Tamoxifen and Exemestane Trial), where they demonstrated better disease-free survival following the treatment with the aromatase inhibitor exemestane (previously suggested only for postmenopausal women) together with pharmacological ovarian suppression (Pagani et al., 2014). Moreover, patients with HR+ metastatic breast cancer are often treated with hormonal therapies. However, some cases of ER+ breast cancers are characterised by *de novo* resistance or develop resistance after an initial response period (Jerusalem et al., 2015, Abdulkareem and Zurmi, 2012). In order to overcome endocrine resistance, new and more targeted drugs are currently being tested. The mTOR inhibitor everolimus for instance, used in combination with endocrine therapy, appears to have the best outcome, even in previously refractory metastatic breast tumours (Jerusalem et al., 2015, Yardley et al., 2013). In fact, the hyperactivation of the mTOR signalling pathway has been previously linked to endocrine therapy resistance (deGraffenried et al., 2004). Besides its positive effects, few adverse events were registered after its use (Fedele et al., 2015). Being such a central metabolic controller, its inhibition will negatively affect several mTOR-controlled metabolic processes such as cellular proliferation, translation initiation and autophagy inhibition (Efeyan et al., 2012, Laplante and Sabatini, 2012) as described in section 1.1.2. Unfortunately, its decreased activity also leads to AMPK activation, which

supports tumour growth and most likely tumour cell resistance to mTOR-inhibitors (Dowling et al., 2010, Faivre et al., 2006).

The overexpression of HER2 is also considered a biomarker, whose presence determines the efficacy of the humanised monoclonal antibody trastuzumab (Herceptin), directed against the extracellular juxtamembrane domain of HER2 (Moulder and Hortobagyi, 2008, Phipps et al., 2008). When trastuzumab is used in combination with conventional chemotherapy, it demonstrates even greater survival benefit (Moulder and Hortobagyi, 2008, Zardavas and Piccart, 2015), even in metastatic breast cancer patients (Wong and Hurvitz, 2014). One of the few known disadvantages of Herceptin is the cardiac toxicity developed independently of drug dose (Sandoo et al., 2015). Despite the above mentioned positive aspects, around 50% of patients do not respond to trastuzumab due to resistance (Wong and Hurvitz, 2014). In recent years, the outcome of HER2 positive metastatic breast cancer has greatly improved, also thanks to new therapeutic agents. Pertuzumab, which is another recombinant humanized monoclonal antibody that, binding to the extracellular dimerization subdomain of HER2, inhibits its pro-proliferation downstream signalling (Baselga et al., 2012), and ado-trastuzumab emtansine, which derives from the conjugation of the monoclonal antibody trastuzumab to the microtubule inhibitory agent DM-1 (Verma et al., 2012). Another class of drugs is the intracellular tyrosine kinase inhibitors (TKIs, lapatinib and neratinib), that act by binding the intracellular phosphorylation domain, therefore blocking the receptor signalling and induction of cellular proliferation (Zhu and Verma, 2015, Hojjat-Farsangi, 2014). The main disadvantage of TKIs is their little specificity, causing the inhibition of several off-target tyrosine kinases (Hojjat-Farsangi, 2014). This would in turn affect metabolic pathways

controlled by those tyrosine kinases, as recently shown for the TKIs used for chronic myeloid leukemia (Breccia et al., 2014). Although lapatinib presents a high tyrosine kinase specificity, it has been shown to induce hepatotoxicity due to the metabolites formed during lapatinib elimination process (Castellino et al., 2012).

Specific treatment guidelines are still lacking for triple-negative tumours, due to the absence of specific targets (Cleator et al., 2007). However, patients appear to derive the major benefits from adjuvant chemotherapy (Lin et al., 2012a).

Targeted therapy approaches have made recent advances given a series of new targets such as fibroblast growth factor (FGF), tyrosine kinases, insulin-like growth factor, hepatocyte growth factor and c-MET (Santarpia et al., 2012), mutated PI3K, deleted PTEN, mutated AKT, cyclin D kinases (CDKs), histone deacetylase (HDAC), and deficient DNA repair capacity. The latter in particular has been exploited to enhance chemotherapy efficacy using poly(ADP-ribose) polymerase (PARP) inhibitors in breast cancer patients with BRCA1/BRCA2 mutations (Tutt et al., 2010). Another targeted agent is the antibody bevacizumab (Avastin), directed against vascular endothelial growth factor A (VEGF-A), therefore inhibiting tumour angiogenesis (Moulder and Hortobagyi, 2008).

Besides classical intra-tumoural targets, new efforts have been made to consider possible targets in the tumour microenvironment (Di Leo et al., 2015) given its contribution to breast tumourigenesis (Tlsty, 2001). First of all, the so-called immunotherapies aimed at enhancing the innate immune response anticancer activity; moreover, drugs targeting tumour necrosis factor-related apoptosis inducing ligand (TRAIL) pathway and matrix metalloproteinases (MMPs) (Di Leo et al., 2015). Other targets could be (Nwabo Kamdje et al., 2014):

- CAFs, given their ability in promoting tumour growth via autophagy and senescence;
- NOTCH, which mediates CAF-induced cancer cell growth and survival, and promotes resistance to therapies, especially for HER2-targeted treatments. One of the most active class of drugs is γ -secretase inhibitors and the R04929097 compound has recently entered clinical evaluation.
- tumour-associated macrophages (TAMs), which often infiltrate triple-negative breast cancer microenvironment and contribute to chemoresistance and tumourigenesis.

One of the main side effects of both systemic and targeted therapies is cardiotoxicity. In response to this issue, *Sharp et al.* pointed out the high potential of stem cells in regenerating cardiac tissue, although pre-clinical and clinical studies investigating the effect of an intramyocardial injection of stem cells derived from the bone marrow, found different results dependent on factors including the injection site. Moreover, mesenchymal stem cells injected percutaneously showed promising outcomes (Hare et al., 2012, Karantalis et al., 2014). New hope in the field was given by the discovery of cardiac-derived stem cells with their capacity of cardiac regeneration manifested in the clinical setting (Sharp and George, 2014).

1.2.2.1 Docetaxel

Docetaxel (registered as Taxotere in 1992, Tax) is a semisynthetic taxoid derived from the needles of *Taxus baccata* (Tankanow, 1998, Cortes and Pazdur, 1995). After showing cytotoxicity against various cancer cell lines, it has been demonstrated that its anticancer activity derives from the anti-mitotic effect due to stabilisation of polymerised microtubules (Cortes and Pazdur, 1995) through binding to the β -tubulin

subunit (Tankanow, 1998). As a consequence, cell proliferation is blocked (Herbst and Khuri, 2003), leading to various effects such as mitotic catastrophe (Morse et al., 2005), apoptosis induction and angiogenesis inhibition (Herbst and Khuri, 2003). Given the promising *in vitro* results, clinical trials started to evaluate docetaxel *in vivo* anticancer activity (Cortes and Pazdur, 1995), where efficacy against breast, lung, prostate, head and neck, gastric and ovarian cancer emerged (Herbst and Khuri, 2003). It was approved in 1996 as second line treatment for locally advanced or metastatic breast cancer, showing additional efficacy in tumours shown to be resistant to alternative therapies (especially to anthracyclines) (Alken and Kelly, 2013, Binder, 2013). Moreover, the combination of docetaxel with other chemotherapeutic agents (i.e. sequential administration of doxorubicin, docetaxel, cyclophosphamide/methotrexate/fluorouracil) in the adjuvant treatment for early breast cancer registered an improvement for recurrence-free survival (Alken and Kelly, 2013). The main concern about docetaxel administration is the appearance of the side effects such as neutropenia, hypersensitivity reactions and fluid retention syndrome, although pre-treatments are available that limit those (de Weger et al., 2014). The hypersensitivity in particular seems to be linked to the solvent used to vehicle the drug, therefore new taxane formulations are currently being explored to overcome this side effect (Yared and Tkaczuk, 2012, Roy et al., 2014). Interestingly, docetaxel has not been shown to induce cardiotoxicity.

1.2.3 Breast cancer resistance to treatments

In recent years, advances in breast cancer treatment and in early detection approaches have contributed to a decrease in breast cancer-related mortality.

However, it still represents the second most common cause of female cancer death in the UK, with 11,600 deaths registered in 2012 (Cancer Research UK) underlining the need for further investigations. Mortality is mainly due to recurrence of the disease after initial regression, or primary resistant tumours leading to absent or incomplete response (Gucalp et al., 2014). The metastatic recidive cancer often presents different features compared to the primary, therefore it most likely loses sensitivity to previously effective drugs, requiring a new estimation of the optimal therapy (Di Leo et al., 2015).

1.2.3.1 Resistance to docetaxel and residual tumours

Despite being one of the most useful drugs in the treatment of metastatic breast cancer, around half of the patients present resistance to docetaxel, rendering this therapy unsuccessful. This therefore leads to early mortality given the absence of valid alternatives. Identifying patients in advance that are most likely to develop resistance, or discovering ways to overcome resistance and to restore sensitivity are therefore central points for future research on breast cancer. Various possible mechanisms of resistance to docetaxel have emerged, the most common being described below (Murray et al., 2012):

- over-expression of proteins responsible of drug efflux, such as P-glycoprotein;
- expression of specific β -tubulin isotypes, i.e. class III, or mutated β -tubulin;
- over-expression of the anti-apoptotic Bcl-2;
- HER2 over-expression that leads to blocked apoptosis via CDK1 inhibition;
- microRNA-452 upregulation (Hu et al., 2014);

However, these data are mainly obtained *in vitro*, while demonstration *in vivo* is still controversial (Murray et al., 2012). Identification of global gene signatures instead

represents the most promising approach offering a closer perspective of the clinical situation, as single genetic biomarkers are often not representative of the complex ensemble of drug targets. Gene expression profiling of patient's breast cancer tissue can also be useful to predict response to docetaxel allowing a more personalised treatment approach. In fact, *Iwao-Koizumi et al.* highlighted a correlation between genes responsible of cellular redox homeostasis and docetaxel resistance (Iwao-Koizumi et al., 2005). Also *Chang et al.* identified a number of genes differentially expressed between sensitive and resistant tumours prior to treatment, with, among others, genes linked to cell cycle and RNA transcription being overexpressed in resistant tumours (Chang et al., 2005).

An initially responsive tumour can later evolve into recurrent cancer if the response to the treatment was incomplete and a portion of the tumour was able to survive. This portion is often represented by single cells therefore clinically undetectable until they restart growth (Ignatiadis and Reinholz, 2011). Interestingly, specific breast cancer subtypes are more likely to manifest residual tumour, such as the luminal A after neoadjuvant chemotherapy (Viale, 2013), while triple negative and HER2+ breast cancers have the smallest risk (Yang et al., 2015). *Creighton et al.*, demonstrated how residual tumour cell populations after docetaxel treatment harbour tumour-initiating capacity (Creighton et al., 2009) and therefore have the potential of being the source of cancer recurrence.

1.2.4 Breast cancer metabolism

As stated above, solid tumours need to rearrange their metabolism in order to be able to cope with the unfavourable conditions of the tumour microenvironment, and breast cancer is no exception (Allinen et al., 2004). In fact, hypoxic areas are present in one

third of breast tumours, contributing to metabolic reprogramming and to the development of resistance to treatments (Vaupel et al., 2002, Ward et al., 2013). There is much evidence supporting the presence of a Warburg effect in breast cancer cells, even though the molecular bases for this effect are not well understood (Robey et al., 2008). *Robey et al.*, have demonstrated that the aerobic glycolytic phenotype in breast cancer cell lines is associated with stabilisation of HIF1 α and activation of c-Myc (Robey et al., 2008). Moreover, HIF1 α overexpression has been demonstrated to be a prognostic factor, associated with poor prognosis for advanced-stage breast cancer (Schindl et al., 2002). Recent work has highlighted changes in mitochondrial structure and function in breast cancer. Electron microscopy studies observed a correlation between ultra-structural mitochondrial abnormalities (round-shape and reduced mitochondrial surface) and a reduction of OXPHOS in breast cancer (Putignani et al., 2012), while gene expression analyses in breast cancer cells confirmed a decreased expression and activity of mitochondrial OXPHOS subunits (complex III in particular), especially in metastatic breast cancer cell lines (Owens et al., 2011). All this evidence clearly supports Warburg's theory. Furthermore, the correlation between type 2 diabetes and increased risk of breast cancer highlights the importance of glucose metabolism deregulation in the pathogenesis of this disease (Ferroni et al., 2015). Many metabolic pathways other than glycolysis have been shown to be altered in breast cancers as recently reviewed (Mishra and Ambs, 2015). Interestingly, glutamine has been shown to cover a central role in breast cancer tumour survival, as confirmed by the anti-tumour effects of glutamine deprivation or glutaminase inhibition (Gross et al., 2014, Timmerman et al., 2013). Moreover, nucleotide synthesis relies on serine pathway, which is often upregulated in breast cancer through PHGDH amplification

(Possemato et al., 2011). Another key process is represented by lipid metabolism, in fact *de novo* fatty acids and phospholipids synthesis is fundamental to sustain cancer cell growth and membrane biogenesis (Hilvo et al., 2011, Menendez and Lupu, 2007). The metabolite signature given by the ensemble of the different metabolic alterations has also been shown to contribute to breast cancer subtypes differentiation, although this not always agrees with the gene-expression based separation (Mishra and Ambs, 2015). The increasing interest in the role of metabolites in breast cancer progression has led to the identification of several “oncometabolites”, such as oncogenic metabolites that can represent therapeutic targets, diagnostic and prognostic biomarkers (Mishra and Ambs, 2015). Alterations in key metabolic genes are often at the origin of these metabolic adaptations. For example, 40-50% of luminal breast tumours have mutated genes of the PI3K-Akt-mTOR pathway, while mutations in TP53 are typical of basal-like and HER2-overexpressing tumours (Cancer Genome Atlas Network, 2012).

1.2.5 Models of breast cancer

Breast cancer is known to be a highly heterogeneous disease (Perou et al., 2000, Skibinski and Kuperwasser, 2015), being characterised by many different subtypes with different clinical outcomes. For this reason, finding an *in vitro* or pre-clinical model that closely resembles the human disease is often challenging (Holliday and Speirs, 2011, Vargo-Gogola and Rosen, 2007). At the same time, working with patients or with patient-derived primary cells also presents disadvantages, such as the need of ethical consent, the availability of a limited amount of sample and the limited lifespan before senescence (Burdall et al., 2003). Issues that can be overcome working with established cell lines and pre-clinical models.

1.2.5.1 *In vitro*: MCF-7 breast cancer cell line

MCF-7 (Michigan Cancer Foundation-7) is one of the most popular breast cancer cell line for research, obtained from a pleural effusion of a patient with metastatic breast adenocarcinoma (Levenson and Jordan, 1997). These cells are a useful tool for research, as they are thought to retain several characteristics of differentiated mammary epithelium. MCF-7 cells are both PR and ER positive and their growth is therefore sensitive to these hormones (Pratt and Pollak, 1993). In fact, treatment with the anti-oestrogen tamoxifen significantly decreases MCF-7 cell proliferation (Pratt and Pollak, 1993). This cell line, which does not overexpress HER2 (Bacus et al., 1990), represents closely the luminal subtype of human breast cancer (Levenson and Jordan, 1997) from a molecular point of view. This aspect is particularly relevant for the purpose of this thesis, given that luminal tumours have been shown to often develop residual disease after neo-adjuvant chemotherapy (Viale, 2013). Moreover, MCF-7 cells ability to undergo apoptosis led to the definition of this cell line as an excellent model to investigate chemoresistance *in vitro* (Simstein et al., 2003).

1.2.5.2 *In vivo*: MMTV-PyMT mouse model of breast cancer

The mouse mammary tumour virus-polyoma middle T antigen (MMTV-PyMT) represents a transgenic mouse model of breast cancer that reflects the complexity of human breast tumours well (Lin et al., 2003). In this model, the oncoprotein polyoma virus middle T antigen is under the control of the mouse mammary tumour virus long terminal repeat (LTR) which is therefore able to initiate tumourigenesis specifically in the mammary epithelium (Lin et al., 2003, Guy et al., 1992), following the activation of a series of downstream signalling proteins such as PP2A, Src, Shc, Ras and PI3K

(Dankort and Muller, 2000, Fluck and Schaffhausen, 2009). Such a model allows obtaining the desired genetic alterations only in the tissue of interest, avoiding the systemic effects that a constitutively expressed mutated gene can induce (Bockamp et al., 2002). Tumour progression then occurs in four stages that closely resemble the multistep progression of breast tumours observed in humans (Figure 1.2): hyperplasia, by 4 weeks of age; adenoma; early carcinoma, between 8 to 12 weeks of age; late carcinoma, at around 14 weeks of age, often accompanied by pulmonary metastases (Guy et al., 1992, Lin et al., 2003). The development of metastases makes this mouse model one of the few able to progress through more advanced and terminal stages, whilst most of the existing models mainly represent early stages of progression (Van Dyke and Jacks, 2002). Besides the morphological similarities, the MMTV-PyMT mouse model also shares the same biomarkers of poor prognosis, such as ER and PR loss, overexpression of ErbB2/Neu and cyclin D1, and altered expression of integrin- β (Figure 1.2) (Lin et al., 2003). The gene expression profiling of the mouse mammary tumour tissue revealed similarities with the human luminal subtype, making this model a good parallel with the above-described *in vitro* model, for studying residual breast tumours. It also showed conserved expression patterns with the human tissue, and a high degree of within-model homogeneity (Lim et al., 2010, Herschkowitz et al., 2007). Moreover, the spontaneous development of the mammary tumour inside the tissue of interest in immunocompetent mice ensures the fundamental communication with the microenvironment, therefore representing a pre-clinical model that closely resembles the human disease (Richmond and Su, 2008). Overall, the 100% tumour incidence (Guy et al., 1992), the parallelism with the human luminal breast cancer subtype and

the tumour growth within its organ-specific microenvironment supported the choice of the MMTV-PyMT mouse model for the purpose of this study.

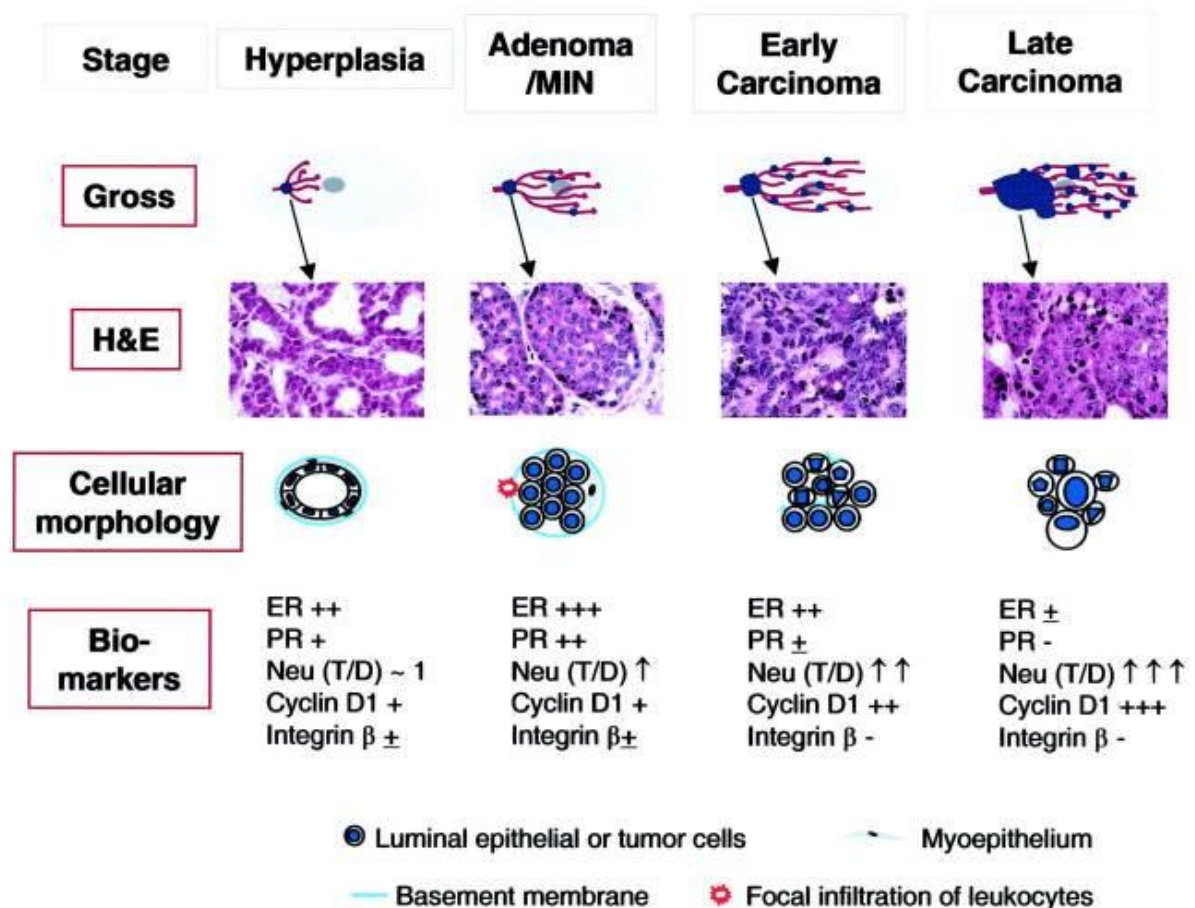


Figure 1.2. Mammary tumour development in the MMTV-PyMT mouse model of breast cancer.

The oncoprotein middle T antigen induces the spontaneous formation of the mammary tumour in the MMTV-PyMT mouse model of breast cancer. Tumour progression goes through four stages, such as hyperplasia, adenoma, early carcinoma and late carcinoma, which resemble the progression of the human disease, both from a morphological and a biomarker point of view. Abbreviations: ER, Oestrogen Receptor; H&E, Haematoxylin and eosine; PR, Progesterone Receptor. Figure taken from (Lin et al., 2003)

1.3 APPROACHES TO DECIPHER CANCER METABOLISM

1.3.1 Tools for metabolic analyses

Metabolism derives its name from the Greek *metabolé* (= change) indicating the enzyme-driven chemical conversion of metabolites, which are defined as low molecular weight organic and inorganic compounds produced through catabolic and anabolic reactions. They constitute, together with genes, transcripts and proteins, all the building blocks of biological systems (Dunn et al., 2011). Hence, in order to study metabolism one needs to identify and quantify metabolites and metabolic reactions. Any alterations in each of the biological components (gene, RNA and protein), as well as changes in the environment, are reflected downstream in the metabolic compartment, therefore the analysis of metabolism represents the most complete and up-to-date readout of a phenotype (Dunn et al., 2011). With the addition of cancer metabolism reprogramming as one of the fundamental cancer hallmarks by *Hanahan and Weinberg* (*Hanahan and Weinberg, 2011*), advances have been made also in the analytical technologies used to analyse metabolism, such as Nuclear Magnetic Resonance (NMR) spectroscopy and mass spectrometry (MS) (Pan and Raftery, 2007, Dunn et al., 2011). In the context of screening a large panel of all metabolites present in a system (the metabolome), it is often called metabolomics (Dunn et al., 2011, Liu et al., 2011). One can choose two different types of workflow, based on the aim of the experiment: targeted studies and metabolic profiling. Metabolic profiling consists of an untargeted analysis (hundreds or thousands of metabolites) with no *a priori* information about the composition of the sample, allowing a hypothesis-generating analysis of the dataset (Dunn et al., 2011). On the contrary, targeted studies look at a specific number

of functionally related metabolites. In this case, the studies are carried out to test a previously formulated hypothesis on metabolites already known (Dunn et al., 2011).

1.3.1.1 NMR spectroscopy

NMR spectroscopy is a powerful technique that offers high reproducibility and the possibility of quantifying metabolites, together with the identification of individual constituents of a metabolite mixture, requiring minimal sample preparation (Griffin and Shockcor, 2004, Dunn et al., 2011). Moreover, the sample does not interact directly with the instrument avoiding any sample alteration or damage (Dunn et al., 2011). However, NMR spectroscopy is a relatively insensitive technique, especially when compared to MS, and requires a high concentration of metabolites to reach a reliable detection and quantification (Dunn et al., 2011, Pan and Raftery, 2007). The simplest NMR acquisition method is the one-dimensional (1D) ^1H spectrum (Claudino et al., 2007), although this type of spectrum derived from a complex mixture is often highly crowded making the correct identification of a compound difficult. Recently, great improvements in sensitivity and resolution have been achieved, in part with two-dimensional (2D) methods such as HSQC (Heteronuclear Single Quantum Correlation), TOCSY (Total Correlation Spectroscopy) and JRES (*J*-resolved) (Keun et al., 2002, Viant, 2003, Ludwig and Viant, 2010), providing a greater dispersion of the signals by adding a second dimension. Sensitivity is also increased in part thanks to the introduction of cryoprobes, that greatly improved the signal to noise (Keun et al., 2002, Dunn et al., 2011).

1.3.1.2 Mass spectrometry

The most often used MS instruments for metabolomics studies are time-of-flight (TOF), quadrupole and hybrid MS (Dunn et al., 2011). Usually the detection step is preceded by a chromatographic separation of the metabolites that can be performed by gas and liquid chromatography (GC and LC respectively), and capillary electrophoresis (CE). While GC-MS is limited to volatile compounds, LC and CE are characterised by a broader applicability (Pan and Raftery, 2007). Compared to NMR spectroscopy, MS has some inherent advantages, such as high sensitivity, fast-scanning times, high mass resolutions, mass accuracy, and the possibility to identify metabolites. At the same time there are some disadvantages: reproducibility is not great because of the physical interaction between the sample and the instrument, that can cause alterations of responses (Dunn et al., 2011). This methodology is mainly applied to targeted studies where the use of standards help the identification and quantification of metabolites in the sample, while it is more difficult to obtain an automated and high-throughput identification necessary for metabolic profiling studies (Dunn et al., 2011). Recently, untargeted analysis has been taken with the application of high-resolution mass spectrometry (HRMS) (Liu et al., 2014). Moreover, reversed-phase- (RP) and hydrophilic interaction liquid chromatography- (HILIC) ultra-performance liquid chromatography- (UPLC) -MS techniques have been recently successfully combined for the untargeted metabolic profiling of diseased cardiac tissue (Vorkas et al., 2015).

1.3.2 Tools for metabolic flux analysis

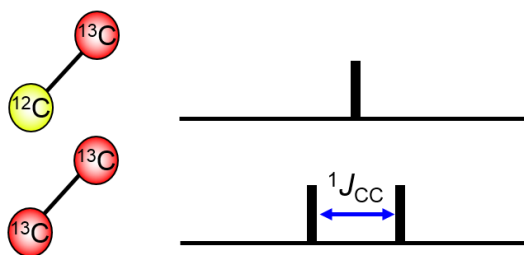
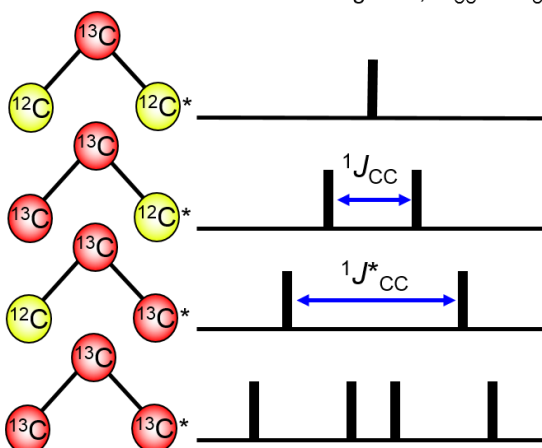
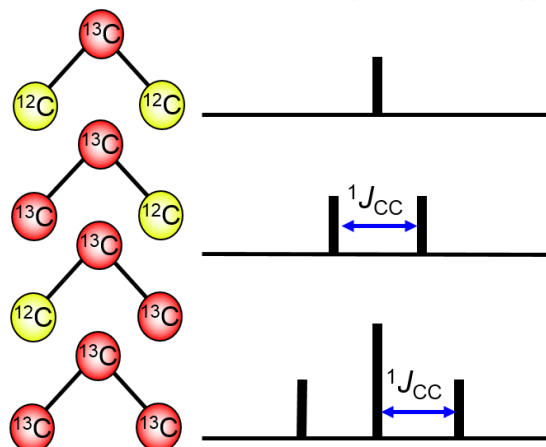
The steady-state quantification of the cellular metabolite concentration is only a static measure that often does not correctly reflect the metabolic alterations happening in the

system and that provides little information on underlying metabolic mechanisms. Metabolic flux analysis (MFA) instead, offers a highly dynamic measure of metabolites at different time points (Wiechert, 2001), helping to understand which alterations are causing a disease (Walther et al., 2012). Although the classical approach to studying pathway fluxes has been through the use of radioactive labelled metabolites (e.g. ^3H , ^{14}C) (Liedtke et al., 1992, Giroix et al., 2002, Nishimura and Kimura, 1965), the use of stable isotopes, i.e. ^{13}C and ^{15}N , is now more popular (Dunn et al., 2011). The commonly-used ^{13}C stable isotope is particularly useful due to the non-labile nature of carbons in eukaryotic organic molecules and the prevalence of carbon-containing metabolites in our cells (Wiechert, 2001, Hiller and Metallo, 2013, Lane et al., 2009, Lane et al., 2011). In order to obtain flux information, cells or tissues are exposed to a nutrient (i.e. glucose) that is enriched in one or more heavy, non-radioactive atoms, and the resulting metabolites into which the isotope is incorporated are analysed. These data from this kind of study can be used to estimate intracellular fluxes and map out pathways used (Wiechert, 2001, Metallo et al., 2009). When the analysis of the different isotopomers is combined into a metabolic profiling approach, this is better defined as Stable Isotope-Resolved Metabolomics (SIRM) (Lane et al., 2011). The importance of the choice of the tracer most suitable for the research purpose has been highlighted by *Metallo et al.*, given that this would determine which pathways one will be able to decipher. Interestingly, their approach evidenced $[1,2-^{13}\text{C}]$ glucose as the best tracer for central carbon metabolism (Metallo et al., 2009). Afterwards, *Crown et al.* proposed a new computational concept for the selection of optimal ^{13}C -tracers termed elementary metabolite units (EMU) decomposition and suggested that $[2,3,4,5,6-^{13}\text{C}]$ glucose can be used to probe the oxidative branch of the PPP (oxPPP)

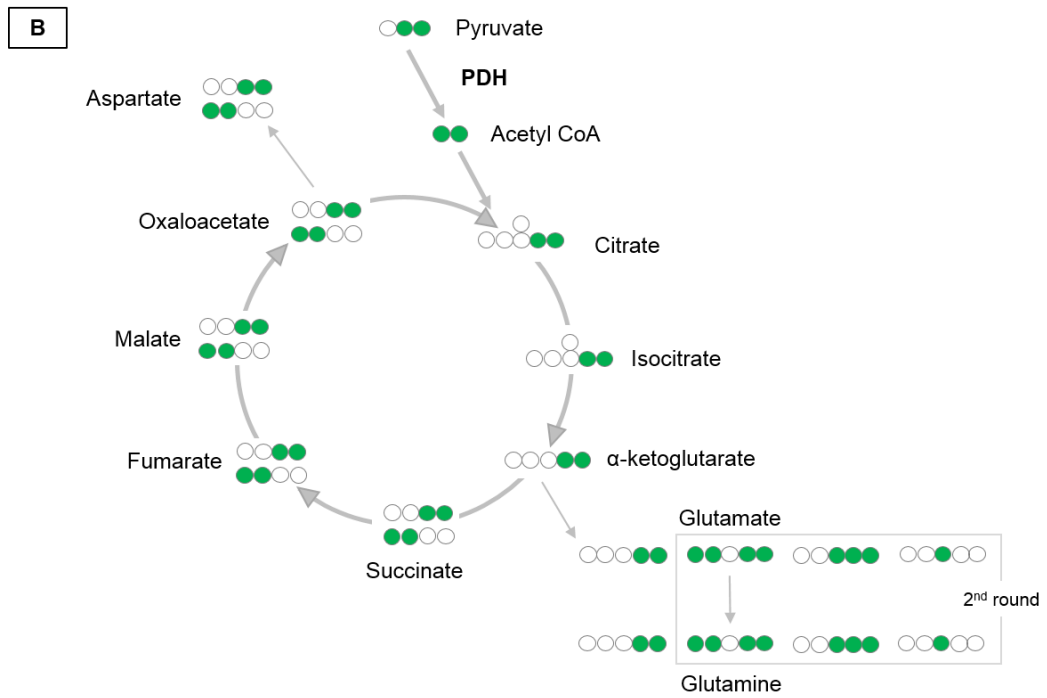
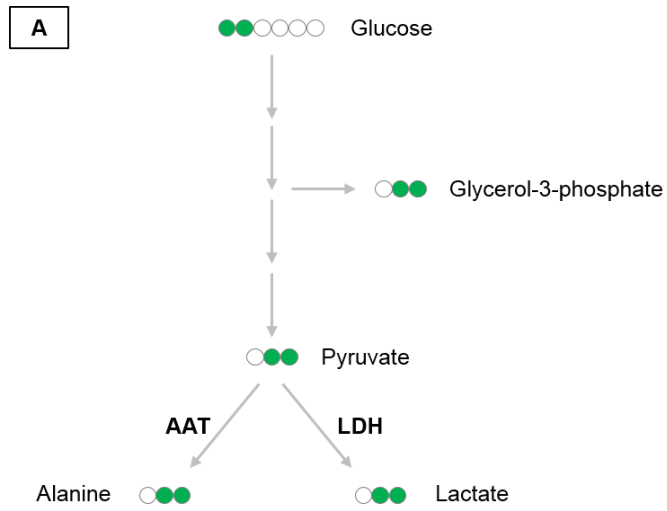
and [3,4-¹³C]glucose for elucidating flux via PC (Crown et al., 2012). 2D ¹H-¹³C-HSQC NMR spectra can provide information on site-specific label incorporation into a range of metabolites and hence on the metabolic pathway usage based on the analysis of the different ¹³C-isotopomers arising from the use of the labelled tracer by cellular metabolic pathways (Szyperski et al., 1996, Günther et al., 2015). In fact, the analysis of multiplet patterns visible in 2D ¹H-¹³C-HSQC spectra arising from the ¹J_{CC} coupling spin-spin coupling of adjacent ¹³C-atoms provides unique and site-specific information about which carbons are labelled in a certain molecule (Szyperski et al., 1999). CH_x-CH_x structures have a typical coupling constant of 42-48 Herz (Hz), while CH_x-COOH fragments demonstrate a coupling constant of 50-60 Hz (Figure 1.3), making them reasonably simple to differentiate between, given a high enough spectral resolution. HSQC spectra benefit from an increased sensitivity compared to the previously used 1D directly observed ¹³C NMR spectra, owing to the acquisition of protons, although at the expense of long measuring times, as the incremented ¹³C-dimension needs to be sampled with a large number of increments in order to resolve ¹J_{CC} couplings in the order of 30Hz. ¹³C-MFA can also be carried out using MS data where the presence of ¹³C atoms introduces a shift in the mass compared to the unlabelled metabolite; the different isotopomers of a molecule are usually indicated as m+n (n= number of different labelled carbons). The analysis of the isotopomer distribution as a consequence of metabolic conversion of a labelled precursor has been termed Mass Isotopomer Distribution Analysis (MIDA) and provides a readout of metabolic pathway usage (Ahmed et al., 2013). As previously mentioned, [1,2-¹³C]glucose has been identified as the most reliable probe for central carbon metabolism (Metallo et al., 2009), therefore it has been chosen as the preferred tracer throughout this thesis.

Specific isotopomer patterns arise following this ^{13}C -labelled substrate catabolism in the cell can be recognised via NMR spectroscopy as illustrated in Figure 1.4. Once $[1,2-^{13}\text{C}]$ glucose is transported into the cell, it is metabolised through glycolysis, producing the end-product $[2,3-^{13}\text{C}]$ pyruvate, which is then reduced to $[2,3-^{13}\text{C}]$ lactate by the LDH enzyme, or converted to $[2,3-^{13}\text{C}]$ alanine by the alanine aminotransferase (AAT) enzyme (Figure 1.4A). Glycolytic intermediates can also be used to fuel other important biosynthetic pathways, for example $[2,3-^{13}\text{C}]$ dihydroxyacetone phosphate is converted to $[2,3-^{13}\text{C}]$ glycerol-3-phosphate (Figure 1.4A) involved in lipid synthesis. $[2,3-^{13}\text{C}]$ pyruvate can be further oxidised into the TCA cycle after being converted to $[1,2-^{13}\text{C}]$ acetyl CoA by the PDH enzyme (Figure 1.4B). This labelled acetyl CoA is then condensed with the oxaloacetate to produce $[4,5-^{13}\text{C}]$ citrate, subsequently metabolised in $[4,5-^{13}\text{C}]$ isocitrate, $[4,5-^{13}\text{C}]$ α -ketoglutarate, $[1,2-^{13}\text{C}]/[3,4-^{13}\text{C}]$ succinate (being a symmetric molecule, these two isotopomers are identical), $[1,2-^{13}\text{C}]/[3,4-^{13}\text{C}]$ fumarate, $[1,2-^{13}\text{C}]/[3,4-^{13}\text{C}]$ malate and $[1,2-^{13}\text{C}]/[3,4-^{13}\text{C}]$ oxaloacetate (Figure 1.4B). TCA cycle intermediates can also be employed as anabolic precursors for different biosynthetic pathways. In fact, amino acids such as glutamate and aspartate are produced from α -ketoglutarate and oxaloacetate respectively. In the case of glutamate, different isotopomers are easily detected based on the number of rounds in the TCA cycle. For instance, $[4,5-^{13}\text{C}]$ α -ketoglutarate in the first round is converted to $[4,5-^{13}\text{C}]$ glutamate, while the second round can give rise to $[1,2,4,5-^{13}\text{C}]$ glutamate, $[3,4,5-^{13}\text{C}]$ glutamate and $[3-^{13}\text{C}]$ glutamate depending on labelled or unlabelled pyruvate being used (Figure 1.4B). All these glutamate isotopomers can be aminated to produce labelled glutamine (Figure 1.4B). An alternative entry-point of $[2,3-^{13}\text{C}]$ pyruvate into the TCA cycle is represented by its carboxylation to $[2,3-^{13}\text{C}]$

^{13}C]oxaloacetate by the PC enzyme (Figure 1.4C), which, condensed with unlabelled acetyl CoA, gives rise to [2,3- ^{13}C]citrate, [2,3- ^{13}C]isocitrate, [2,3- ^{13}C] α -ketoglutarate, while succinate, fumarate and malate are the same as before. [2,3- ^{13}C]oxaloacetate and [2,3- ^{13}C] α -ketoglutarate are then converted to [2,3- ^{13}C]aspartate and [2,3- ^{13}C]glutamate respectively (Figure 1.4C). An alternative pathway that uses glycolytic intermediates is the PPP. As soon as labelled glucose is phosphorylated to [1,2- ^{13}C]glucose-6-phosphate, this metabolite can be diverted into the oxidative branch of the PPP where it is oxidised to [1,2- ^{13}C]6-phosphogluconate, further decarboxylated to [1- ^{13}C]ribulose-5-phosphate (Figure 1.4D). The following steps belong to the non-oxidative branch of the PPP, where a series of reactions lead to the production of [1- ^{13}C]ribose-5-phosphate, that is used in nucleotide synthesis, and [1- ^{13}C]fructose-6-phosphate and unlabelled glyceraldehyde-3-phosphate that are glycolytic intermediates. If [1- ^{13}C]fructose-6-phosphate is then further metabolised in the glycolysis, it will result in the production of [3- ^{13}C]pyruvate, [3- ^{13}C]alanine and [3- ^{13}C]lactate (Figure 1.4D).

A: Terminal ^{13}C atomB: ^{13}C -atom embedded in a C3-fragment, $^1J_{\text{CC}} \neq ^1J_{\text{CC}}^*$ C: ^{13}C -atom embedded in a C3-fragment (equal $^1J_{\text{CC}}$)**Figure 1.3. Multiplet patterns derived from adjacent ^{13}C atoms.**

Adjacent ^{13}C atoms in a molecule result in typical scalar coupling constants (J_{CC}) that give information on the fragment structure and on the precise position of the ^{13}C -labelled atom. $\text{CH}_x\text{-CH}_x$ fragments have a typical coupling constant of 42-48 Hz, while a 50-60 Hz coupling is typical for $\text{CH}_x\text{-COOH}$ fragments. Figure taken from (Günther et al., 2015).



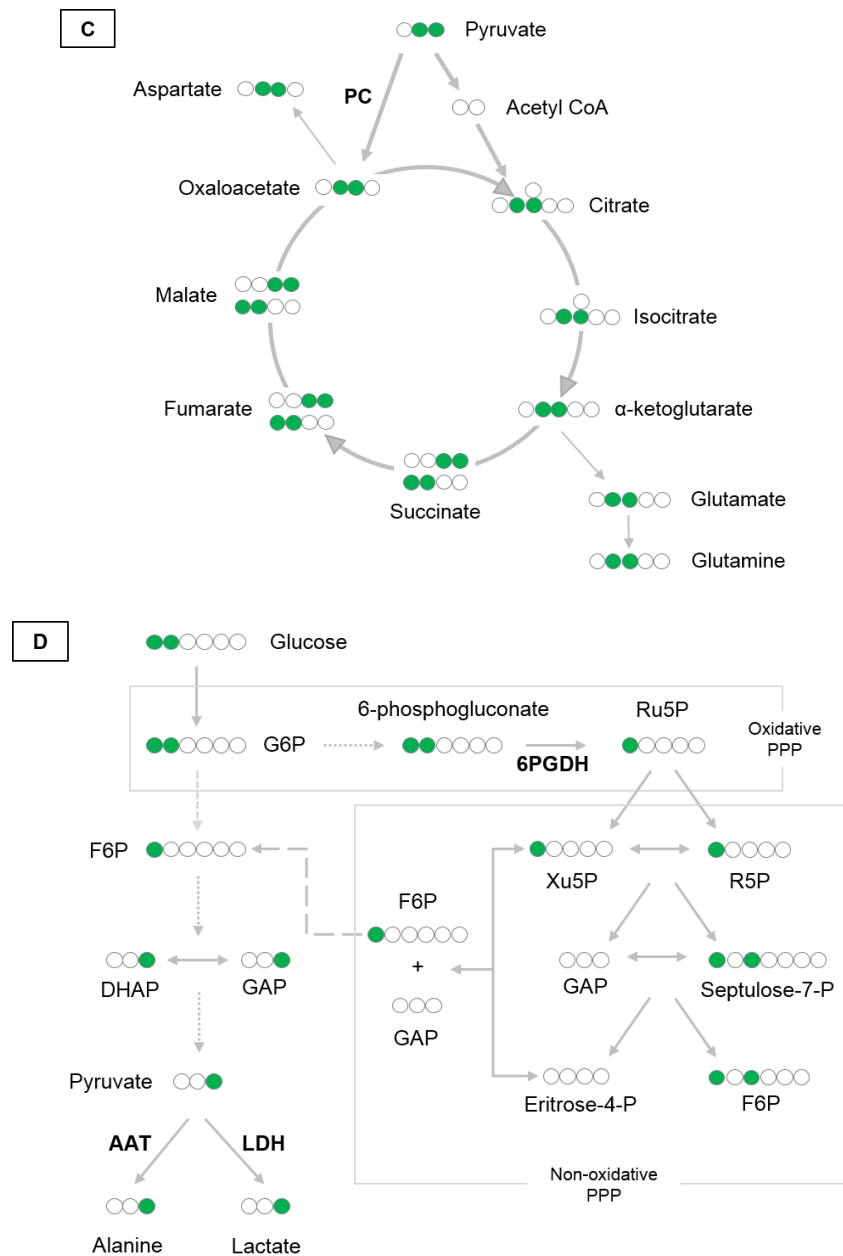


Figure 1.4. ^{13}C isotopomer patterns following $[1,2-^{13}\text{C}]$ glucose catabolism.

Illustration showing schematic $[1,2-^{13}\text{C}]$ glucose catabolism through glycolysis (A), TCA cycle via PDH activity (B), TCA cycle via PC activity (C), and PPP (D), arising in different metabolite isotopomers detectable by NMR spectroscopy. Abbreviations: 6PGDH, 6-phosphogluconate dehydrogenase; AAT, alanine aminotransferase; DHAP, dihydroxyacetone phosphate; GAP, glyceraldehyde-3-phosphate; F6P, fructose-6-phosphate; G6P, glucose-6-phosphate; LDH, lactate dehydrogenase; PDH, pyruvate dehydrogenase; PC, pyruvate carboxylase; PPP, pentose phosphate pathway; R5P, ribose-5-phosphate; Ru5P, Ribulose-5-phosphate; Xu5P, xilulose-5-phosphate.

1.3.2.1 ^{13}C -MFA in cancer cells

In vitro ^{13}C -MFA studies aimed at understanding cancer metabolism have been conducted mainly on cancer cell lines, such as melanoma (Scott et al., 2011), renal cancer (Metallo et al., 2012, Mullen et al., 2012), pancreatic ductal adenocarcinoma (Lee et al., 2004), glioblastoma (Wise et al., 2011), and leukemia (Miccheli et al., 2006, Boren et al., 2001) cells.

Among the wide plethora of *in vitro* ^{13}C -MFA studies, we will narrow down the focus to few studies conducted on breast cancer cells, being this type of tumour the main focus of this thesis. As described in section 1.2.4, previous studies have demonstrated a link between metabolic reprogramming and breast cancer. One tracer-based investigation of central carbon metabolism using $[\text{U-}^{13}\text{C}]$ glucose evidenced increased flux through most of the central pathways (i.e. PPP, TCA cycle, proline and glutathione synthesis) in order to support cellular transformation (Richardson et al., 2008), while increased glycolytic flux was observed in H-ras transformed breast cancer cells occurring already in early stages of tumour progression (Zheng et al., 2015). ^{13}C -MFA has also been exploited to unravel the mechanisms underpinning estradiol-induced breast cancer cell growth, involving increased flux through biosynthetic pathways as a consequence of increased glucose and glutamine consumption (Forbes et al., 2006). Despite the studies cited above, the application of ^{13}C -MFA to investigate breast cancer metabolism is still poor.

1.3.2.2 *In vivo* ^{13}C -MFA

Despite the great utility of the *in vitro* models to investigate basic mechanisms of cellular metabolism, they do not mimic real tissue complexity and physiology, requiring

the introduction of *in vivo* models (i.e. animals and humans). However, the experimental setup for flux analysis in animals is more complex and the degree of experimentally controllable conditions more limited (Metallo and Vander Heiden, 2013). For instance, while feeding cells *in vitro* with labelled substrates only requires the addition of a ^{13}C -labelled tracer in the growth medium, the administration of labelled tracers *in vivo* is much more challenging. In fact, the protocol for the administration of metabolic precursors such as glucose requires optimisation for each *in vivo* model and for the tissue of interest in order to observe label incorporation into a meaningful pool of metabolites. Ayala *et al.*, addressed this issue suggesting methods for standardised procedures in mice, focusing in particular on the parameters one needs to take care of when investigating glucose metabolism, as potential source of inter-animal variability: animal-strain, age, sex, diet, use of anaesthesia, dark/light cycles, fasting and route of glucose administration (Ayala *et al.*, 2010). The latter is of particular interest for the purpose of this thesis. Two main ways of administering substances exist: the enteral or the parenteral routes (Turner *et al.*, 2011). When the administration is given directly to the digestive system (enteral), substances can be altered and digested by the juices and the enzymes in the stomach and absorption can be influenced as well depending on food presents in the stomach (Shimizu, 2004). Moreover, glucose administration via oral route would induce an incretin hormone response that causes insulin release (Ayala *et al.*, 2010). This method therefore represents the least recommended for metabolic studies. Parenteral routes instead are reached using either injections (mainly sub-cutaneous, intraperitoneal and intravenous routes) or infusions (Shimizu, 2004, Turner *et al.*, 2011). The incretin response in fact can be avoided when glucose is administered via either intraperitoneal (i.p.) or intravenous (i.v.) injection

(Andrikopoulos et al., 2008, Ahren et al., 2008). However, i.p. injection has inherent risks, e.g. the piercing of visceral organs (Arioli and Rossi, 1970), although it is less technically demanding compared to the i.v. injection route, especially when working with small laboratory animals (Wong et al., 2011). Mice represent the preferred model for most *in vivo* studies, but there are still very few reports showing the application of labelled tracers in humans (Lane et al., 2009, Fan et al., 2009, Maher et al., 2012).

The application of ^{13}C -MFA on pre-clinical models led to interesting discoveries about the metabolic phenotype of various type of cancers. In particular, PC activity emerged as a unique trait for human lung cancer compared to normal lung tissue (Fan et al., 2011). Furthermore, the fate of glucose and glutamine in liver cancer has been shown to depend upon the expression of Myc and MET (Yuneva et al., 2012). Another interesting study showed active mitochondrial oxidative phosphorylation in human glioblastoma (Marin-Valencia et al., 2012). The high potential of the ^{13}C -MFA approach in uncovering *in vivo* metabolic alterations should therefore be further exploited.

1.4 AIM OF THE THESIS

It is increasingly clear that cancer presents altered metabolism under many different aspects, giving a strong rationale for the investigation of cancer cell metabolism as a readout of cellular phenotype (Cantor and Sabatini, 2012, Dang, 2012). The overall aim of this thesis was to study the metabolic phenotype of residual cells in a breast cancer cell line and a breast cancer mouse model, after docetaxel treatment. The approach used in this thesis can be defined as “targeted”, looking specifically at the polar fraction of cellular metabolic extracts (Dunn et al., 2011). Beyond a standard approach of quantifying metabolite levels, a tracer-based approach was used where [1,2-¹³C]glucose was given as a metabolic precursor (¹³C-metabolic flux analysis, ¹³C-MFA).

The objectives of this thesis were the following:

- to establish an *in vitro* model of residual breast cancer after docetaxel treatment,
- to establish an *in vivo* model of residual mouse mammary tumour after docetaxel treatment,
- to conduct an *in vitro* and *in vivo* quantification of the polar metabolites in the residual breast tumour after docetaxel treatment,
- to investigate pathway usage in a breast cancer cell line using ¹³C-MFA,
- to develop a method for the administration of ¹³C-labelled glucose to a mouse model, aimed at investigating metabolic pathways used in residual mouse mammary tumours, using ¹³C-MFA and gene expression analysis,
- to explore *in vitro* the ability of residual breast cancer cells to result in tumour relapse

CHAPTER 2

MATERIALS AND METHODS

2.1 BREAST CANCER CELL LINE MODEL

The MCF-7 breast cancer cell line (ATCC) was maintained in high glucose Dulbecco's Modified Eagle Medium (DMEM, HyClone), supplemented with 10% fetal bovine serum (HyClone) and L-glutamine (2 mM, HyClone). The cells were cultured in a humidified incubator at 37 °C and 5% CO₂ and routinely passaged using a standard procedure: after media removal, adherent cells were washed with warm 1X Phosphate buffered saline, pH 7.4 (PBS, HyClone) and incubated with 0.05% Trypsin-EDTA in PBS (Gibco) at 37 °C. When the cells were completely detached from the dish, as assessed using light microscopy, trypsin was inactivated adding at least three volumes of complete media before sub-culturing the cells at a seeding density optimal for the experiment to be performed.

For cell growth in hypoxic conditions, cells were allowed to attach to the plate before being transferred to an H35 Hypoxystation (Don Whitley Scientific) at 37 °C in a humidified atmosphere of 1% O₂, 5% CO₂, balance N₂.

Cells were routinely tested for mycoplasma infection using the kit EZ-PCR (Biological Industries).

2.2 *IN VITRO* DOCETAXEL TREATMENT OF MCF-7 BREAST CANCER CELLS

2.2.1 Determining the optimal concentration of docetaxel

To determine the concentration of drug that resulted in 50% cell killing, MCF-7 cells were seeded in a 12-well plate at 3×10^4 cells per well, in normoxic or hypoxic conditions.

Docetaxel (Sigma) was dissolved in DMSO (Fisher Scientific) to make a 1 mM stock solution subsequently diluted in normal media to reach the treatment concentrations of 10, 50, 100 and 500 nM. Cells were also left untreated as control. Four hours post-treatment, Tax-containing medium was removed from the cells and replaced with fresh complete DMEM. Cell viability was determined 24 and 48 hours post-treatment via Sulforhodamine B colorimetric assay (SRB assay, see 2.2.4).

2.2.2 Time-course of docetaxel effect on MCF-7 cell growth

To monitor the drug effect over five days, MCF-7 cells were seeded at 3×10^4 cells per well onto a 6-well plate, treated in triplicate for 4 hours with the Tax concentration of 10 nM, or left in DMEM as control, in normoxia and in hypoxia. Afterwards, the treatment was replaced with fresh normal DMEM and cells left to grow. Cell growth was evaluated using an SRB assay at 24, 48, 72, 96 and 120 hours post treatment removal.

2.2.3 Glutathione synthesis inhibition during docetaxel treatment

To assess the efficacy of the inhibitor L-Buthionine-sulfoximine (BSO) in effectively reducing glutathione production, cells were seeded in 15-cm dishes at 3×10^6 cells per plate. A BSO (Sigma) 0.1 M stock solution was prepared in sterile distilled water, and diluted in DMEM immediately prior to cell treatment. One plate was treated with 1 mM BSO and one plate left untreated as control. Metabolites were extracted from cells (as described in 2.3.1) after 24 hours treatment, and the polar fraction was collected for analysis by NMR spectroscopy.

To investigate the additive effect of BSO and Tax treatment, MCF-7 cells were seeded in 6-well plates at 3×10^4 cells per well in triplicate. The day after, three wells were

fixed with 4% Trichloroacetic acid (TCA, final concentration) and used as time-zero cell density. The other wells were treated with 10 nM Tax for 4 hours or left in normal DMEM as control. After docetaxel removal, treated cells were incubated with 1 mM, 100 μ M BSO or normal DMEM. Untreated cells were left in normal media or treated with 1 mM or 100 μ M BSO only. All cells treated with 1 mM BSO were fixed after 24 hours, while the remaining were fixed 48 hours post-initial treatment, and stained using the SRB assay.

2.2.4 Sulforhodamine B colorimetric assay

In order to assess cells remaining after an experimental treatment, the SRB assay was used, where the cellular protein content, bound to the SRB dye, can be used as a surrogate to measure cell number. Cells at the experimental endpoint were fixed adding cold 20% TCA (v/v, Sigma) to the media in the wells in order to obtain a final TCA concentration of 4%, and were left for 30 minutes at 4 °C. Subsequently, media with TCA was washed off the fixed cells with tap water, and the plates were left to dry at room temperature overnight. The staining was performed adding sufficient amounts of 0.4% SRB (w/v, Sigma) in 1% acetic acid (Fisher) to cover the well surface and leaving it for 10 minutes at room temperature. The SRB solution was removed and unbound SRB washed off with four washes with 1% acetic acid. Plates were then left to dry overnight and protein-bound SRB was dissolved in 50 mM Tris (pH 8.8). The absorbance for 200 μ L of each well was measured in a 96 well plate using the FLUOstar Omega plate reader (BMG LABTECH) at 510 nm. The Tris-based solubilisation buffer alone was used as blank, in order to subtract the background absorbance from the experimental absorbance. The final sample absorbance value

was determined calculating the mean among the blank-corrected absorbances for each replicate.

2.3 RESIDUAL MCF-7 CELL CHARACTERISATION POST- DOCETAXEL TREATMENT

2.3.1 Metabolic analysis

For the metabolic analysis, MCF-7 cells were seeded at 1.2×10^6 cells for the control plate and at 5.5×10^6 for the treatment plate, one 15-cm dish per condition. Count plates were also seeded at the same time. The day after, cells were treated for 4 hours with 10 nM Tax or with normal DMEM as control, and left to recover for 48 hours in media after treatment removal. The morphology of residual and control cells was imaged using a Nikon ECLIPSE TS100 equipped with a QImaging Rolera-XR camera. Metabolites were then extracted from the media and cells using a methanol/chloroform/water protocol.

Briefly, medium was removed, and an aliquot from each plate (1.2 mL) was quenched with an equal volume of methanol. Cells were washed with ice-cold 1X PBS, and quenched with 1.2 mL of ice-cold methanol (Fisher) before collection by scraping into pre-chilled 15-mL tubes (Greiner bio-one). An equal volume of chloroform (Scientific Laboratory Supplies) was added to all the samples, the extracts vigorously shaken at 4 °C for 10 minutes and left on ice for 10 minutes. Finally, an equal volume of distilled water was added to the cell extracts and all the samples centrifuged at $1300 \times g$ for 15 minutes at 4 °C. Two distinct layers appeared at this stage, with a protein-containing interphase. 2 mL of cell extract- and 750 μ L of media-derived upper polar phase was

collected into 2-mL tubes (Eppendorf) and dried at 2000 rpm using a Centrifuge for vacuum Concentrator (SCANVAC).

2.3.2 Metabolic flux analysis

To perform MFA, residual and control cells were cultured in glucose-free, phenol red-free DMEM (Sigma) with the addition of 10 mM [1,2-¹³C]glucose (Sigma) or unlabelled glucose (Sigma) as control. After 6 hours of incubation, metabolites were extracted from the cells and the media following the protocol previously described (see 2.3.1).

2.3.3 Establishment of residual clones

Cells were seeded onto 6-well plates at 3×10^4 cells/well and treated the day after with 10 nM Tax for four hours as previously described. After treatment removal, residual cells were left to recover in normal media until they resumed proliferation and were subsequently further expanded. The same experiment was performed three times and the regrowth cells were named Clone 1, Clone 2 and Clone 3. However, further experiments were carried out only on Clone 1 and Clone 2.

2.3.4 Growth curves

Cells were seeded in triplicate in 6-well plates at 3×10^4 cells per well. In order to determine growth parameters, cells were trypsinised and counted using a Neubauer chamber (Immune systems) daily for four days. Data from the exponential growth phase (between day 2 and day 4) were then used to calculate the population doubling time (dt) using the following formula (ATCC):

$$Dt = t \cdot \ln 2 / \ln(Cf/Ci)$$

Where t is the duration time; C_f is the final number of cells and C_i is the initial number of cells.

2.3.5 Western blotting

2.3.5.1 Sample preparation

MCF-7 control (0.4×10^6 /plate), 10 nM Tax treated (1.8×10^6 /plate), Clone 1 and Clone 2 (both 1×10^6 /plate) cells were seeded onto 10-cm dishes and harvested after 48 hours by scraping into 1 mL ice-cold RIPA buffer (50 mM Tris-HCl pH 8.0, 150 mM NaCl, 1% Triton X-100, 0.1% SDS, 0.5% sodium deoxycholate) with 1X Protease Inhibitor Cocktail (Sigma) and 10 mM NaF (Sigma). Complete cell lysis was achieved by incubation on ice for 30 minutes. Samples were centrifuged at $14000 \times g$ for 15 minutes at 4°C and supernatants transferred to a new tube. Protein quantification was performed using Pierce bicinchoninic acid (BCA) Protein Assay kit (Thermo scientific). Briefly, an aliquot of each protein sample was diluted 1:4 in dH_2O and $10 \mu\text{L}$ added to a well of a 96-well plate in triplicate before adding $200 \mu\text{L}$ of BCA working reagent (reagent A: reagent B, 50:1) to each well. The plate was then incubated at 37°C for 30 minutes, and the absorbance at 562 nm measured on the FLUOstar Omega plate reader (BMG LABTECH). Sample protein concentration was determined based on a Bovine Serum Albumin (BSA) standard curve. Lysates were then diluted to the required concentration in 2X Laemmli buffer (Sigma) and dH_2O , and heated to 100°C for 10 minutes.

2.3.5.2 Protein separation and transfer

Size-based protein separation was performed through SDS PAGE (sodium dodecyl sulphate polyacrylamide gel electrophoresis), using the Mini-PROTEAN Tetra System (BIO-RAD). 10% resolving gels and 5% stacking gels were prepared following the Laemmli method (Laemmli, 1970). Once the gel apparatus was assembled, the tank was filled with 1X running buffer (25 mM Tris/192 mM Glycine/0.1 % SDS, Geneflow) and lysates loaded into wells within the stacking gel (9 - 15 µg of total protein/well) next to a molecular weight ladder. Samples migration was carried out at constant voltage: 80V through the stacking gel, and then 100-150V until the migration front reached the bottom of the gel.

Transfer onto a nitrocellulose blotting membrane (GE Healthcare) was performed using the Mini Trans-Blot Cell (BIO-RAD) in wet conditions. The assembled sandwich was immersed in 1X transfer buffer (20 mM Tris/150 mM Glycine with 20% methanol) and transfer allowed for 1 h 15 minutes at constant voltage (100V).

2.3.5.3 Protein detection

Non-specific binding of antibodies to the membrane was blocked by incubation with 5% milk (non-fat skimmed milk powder, 5% w/v, Marvel) in PBST (1X PBS with 0.1% Tween-20) at room temperature for 1 hour on a rotating platform. Subsequently, the blocked membrane was incubated overnight at 4 °C with the specific primary antibody (see Table 2.1) diluted in 1% milk/PBST. After washing the membrane for 25 minutes in PBST, the relevant horseradish peroxidase (HRP)-conjugated secondary antibody (1:4000 in 1% milk/PBST, Cell Signalling) was added for 1 hour at room temperature with shaking. The membranes were then washed 3 times for 10 minutes each in PBST

before protein detection with ECL Prime Western Blotting Detection Reagent (GE Healthcare), onto Amersham Hyperfilm ECL (GE Healthcare).

Antigen	Dilution	Secondary	Supplier
p70 S6K	1:1000	α -rabbit	Cell Signalling
Phospho-p70 S6K (Thr389)	1:1000	α -rabbit	Cell Signalling
β -actin	1:2000	α -mouse	Sigma

Table 2.1. List of primary antibodies used in this thesis.

2.4 MMTV-PYMT: TRANSGENIC MOUSE MODEL OF BREAST CANCER

MMTV-PyMT male mice on a FVB background were crossed to wild-type females to obtain heterozygous females to be used for the experiments, and heterozygous males for breeding purposes. Mice were group housed in temperature and humidity-controlled rooms on a 12-hour light-dark cycle with access to normal chow and water *ad libitum* in accordance with the Animals (Scientific Procedures) Act (1986). All procedures were performed under Dr Daniel Tennant's Project License number 30/2881 and my Personal License number I5A5EFA78. Tumour burden was assessed by palpation starting when the female mice were 8 weeks of age. Upon sacrifice, tumour volumes were determined measuring the two axes using a digital caliper and calculated using the formula: D (long diameter) $\times d^2$ (short diameter) $\times 0.52$ (Bai et al., 2009).

2.4.1 Genotyping

2.4.1.1 DNA extraction

Mouse ear-clips were used to extract DNA in order to determine the mouse genotype. Briefly, biopsies were lysed for 3 hours at 65 °C in 200 µL TNES buffer (10 mM Tris pH 7.5, 400 mM NaCl, 100 mM EDTA, 0.6% SDS) and 15 µL Proteinase K (Promega, from 10 mg/mL stock solution). Protein precipitation was aided by adding 6 M NaCl to obtain a 1.2 M final concentration prior to centrifugation of the lysates at 14000 x g for 15 minutes at 4 °C. Supernatants were transferred to clean 1.5 mL Eppendorf tubes and DNA precipitation was started adding two volumes of cold 100% ethanol (VWR chemicals) and mixing by inversion. Precipitated DNA was pelleted by centrifuging each sample at 14000 x g for 20 minutes at 4 °C. After removal of the supernatant, the DNA pellet was washed with 1 mL of 70% EtOH and centrifuged as above. The DNA pellet was then left to air-dry after ethanol removal, before being re-suspended in 50-500 µL (depending on pellet size) of 10 mM Tris buffer, pH 8, and incubated overnight at 37 °C. Extracted DNA was then quantified using a NanoDrop spectrophotometer (Thermo Scientific).

In some cases, the KAPA Express Extract kit (KAPA BIOSYSTEMS) was used for the DNA extraction. Briefly, each biopsy was lysed in 100 µL mix containing 2X KAPA Express Extract Buffer and 2U KAPA Express Extract Enzyme, at 75 °C for 40 minutes. The enzyme was inactivated at 95 °C for 5 minutes before spinning the extract down at 14000 x g for 1 minute. The DNA-containing supernatant could be used straightaway for PCR.

2.4.1.2 Amplification of the middle T antigen by PCR

50 ng of isolated DNA were used in the PCR reaction to assess the presence of the middle T antigen. Amplification of this specific gene was performed using the following primers (IMR0384/0385):

5'- GGA AGC AAG TAC TTC ACA AGG G -3'

5'- GGA AAG TCA CTA GGA GCA GGG -3'

The mastermix, set up on ice, contained 1X MyTaq Reaction buffer, 1 μ M of the primer mix (IMR0384/0385) and 3.125 U of MyTaq DNA Polymerase (Bioline) in a 12 μ L total reaction.

When extracting the DNA using the KAPA Express Extract kit, 1 μ L of sample was used for the PCR with the KAPA2G Robust HotStart kit (KAPA BIOSYSTEMS). The mastermix included 1X KAPA2G buffer A, 1.5 mM MgCl₂, 1X KAPA Enhancer 1, 0.2 mM each dNTP, 1 μ M of the primer mix (IMR0384/0385) and 0.5 U KAPA2G Robust HotStart DNA Polymerase in a 25 μ L total reaction. In both cases, the PCR was carried out under the following cycling conditions on a GeneAmp PCR System 9700 machine (Applied Biosystems):

initial denaturation	95 °C	3 min	
denaturation	95 °C	15s	} for 35 cycles
annealing	64 °C	1 min	
extension	72 °C	1 min	
	72 °C	2 min	
End	4 °C	∞	

2.4.1.3 Detection of the PCR product by agarose gel

The PCR products were subsequently visualised through agarose gel electrophoresis and the presence of the middle T antigen was identified with a 556 bp band in the gel. The 1.5% agarose gel was prepared by dissolving 0.75 g of agarose powder (Invitrogen) in 50 mL 1X TAE buffer (40 mM Tris acetate, 1 mM EDTA) and boiling it using a microwave. Once the agarose was dissolved, it was left to cool before the addition of ethidium bromide (0.5 µg/mL, Sigma) for the visualisation of DNA. The gel solution was then poured into a gel tray and allowed to polymerise with the appropriate comb to produce wells. Once set, the gel was placed in 1X TAE running buffer in a horizontal electrophoresis tank before 6 µL of PCR reaction and loading dye (3 µL of each PCR reaction, 1 µL of 6X loading dye (New England BioLabs) and 2 µL of ddH₂O) were loaded into the wells. A 100 bp DNA ladder (Invitrogen) was loaded next to the samples in order to determine approximate PCR product size. The gel was run at 100V for about 45 minutes at constant voltage, and the bands visualised using a 312 nm UV lamp (Spectroline) connected to a EDAS 290 camera (Kodak).

2.5 IN VIVO DOCETAXEL TREATMENT OF MOUSE MAMMARY

TUMOUR

Docetaxel treatment of mammary tumour was performed when the neoplasia was at the early carcinoma stage. Tax was freshly dissolved in polysorbate 80:ethanol (1:1, v/v) and diluted in 0.9% saline to 1 mg/ 100 µL prior to injection. The treatment schedule was chosen to mimic the clinical protocol applied to patients (Cancer Research UK, Korde et al., 2010). In fact, tumour-bearing females received two weekly doses of treatment, starting at 9 weeks of age, consisting in a single i.p. injection of

100 μ L of Tax (35 mg/kg) or 100 μ L of 0.9% saline as placebo per week. Mice were sacrificed via cervical dislocation at 11 weeks of age, one week after the last dose, mammary tumours were collected and flash-frozen in dry-ice for subsequent analysis. The cancer cells/tumour that survived and recovered from Tax treatment *in vivo* were defined as residual tumour.

2.5.1 Gene expression analysis

2.5.1.1 Extraction of total RNA

Total RNA was extracted from a piece of each of four tumours from placebo and four from Tax-treated animals, using the RNeasy Mini kit (Qiagen). Briefly, 25 mg of each tumour was homogenised into 600 μ L RLT buffer with β -Mercaptoethanol (Fisher Chemical, 10 μ L/mL of RLT buffer) using a Precellys®24 instrument with 2 x 20 seconds at 5000 rpm. The homogenate was then spun down at 19000 x g for 3 minutes and supernatant transferred to a 2-mL tube for RNA isolation.

One volume of 70% ethanol was added to the sample, mixed and transferred to an RNeasy spin column. Samples were centrifuged for 15 seconds at 8000 x g and the flow-through discarded. The column was washed with 350 μ L of buffer RW1 before sample treatment with 80 μ L of Dnase I from the RNase-Free DNase set (Qiagen, 10 μ L in 70 μ L buffer RDD) for 15 minutes at room temperature. The treatment was stopped applying another wash with 350 μ L of buffer RW1. Columns were centrifuged as before and flow-through discarded, followed by two washes with 500 μ L buffer RPE each time. After the last wash, the samples were centrifuged for 2 minutes at 8000 x g, and the column transferred to a new 2 mL collection tube and centrifuged for 1 minutes at 13000 x g to ensure the removal of all residual buffer. Finally, isolated RNA

was eluted into a clean 1.5 mL Eppendorf tube using 30 μ L of RNase-free water and RNA quality and quantity was determined as before.

2.5.1.2 RNA sequencing

The extracted total RNA was sent to Microsynth (Switzerland) to perform RNA sequencing. Firstly, the mouse tissue-derived total RNA was enriched for mRNA using a poly(A) tail-based method. Subsequently, a cDNA library was generated and sequenced using the Illumina NextSeq500 system. The reads were mapped to the UCSC mm10 reference sequence using TopHat, and counted using HTSeq (Anders et al., 2014). The differential gene expression analysis between the two conditions was carried out using the DESeq2 package performing Wald statistic. The p-values obtained were adjusted with the Benjamini & Hochberg test.

2.5.2 *In vivo* metabolic analysis

For metabolic analyses, mice were sacrificed and tumours collected and flash-frozen on dry-ice. Metabolite extracts were obtained from the frozen biopsies using a methanol/chloroform/water protocol. Tumours were homogenised into ice-cold methanol (1.7 mL/200 mg of tissue) using a Precellys®24 instrument with 2 x 20 seconds at 5000 rpm. The homogenate was transferred to a 15 mL polypropylene tube (Greiner Bio-One) and an equal volume of chloroform added. The subsequent steps used were the same as for cell extracts (see 2.3.1). A 1.36 mL aliquot of polar metabolites was dried from each sample for subsequent NMR spectroscopy analysis.

2.5.3 *In vivo* [1,2-¹³C]glucose flux

To determine the most suitable means by which to monitor glucose usage by the mouse mammary tumours, we needed to determine the best injection site and the best time point for tissue sampling.

To compare different injection sites, mice were divided in two cohorts: one cohort received bolus i.v. injection, while the other received bolus i.p. injection, of 100 μ L 1M unlabelled glucose in both cases. Mammary tumours were then collected 20 minutes post-glucose administration, extracted as above and metabolites identified and quantified by 1D-¹H NMR spectroscopy (see 2.6.2).

The sampling time point was evaluated administering a 100 μ L i.p. injection of 1M [1,2-¹³C]glucose to tumour-bearing mice and sacrificing them 10, 20, 30 or 45 minutes after injection. The percentage of [1,2-¹³C]glucose enrichment over time in the mammary tumour was then assessed using the 2D ¹H-¹³C-HSQC improved spectra (see 2.6.2).

Once the method had been established, it was possible to compare glucose metabolism between residual and untreated mammary tumours. One week following the second dose of Tax (or placebo) treatment, mice received 100 μ L i.p. injection of 1M [1,2-¹³C]glucose (Sigma) in 0.9% saline. Mice were then sacrificed 45 minutes (Tax-treated) or 30 minutes (placebo) post-labelled glucose injection by cervical dislocation. Mammary tumours were collected and flash-frozen in dry-ice, and underwent metabolites extraction as previously described (see 2.5.2). To analyse the ¹³C incorporation, a 1.36 mL aliquot of each polar extract was dried for NMR analysis, and a 340 μ L aliquot for GC-MS analysis.

2.5.4 GC-MS analysis

The GC-MS analysis was carried out in collaboration with Professor Marta Cascante (University of Barcelona).

Dried metabolites derived from residual or control mouse mammary tumours were re-suspended in 50 μ L of 2% methoxyamine–hydrogen chloride in pyridine (Sigma), used in prevention of multiple derivatives formation when silylation occurs in presence of enols, vortexed and shaken at 37 °C for 90 minutes. Samples were then derivatised adding 30 μ L of *N*-Methyl-*N*-*tert*-butyldimethylsilyltrifluoroacetamide (MBTSTFA) + 1% *tert*-Butyldimethylchlorosilane (TBDMCS) (Sigma) and incubating them at 55 °C for 1 hour. The derivatised polar metabolites were transferred to glass vials before being subjected to separation by gas chromatography on a 7890A System (Agilent Technologies) and then mass spectrometric detection of metabolites (5975C EI MSD with Triple-Axis detector [Agilent Technologies]). 1 μ L of derivatised sample was injected into the GC-MS with a split ratio of 1:10 (sample:helium) and metabolites were separated through an HP-5MS column (Agilent Technologies). Samples were ionised by Electron Impact (EI) and detected in selected-ion monitoring (SIM) mode based on their different retention time by a TOF mass analyser. Each sample was analysed twice. The mass peaks visualised were manually integrated using the MSD ChemStation software (Agilent Technologies). Results were corrected for ^{13}C natural abundance using an in-house macro.

2.6 NMR EXPERIMENTS

2.6.1 Sample preparation

Dried metabolites were re-suspended in 100 mM phosphate buffer (pH 7.0), 500 μ M Trimethylsilyl propanoic acid (TMSP), 10% deuterium oxide (D_2O) (60 μ L for cells and mouse-derived metabolites and 550 μ L for media-derived metabolites) for subsequent investigations via NMR spectroscopy. Samples were sonicated and vortexed to ensure efficient solubilisation of metabolites, before centrifugation at 13000 x g for 10 minutes. 35 μ L of resuspended metabolites were then transferred to a 1.7 mm NMR tube (Bruker Biospin) using a Gilson 215 Liquid handler robotic sample preparation system (Bruker Biospin).

2.6.2 NMR experiments

The sample-containing 1.7 mm NMR tubes were transferred to an automatic NMR sample-changing robot (SampleJet, Bruker Biospin). NMR data were acquired on a Bruker 600 MHz NMR spectrometer equipped with a 1.7mm cryogenic probe with z-axis pulsed field gradients running the Topspin 3.2 software interface.

Prior to acquisition, the spectrometer was locked on the D_2O signal, the probe was tuned and matched for the relevant channels (1H and ^{13}C) and shimmed using automated three-dimensional (3D) and 1D gradient-based TopShim procedures. All spectra were acquired at 300 K.

For the *in vitro* study, 1D- 1H and 2D 1H - ^{13}C -HSQC NMR spectra were collected with the following parameters:

- $1D$ - 1H spectra were acquired with 256 scans, 32768 data points, 16 dummy scans to reach a steady-state, a 4 seconds delay 1 and 2.28 seconds acquisition time. The solvent resonance was suppressed either using NOESY-presaturation (Wider et al., 1983) or excitation sculpting (Hwang and Shaka, 1995).
- HSQC spectra were acquired with 4096 data points in both dimensions, 8 steady-state scans and 2 transients per increment. Coherence selection was performed using gradients with the echo/anti-echo method. Suppression of the solvent resonance was enhanced using presaturation during the interscan relaxation delay (1.5 sec). The spectral width in the proton dimension was 13.0349 ppm, and 160 ppm in the carbon dimension.

For the *in vivo* study, additional spectra were acquired.

Besides the proton $1D$ spectra (as previously described for the *in vitro* work), an improved version of the $2D$ 1H - ^{13}C -HSQC spectra was acquired. In fact this was characterised by non-uniform sampling (NUS), acquired with 1024 data points in the direct dimension and 16384 data points in the indirect dimension (as a 30% sampling was performed, the number of actually acquired data points was 4915), 8 steady-state scans and 2 transients.

2.6.3 NMR data analysis

All NMR spectra were processed using the NMRLab software (Ludwig and Günther, 2011).

1D-¹H spectra

The free induction decay (FID) for each spectrum was apodised using a 0.3 Hz exponential line broadening and then zero-filled up to 128k data points prior to Fourier transformation. The resulting NMR spectra were then manually phase corrected. Different spectra acquired at the same time were aligned and referenced using the TMS signal, and baseline defects were corrected using a user defined linear-spline function (Ludwig and Günther, 2011). These processed spectra were then exported from NMRLab to Chenomx NMR suite 7.0 (Chenomx Inc., AB, Canada) where metabolites were assigned and quantified for each sample, using the TMS concentration as a reference. The concentration (mM) of each assigned intracellular metabolite was determined, then converted to total nmol of metabolite and subsequently normalised by the total cell number in order to obtain a nmol/cell quantity.

The formula used was the following:

$$\text{nmol/cell} = ((\text{mM} * 60 \mu\text{L}) * 1.2) / \text{total number of cells}$$

where 60 μL is the amount of phosphate buffer used to resuspend the dried metabolites before acquisition of NMR spectra (see 2.6.1), and 1.2 is the factor to obtain the total nmol in the total polar fraction (from a total polar fraction of 2.4 mL 2 mL were analysed: $2.4/2 = 1.2$, see 2.3.1).

The concentration (mM) of mouse mammary tumour-derived polar metabolites did not need further normalization as they were extracted from always the same amount of tissue.

Whereas for the media, the concentration (mM) of each metabolite obtained with Chenomx was converted to nmol/1.2 mL using the following equation:

$$\text{nmol}/1.2 \text{ mL} = 3.2 * (\text{mM} * 550 \mu\text{L})$$

where 1.2 mL is the volume of fresh or spent medium extracted for each sample, 550 μL is the amount of NMR phosphate buffer used to resuspend the dried metabolites. The nmols in 550 μL are representative of a fraction of the total polar extract (from a 2.4 mL of media-derived polar phase only a 750 μL -aliquot was analysed: $2.4/0.75 = 3.2$), it is therefore necessary to multiply the nmols by 3.2 to obtain the total nmols of polar metabolites extracted from the 1.2 mL aliquot of media. Once converted to the total nanomoles of metabolite in the fresh and spent medium (25 mL), it was possible to compare the initial nmols (nmol_i) with the final nmols (nmol_f) to determine uptake and secretion: $\Delta \text{nmol} = \text{nmol}_f - \text{nmol}_i$.

If $\Delta > 0$ = metabolite excreted; If $\Delta < 0$ = metabolite uptaken. At last, the nmol difference was normalised by the total cell number to obtain $\Delta\text{nmol}/\text{cell}$.

2D ^1H - ^{13}C -HSQC spectra

HSQC spectra acquired from MCF-7-derived samples underwent the following steps: suppression of the water resonance was enhanced by a convolution filter on the FID prior to apodisation with a squared cosine window function, zero filling up to 1024 data points for the direct dimension prior to Fourier transformation. The indirect dimension was apodised using a squared cosine window function and the data was zero-filled to 4096 data points before Fourier transformation. These 2D-NMR spectra were then manually phase corrected in both dimensions. Spectra were referenced on the alanine C(3) signal. Once processed, the metabolites in these HSQC spectra were assigned using the AssignTool in NMRLab (Ludwig and Günther, 2011), and the amount of ^{13}C -enrichment was calculated and obtained automatically through the HSQC report tool. Briefly, for each metabolite the peak intensities in the labelled spectra are divided by

the peak intensity in the unlabelled spectra to determine the ^{13}C enrichment; in case of multiplets in the ^{13}C -enriched spectra, all the peaks are added up to obtain the peak overall intensity. The taurine peak intensity was used for inter-experiments normalisation.

2D ^1H - ^{13}C -HSQC (with NUS)

These NMR spectra were processed to 1024 points in the direct dimension and 16384 points in the indirect dimension using the mddnmr/nmrpipe software (Delaglio et al., 1995, Orekhov and Jaravine, 2011) to reconstruct the 2D spectrum using a compressed sensing algorithm. Subsequently, they were phased using the NMRPipe software (Delaglio et al., 1995) and the phased spectra were opened in NMRLab where they were again referenced on alanine, and analysed.

For each peak, the multiplets were analysed with a quantum mechanical spin system simulation using the C++ and python based PyGamma NMR simulation library (Smith et al., 1994); once all the peaks of the metabolite of interest were simulated and fitted, a self-consistent approach was used to extract the ^{13}C isotopomers from the information in the HSQC spectra.

2.7 STATISTICAL ANALYSIS

When the number of replicates was higher than three, data normality distribution was tested by Kolmogorov-Smirnov test using GraphPad 5.0d software. Results are expressed as mean \pm standard error of the mean (SEM) except for data shown in box-and-whiskers where the median is calculated instead, and in scatter dot-plot where results are expressed as mean \pm standard deviation (SD). Unpaired, two-tailed

student's *t* test with 95% confidence intervals was used to compare groups using GraphPad 5.0d software. The p-values obtained using the Wald test on the differential gene expression analysis, were adjusted with the Benjamini & Hochberg test. In all cases, p-values < 0.05 were considered statistically significant.

CHAPTER 3

***IN VITRO* CHARACTERISATION OF
RESIDUAL BREAST CANCER
CELLS AFTER DOCETAXEL
TREATMENT**

3.1 INTRODUCTION

Improvements in early-stage detection and introduction of new therapies have contributed to the reduction in breast cancer mortality in recent years (Broeders et al., 2012, Gunsoy et al., 2014). Nevertheless, this type of tumour still represents the second most common cause of cancer-related death in women in the UK (2012).

Among the various possible therapeutic approaches for breast cancer, taxane-based treatment represents one of the most effective (Valero et al., 1995, Alken and Kelly, 2013), involving mainly the anti-microtubule agents paclitaxel and docetaxel, either as single agents or in combination with other drugs (Moulder and Hortobagyi, 2008, Kim et al., 2014, Zardavas and Piccart, 2015). The semisynthetic taxoid docetaxel, approved in 1996, represented the preferential second line treatment for locally advanced or metastatic breast cancer (Yalcin, 2013, Hassan et al., 2010). However, many patients do not reach complete remission of the disease or develop resistance to the drug (Chang et al., 2005), leading to the presence of residual breast cancer. In particular, it has been shown that the tumour that remains after docetaxel treatment is enriched in cells presenting tumour-initiating markers (Creighton et al., 2009). Therefore, this subpopulation of the original tumour represents a possible source of cancer relapse. Recurrence, together with resistance to therapy and metastasis, are the main factors contributing to cancer patient mortality. For these reasons, preventing the development of these situations is of seminal importance for increasing patient survival. In order to be able to do that, it is necessary to understand the biological advantage exploited by the breast tumour cells to survive docetaxel treatment. A number of *in vitro* studies have outlined the possible mechanisms of resistance to docetaxel, most of which include alterations in gene expression levels (Chang et al.,

2003, Chang et al., 2005, Korde et al., 2010, Tan et al., 2012, Ghanbari et al., 2014, Hu et al., 2014, Iwao-Koizumi et al., 2005). However, to our knowledge, none have examined at residual cell metabolism post-docetaxel. It is already well known that cancer cells undergo metabolic adaptations in order to survive and proliferate despite many adverse conditions during tumour growth (Tennant et al., 2009, Griffin and Shockcor, 2004, Ward and Thompson, 2012). These adaptations are mediated by changes in the metabolome, described as the sum of all the metabolites within a cell, which represents the most dynamic cellular component; able to respond to the requirements of the cell at any given time. This means that any alterations in the genome, proteome or microenvironment that requires a change in phenotype must be supported by a metabolic shift in order to occur.

Given all these premises, the *in vitro* metabolic response of residual breast cancer cells that survived docetaxel treatment will be investigated. This chapter will therefore be focused on the *in vitro* model, the MCF-7 breast cancer cell line, which is a well-established model of ER+ breast adenocarcinoma (Brooks et al., 1973, Levenson and Jordan, 1997, Holliday and Speirs, 2011), sharing markers with the luminal subtype A of human breast cancer (Holliday and Speirs, 2011).

3.2 MCF-7 RESPONSE TO DOCETAXEL TREATMENT

3.2.1 Determining the optimal concentration of docetaxel

The purpose of this study was to investigate residual breast cancer cells after Tax treatment. Hence, it was important to apply a drug concentration that did not cause death of all the cells used in the experiment, but allowed the survival of some of the original cell population, defined as residual cells (TAX). Therefore, was necessary to identify the concentration of docetaxel able to kill 50% of the cells in culture. In order to determine the MCF-7 dose-response to Tax treatment, cells were treated for 4 hours in normoxia (21% oxygen) and hypoxia (1% oxygen) with a range of drug concentrations from 10 nM to 500 nM (Morse et al., 2005, Sanli et al., 2002). The cytotoxicity effect was evaluated via SRB assay (see 2.2.4) at 24 and 48 hours post treatment removal, normalising the absorbance of the treated cells with the absorbance of the untreated control cells (Figure 3.1). We found that 10 nM Tax represented the concentration at which 50% viable cells remained in culture 48 hours post treatment removal, and was therefore defined as the optimal concentration for our purposes. Interestingly, no differences in cell viability were noted between normoxic and hypoxic treatment.

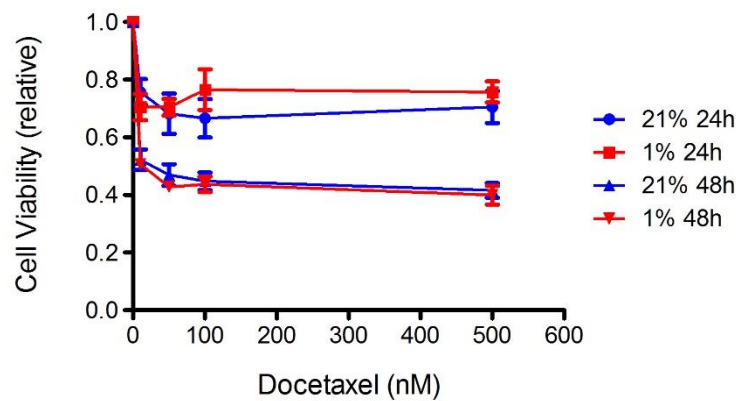


Figure 3.1. 10 nM is the Tax concentration able to kill 50% of the MCF-7 breast cancer cells in culture.

Graph representing MCF-7 breast cancer cells viability 24 and 48 hours following Tax treatment with 10, 50, 100 and 500 nM, in normoxia (21%) and hypoxia (1%), relative to normoxic and hypoxic untreated cells, determined through SRB assay. Data shown are average of four experiments \pm SEM. 10 nM is the Tax concentration able to kill 50% of the cells in culture, 48 hours post treatment removal.

3.2.2 Docetaxel time-course

The mechanism of action of docetaxel is through the stabilisation of polymerised microtubules therefore blocking cell division and proliferation (Herbst and Khuri, 2003, Cortes and Pazdur, 1995, Tankanow, 1998). In order to investigate if this is a long-term effect on the MCF-7 cells, we performed a time-course experiment to detect the proliferation behaviour of the cells several days after treatment. Cells were treated with the previously determined optimal Tax concentration (10 nM) or left untreated as control, in normoxia and hypoxia. Cell density was evaluated via SRB assay 24, 48, 72, 96, 120 hours post treatment removal (Figure 3.2). As expected, MCF-7 control cells proliferated less in hypoxia than in normoxia. The Tax treated cells did not show increase in cell number between the first and the fifth day post treatment. Given the

presence of dead cells in the media during these days (see Figure 3.3B and C), it is possible to infer that the stable protein content evidenced by SRB could derive from a balance between few cells proliferating and cells dying. However, the major part of these cells underwent a cell cycle arrest, in accordance with the Tax mechanism of action. Moreover, this experiment did not show any evidence of differential activity of the drug on cells under normoxia and hypoxia (as well as in section 3.2.1). For this reason, the subsequent *in vitro* experiments have been conducted in normoxic conditions only.

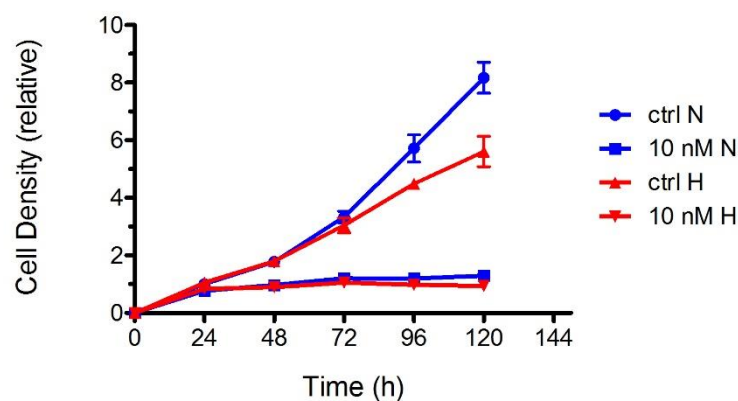


Figure 3.2. Tax inhibits MCF-7 cells proliferation for several days.

Curves showing MCF-7 cell density in normoxia and in hypoxia 24, 48, 72, 96 and 120 hours post Tax treatment with the 10 nM drug concentration. Results are average of three independent experiments \pm SEM, each value is relative to the 24 hours normoxic control. After four hours incubation with Tax, MCF-7 cells arrest their proliferation at least for the duration of the time-course experiment (five days).

3.3 RESIDUAL BREAST CANCER CELLS METABOLIC PHENOTYPE

3.3.1 Residual cells morphology

The MCF-7 breast cancer cells present an epithelial-like phenotype, characterized by polygonal cells in tight contact with each other, with well-defined boundaries (Figure 3.3A). Following treatment with Tax, cell morphology was altered: cells flattened, boundaries were less visible, and nuclei contained large inclusions that could be considered as multiple micronuclei (Figure 3.3B-C). These characteristics are suggestive of induction of Tax-mediated senescence as previously described (Ewald et al., 2010) and mitotic catastrophe (Morse et al., 2005, Portugal et al., 2010).

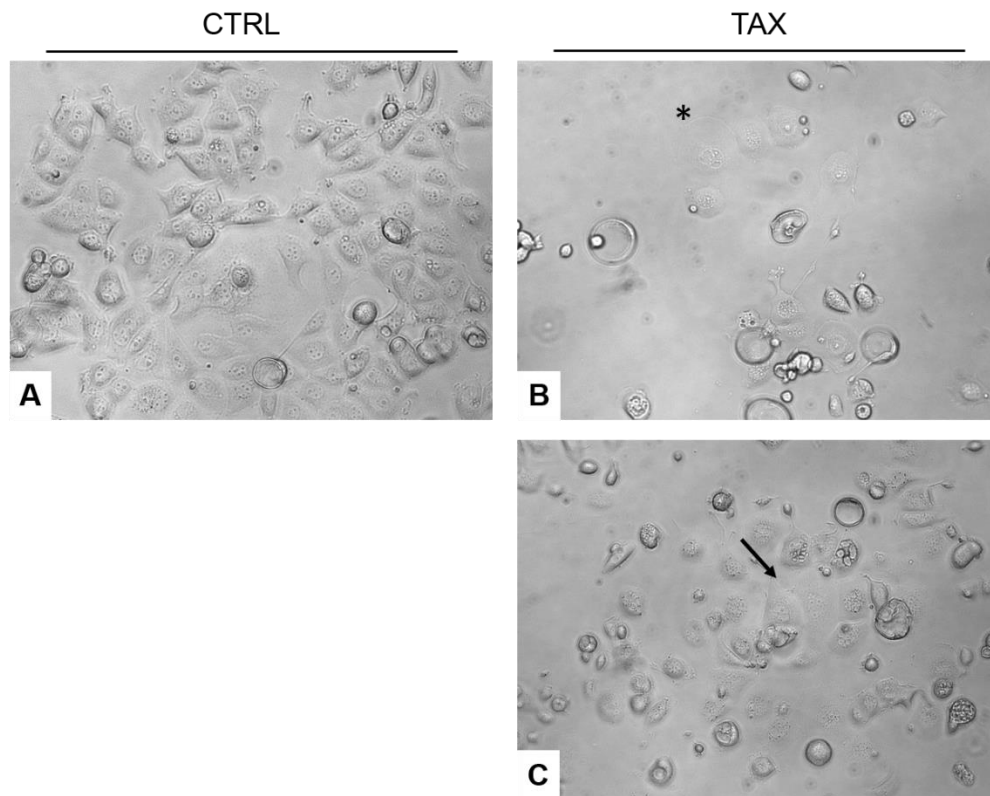


Figure 3.3. Tax induces changes in MCF-7 cells morphology.

Phase contrast images showing morphology of untreated MCF-7 cells (CTRL, A) and residual cells 48 hours after Tax treatment removal (TAX, B and C). Magnification: 20X. Dead floating cells are visible in the media (B and C). B) The star indicates a large flattened senescent-like cell; C) the arrow points at large cells with multiple inclusions similar to micronuclei that underwent mitotic catastrophe.

3.3.2 Residual cells metabolic analysis

As the purpose of this thesis is to investigate the metabolic phenotype of the cells able to survive docetaxel treatment, MCF-7 cells were treated with 10 nM Tax for 4 hours, and the residual cells underwent metabolic analysis 48 hours post treatment removal, compared to the untreated cells (CTRL). The polar fractions of the metabolic extracts derived from six replicates for each condition have been analysed by 1D-¹H NMR spectroscopy. After data processing, assignment and quantification of metabolites in each spectrum was performed using Chenomx, which uses the TMS⁺ signal as reference for metabolite quantification. The assignment process led to the identification of 21 metabolites in each spectrum.

The metabolite quantification revealed statistically significant differences between CTRL and Tax-treated residual cells as listed in Table 3.1. Among these metabolites, particular interest is driven by the essential (Figure 3.4A) and non-essential amino acids (Figure 3.4B), as well as glycolysis-derived metabolites (Figure 3.4C), which are more abundant in the residual cells. Accumulation of two other interesting metabolites, the phospholipid-precursor glycerophosphocholine and the antioxidant glutathione (Figure 3.4D), characterised these breast cancer residual cells. Moreover, the concentration of a number of other metabolites was not altered between the two conditions, such as aspartate ($p=0.0510$), phosphorylcholine ($p=0.4037$), fumarate ($p=0.2359$) and taurine ($p=0.0933$).

Metabolite	CTRL	TAX	P value
Alanine	8.470e-006 ± 1.145e-006	2.443e-005 ± 2.621e-006	0.0014
Creatine phosphate	3.539e-006 ± 5.581e-007	6.462e-006 ± 8.268e-007	0.019
Glutamate	2.125e-005 ± 1.848e-006	3.741e-005 ± 4.555e-006	0.0167
Glutathione	5.551e-006 ± 7.462e-007	9.953e-006 ± 8.651e-007	0.0039
Glycerophosphocholine	6.379e-006 ± 1.032e-006	1.242e-005 ± 2.052e-006	0.0338
Glycine	2.005e-005 ± 2.481e-006	4.017e-005 ± 4.321e-006	0.005
Isoleucine	6.405e-006 ± 7.287e-007	1.333e-005 ± 1.398e-006	0.0032
Lactate	2.298e-005 ± 2.242e-006	7.309e-005 ± 1.246e-005	0.0108
Leucine	5.290e-006 ± 6.131e-007	1.217e-005 ± 1.463e-006	0.0049
Phenylalanine	3.678e-006 ± 4.325e-007	9.164e-006 ± 1.014e-006	0.0025
Threonine	1.591e-005 ± 1.464e-006	3.684e-005 ± 4.065e-006	0.0029
Tryptophan	9.918e-007 ± 1.187e-007	2.553e-006 ± 2.739e-007	0.002
Tyrosine	5.143e-006 ± 4.886e-007	1.305e-005 ± 1.605e-006	0.0053
Valine	7.499e-006 ± 8.383e-007	1.711e-005 ± 1.865e-006	0.0033

Table 3.1. Metabolites more abundant in residual cells.

List of metabolites whose concentration changed significantly between CTRL and residual cells post-Tax treatment (TAX). Values are represented as nmol/cell mean ± SEM. P value < 0.05 are considered statistically significant.

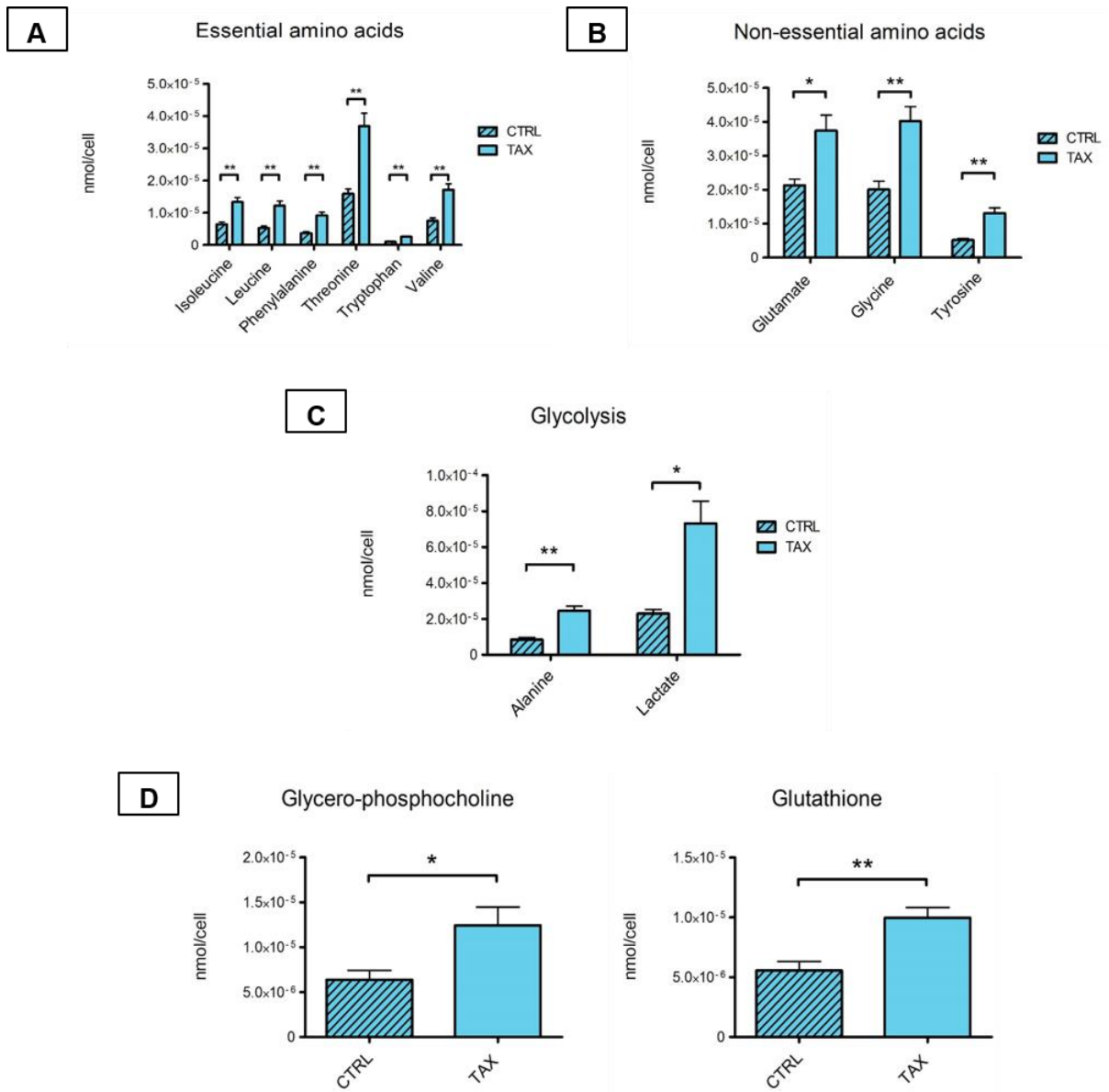


Figure 3.4. Metabolites more abundant in residual cells.

Histograms representing the quantification of metabolites (in nmol/cell) within residual (TAX) or untreated (CTRL) cells polar metabolic extracts, obtained analysing the 1D-proton NMR spectra. Each value is normalised based on total cell number. Statistics is based on six replicates each condition ($p < 0.05$), and presented as mean \pm SEM. A) essential amino acids, B) non-essential amino acids, C) glycolysis-derived metabolites, D) phospholipid-precursor glycerol-phosphocholine and antioxidant glutathione were more abundant in the residual cells post Tax treatment.

3.3.3 Residual cell media metabolic analysis

In order to evaluate differences in uptake or secretion of metabolite between the untreated and the residual cells, a metabolic analysis of the growth media was performed. Medium that had been incubated with cells, as well as fresh medium for comparison underwent extraction of polar metabolites and was subsequently subjected to metabolite identification and quantification through NMR spectroscopy as described above.

Particular attention was focused on the essential amino acids given their intracellular accumulation in the residual breast cancer cells post Tax treatment (Figure 3.4A). The analysis of the media evidenced the uptake of similar amount of isoleucine and valine, and secretion of methionine, phenylalanine, threonine and tryptophan in both conditions (Figure 3.5A). Leucine shows an opposite behaviour between control and residual cells, however the high variability between the 3 replicates meant that these results did not reach statistical significance. In terms of non-essential amino acids, glutamine was the only one consumed, while arginine, glycine, serine and tyrosine were excreted, but again control and residual cells behaved in the same way (Figure 3.5B). The glycolysis-derived metabolites alanine and lactate accumulated into the media in both conditions, but to a higher extent in the residual cells (Figure 3.5C). However, only alanine reached statistical significance ($p=0.0040$), while lactate did not ($p=0.0931$).

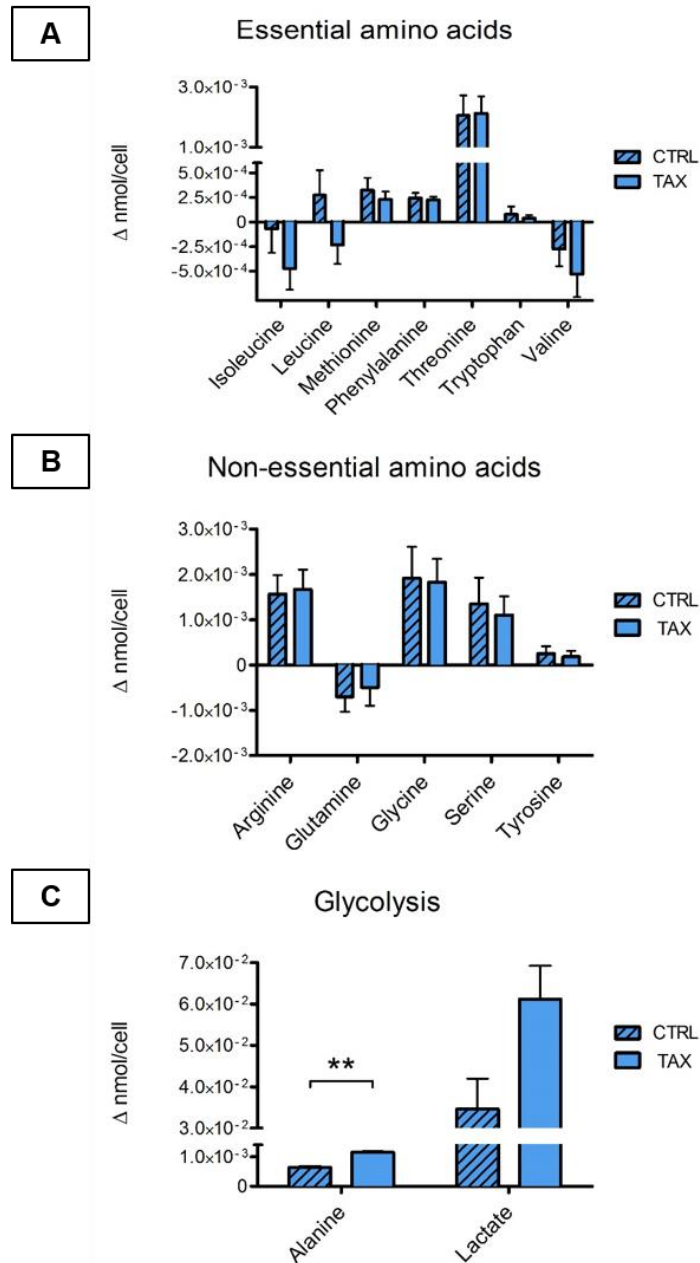


Figure 3.5. Metabolites uptaken and secreted in the media.

Histograms representing the variation between initial and final nmol of polar metabolites per cell (Δ nmol/cell) in the media of residual cells (TAX) compared to untreated (CTRL) cells. Metabolites with $\Delta > 0$ are secreted, while with $\Delta < 0$ are uptaken from the media. Statistics is based on three replicates each condition ($p < 0.05$), results are show as mean \pm SEM. A) essential amino acids, B) non-essential amino acids and C) glycolysis-derived metabolites. Alanine is significantly more abundant in the residual cell media.

3.3.4 Residual cell ^{13}C -MFA

The quantification of intracellular metabolites offers information on the total metabolite pool in a biological system at a specific time. However, this approach does not unravel the metabolic pathways involved in the production or consumption of a certain metabolite. ^{13}C -labelled molecules are employed as metabolic substrates that allow tracing of downstream metabolic pathways involved in their consumption. Given the importance of glucose and central carbon metabolism in malignant adaptations for tumour survival (Koppenol et al., 2011), MCF-7 breast cancer control and residual cells were fed with [1,2- ^{13}C]glucose (Metallo et al., 2009) for 6 hours.

After intracellular polar metabolites extraction, ^{13}C isotope incorporation was identified and quantified on the 2D ^1H - ^{13}C -HSQC NMR spectra (see 2.6.2 and 2.6.3), which allow the determination of the specific intramolecular position of the ^{13}C nuclei (Wiechert, 2001). The metabolite assignments of these spectra were conducted using a library in NMRLab, and label enrichment into the individual carbon atoms was calculated comparing the signal intensity in the spectra derived from samples incubated with [1,2- ^{13}C]glucose to the signal intensity in those derived from ^{13}C - natural abundance (unlabelled glucose-incubated) samples. In this way, the percentage of ^{13}C enrichment in a specific carbon can be obtained relative to its natural abundance. Further information on the metabolic pathway usage is possible to extract from the ^{13}C isotopomers present in the cell extract, which can be identified through the analysis of coupling patterns derived from the spin - spin coupling (J_{CC} coupling) of adjacent ^{13}C -atoms as described in section 1.3.2. The possible difference in cell number among different samples was accounted normalizing in each sample the intensities of all the

metabolites to the intensity of taurine. This analysis was conducted on three replicates for control and four replicates for residual cells.

The ^{13}C enrichment into each labelled carbon was therefore compared between residual (TAX) and untreated (CTRL) cells (Figure 3.6). Starting from the $[1,2-^{13}\text{C}]$ glucose substrate, the downstream glycolytic end-product lactate and alanine showed high ^{13}C incorporation into carbon 2 and 3, therefore leading to the formation of $[2,3-^{13}\text{C}]$ lactate and $[2,3-^{13}\text{C}]$ alanine isotopomers (Figure 3.6A). While alanine had similar incorporation levels in both conditions, lactate showed a slight increase in the residual cells, although not statistically significant. This would suggest no differences in the relative ^{13}C enrichment between the two conditions, however the metabolite quantification already suggested an increased glycolytic flux in Tax-treated cells (Figure 3.4C). Consistent with this, the isotopomer $[2,3-^{13}\text{C}]$ glycerol-3-phosphate, derived from the glycolytic intermediate dihydroxyacetone phosphate, was produced to a higher extent by the residual cells (carbon 2 $p=0.0422$, carbon 3 $p=0.0045$, Figure 3.6A). As a lipid precursor, glycerol-3-phosphate may support residual cells anabolism and membrane synthesis. However, it is necessary to point out that the natural abundance signal of these carbons was very weak, which may result in an overestimation of the label incorporation. Furthermore, both conditions demonstrated the coexistence of glycolysis and oxidative mitochondrial metabolism of glucose, as evidenced by the incorporation of labelled carbons into TCA cycle-derived metabolites such as glutamate, aspartate and malate. Glutamate showed predominant incorporation into carbon 4 in both conditions (Figure 3.6B), which gets labelled directly after the oxidation of $[2,3-^{13}\text{C}]$ pyruvate to $[1,2-^{13}\text{C}]$ acetyl CoA (not detected) by the PDH enzyme during the first round of the TCA cycle, leading to the production of

the [4,5-¹³C]glutamate isotopomer (Figure 1.4B). Label was also present into C(2) and C(3) of glutamate (Figure 3.6B) as a consequence of the activity of pyruvate carboxylase – an alternative entry point of glucose into the mitochondria – for the biosynthesis of the [2,3-¹³C]glutamate isotopomer. Interestingly, the incorporation of ¹³C nuclei from glucose into C(3) was significantly higher in the residual cells-derived glutamate ($p=0.0475$) (Figure 3.6B), which may indicate that these cells use multiple TCA cycle rounds (Figure 1.4B). These results highlighted the central role of glutamate as a substrate for the biosynthesis of many metabolites in this breast cancer cells. In fact, a fraction of ¹³C-labelled glutamate was employed in the synthesis of glutamine, as evidences by the detection of the [2,3-¹³C] and [4,5-¹³C]glutamine isotopomers in both conditions, although to an higher extent in the Tax treated cells (C(2) $p=0.0399$; C(3) $p=0.0005$; C(4) $p=0.0109$) (Figure 3.6B). It was also used as a precursor for the synthesis of the anti-oxidant glutathione, as confirmed by the ¹³C enrichment into C(4) in both conditions (Figure 3.6B) as part of the [4,5-¹³C]glutathione isotopomer. Despite similar enrichment levels, the metabolite quantification had already evidenced a bigger glutathione pool in the residual cells (Figure 3.4D). However, the [4,5-¹³C]pyroglutamate isotopomer was only observed in the Tax-treated cells (Figure 3.6B). Being pyroglutamate part of the glutathione degradation pathway, this result may represent increased glutathione turnover in the residual cells. Unfortunately, pyroglutamate was absent in one CTRL sample, therefore statistical tests could not be performed on two values. Glutamate was also required for the synthesis of the non-essential amino acid proline, which is observed to be labelled in both C(4)&(5) (Figure 3.6B). Although there appears to be a trend towards increased ¹³C incorporation in the residual cell's proline, the difference is not significant. Keeping on tracing the ¹³C atoms

fate in the TCA cycle, it is possible to identify the [3,4-¹³C]malate isotopomer (Figure 3.6C). The abundance of this metabolite is usually very low, therefore the natural abundance-derived signal in the HSQC spectra is very weak making it difficult to properly quantify the enrichment. Moreover, ¹³C label incorporation into aspartate was observed, mainly as the [2,3-¹³C]aspartate isotopomer (Figure 3.6C), which can only be obtained through PC activity (Figure 3.7), at a similar rate in the two conditions. The presence of the isotopomers described above is consistent with ongoing glucose metabolism using both oxidative and non-oxidative mitochondrial pathways in both CTRL and the residual cell population. Using the ¹³C-MFA approach we were therefore able to trace the metabolic pathways involved in the catabolism of [1,2-¹³C]glucose in the MCF-7 cells, such as glycolysis, TCA cycle, glutathione synthesis, glycerophospholipid synthesis and non-essential amino acids production.

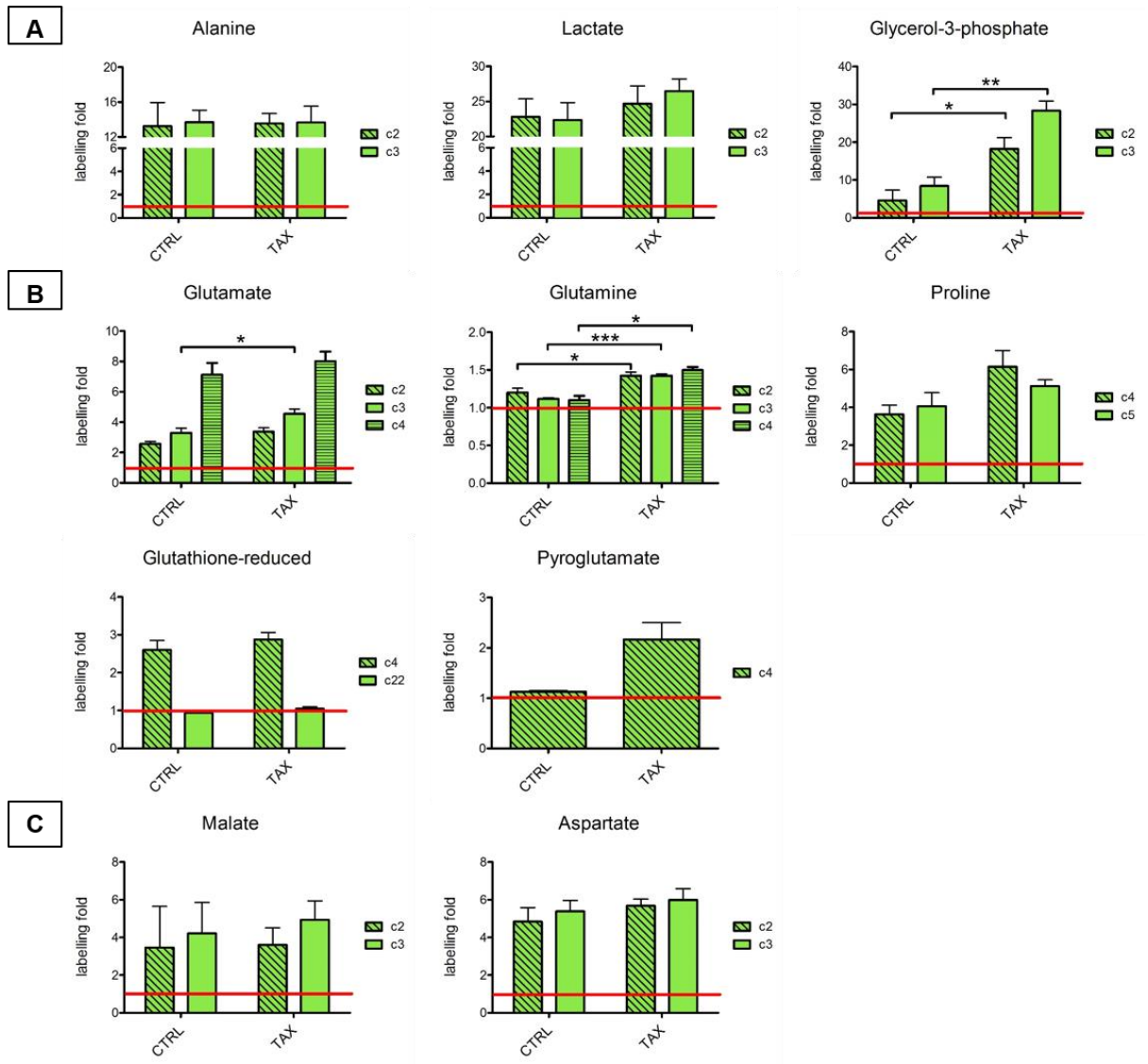


Figure 3.6. Relative ^{13}C isotope enrichment into glucose-derived metabolites.

Histograms showing ^{13}C incorporation into specific residual (TAX) and untreated (CTRL) cell metabolite's carbons, after 6 hours incubation with $[1,2-^{13}\text{C}]$ glucose, relative to natural abundance. The red line represents the ^{13}C isotope natural abundance (here approximated with 1%). Analysis derived from $^1\text{H}-^{13}\text{C}$ -HSQC NMR spectra, three replicates for CTRL and four for TAX ($p < 0.05$). A) glycolysis-derived; B) glutamate-derived and C) TCA cycle-derived metabolites.

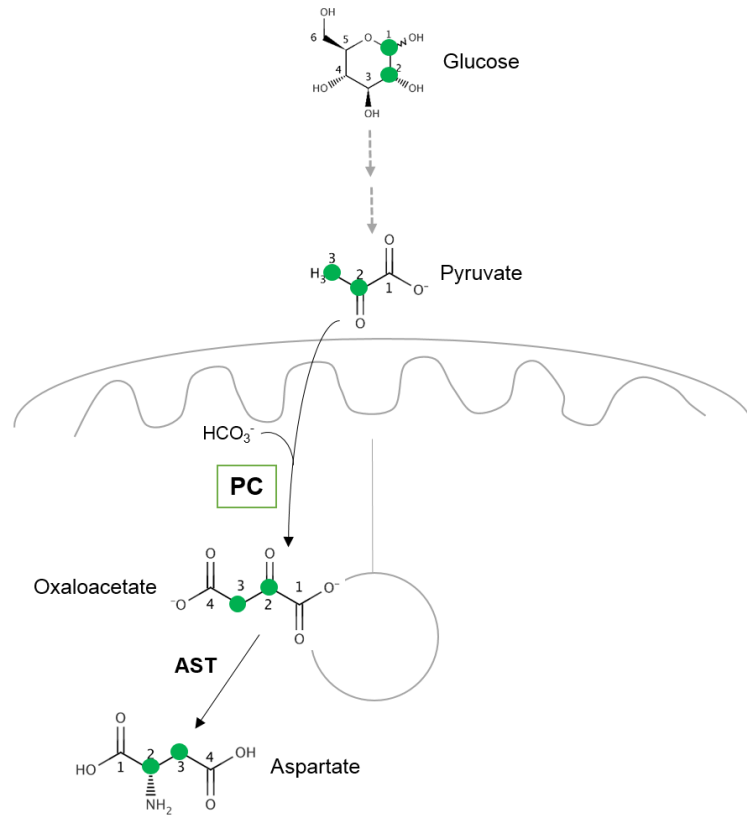


Figure 3.7. [2,3-¹³C]aspartate production via pyruvate carboxylase activity.

Illustration showing ¹³C atoms transition between the substrate [1,2-¹³C]glucose and the product [2,3-¹³C]aspartate via pyruvate carboxylase-dependent conversion of pyruvate into oxaloacetate. Abbreviations: PC, pyruvate carboxylase; AST, aspartate transaminase.

3.3.5 Residual cell media ¹³C-MFA

During the 6 hours incubation period in which the cells are exposed to [1,2-¹³C]glucose, dynamic exchange of nutrients and metabolic products with the extracellular environment occurs. In order to collect this type of information, ¹³C-MFA was also conducted on the conditioned media collected at the endpoint of the experiment, as described in *Materials and methods* (see 2.3.1, 2.3.2). Unfortunately, the taurine signal, which was used as a normaliser in the previous cell flux analysis, was not detected in the spectra derived from the media samples. Consequently, the metabolite intensities were normalized using threonine signals, given that this metabolite was demonstrated not to be affected by treatment (see 3.3.3 and Figure 3.5A). A number of ¹³C labelled metabolites were detected in the media samples, indicative of them having been produced from glucose (Figure 3.8). Among the metabolites identified during the analysis, ¹³C-incorporation into lactate and alanine was observed at significant levels, indicative of a highly active glycolytic metabolism in both treated and untreated cells. In particular, the major lactate isotopomer identified was found to be [2,3-¹³C]lactate, which would be predicted as the result of simple glycolytic metabolism of glucose. This isotopomer was found to be equally present in both conditions (Figure 3.8A). The equivalent isotopomer of alanine, [2,3-¹³C]alanine, was also observed in both control and residual cells (Figure 3.8A). However, the signal derived from alanine C(2) was weak in most of the samples, and entirely undetectable in one replicate. At the same time, the C(3) position was still labelled in these samples, from which we inferred the presence of the alternative [3-¹³C]alanine isotopomer in the media of both conditions. This isotopomer would be predicted to be formed from the involvement of the oxidative branch of the pentose phosphate pathway in the metabolism of glucose.

This not only suggests the induction of the oxPPP in these cells, but that the metabolic intermediates derived from this pathway were used preferentially in the synthesis of alanine, rather than lactate. Other metabolites not identified in the 1D-¹H NMR spectrum during the metabolic analysis of intracellular metabolites presented label incorporation: a-fructose and b-fructose (Figure 3.8A), along with the remaining [1,2-¹³C]glucose (Figure 3.8B). Unfortunately, the experimental variation in fructose labelling percentage within different samples was high, making it difficult to draw meaningful conclusions. The presence of [1,2-¹³C]glucose in the media at the experimental endpoint confirms the availability of the labelled tracer throughout the whole experiment.

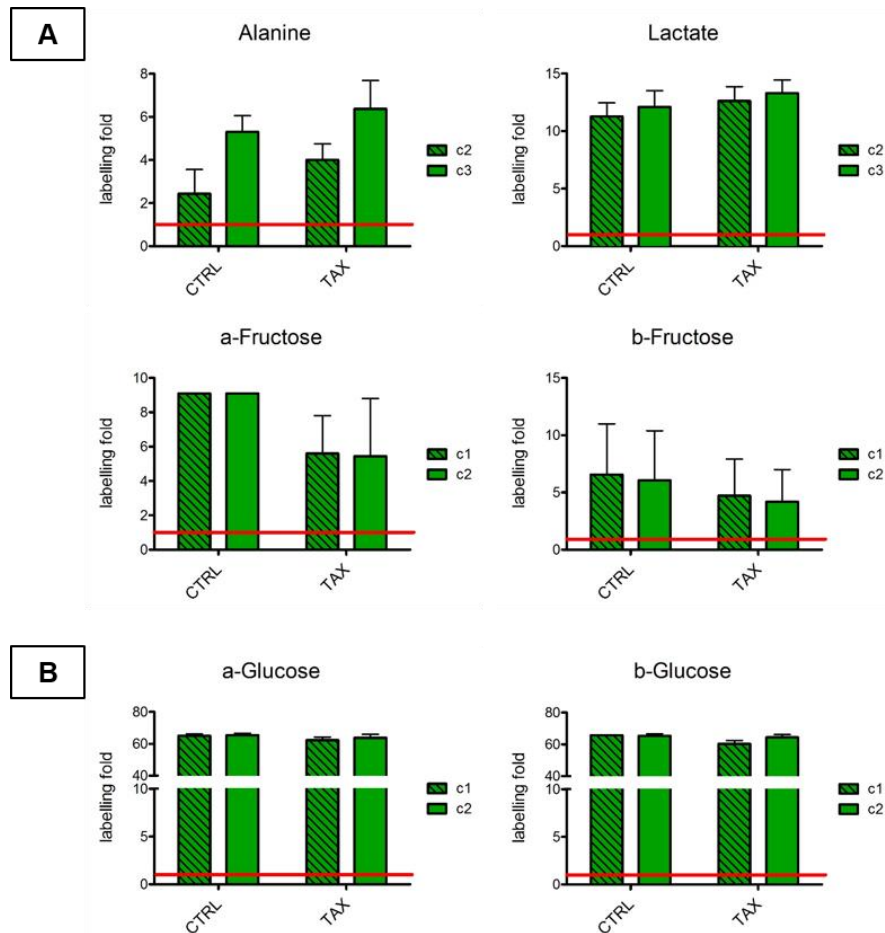


Figure 3.8. Relative ¹³C isotope enrichment into media-derived metabolites.

Histograms showing ¹³C incorporation (relative to natural abundance) into specific metabolite's carbons in the media of residual cells (TAX), compared to untreated cells (CTRL), after 6 hours incubation with [1,2-¹³C]glucose. The red line represents the ¹³C isotope natural abundance (here approximated with 1%). Analysis derived from ¹H-¹³C-HSQC NMR spectra, three replicates for CTRL and four for TAX (p< 0.05). A) glucose-derived metabolites secreted in the media; B) left-over of [1,2-¹³C]glucose used to feed the cells.

3.3.6 Glutathione role in residual cell survival

The metabolic analysis of the intracellular metabolites extracted from control and residual cells highlighted, among others, an increase in glutathione concentration per cell in the residual breast cancer cells (Figure 3.4D). Moreover, from the ^{13}C isotope incorporation into glutathione C(4) (Figure 3.6B) it is possible to infer the metabolic pathway leading to its synthesis following the administration of the metabolic substrate $[1,2-^{13}\text{C}]$ glucose: through the formation of $[4,5-^{13}\text{C}]$ glutamate, which is subsequently used in the production of $[4,5-^{13}\text{C}]$ glutathione. Although the relative ^{13}C enrichment of C(4) does not differ between the two conditions, one can assume a higher absolute amount of labelled glutathione given the presence of a bigger glutathione pool in the residual cells (Figure 3.4D). Glutathione is a well-known intracellular antioxidant (Meister, 1983) that has a fundamental role in cancer cell survival (Arrick and Nathan, 1984, Cazenave et al., 1989). We therefore hypothesised that glutathione production was fundamental to breast cancer cell survival after Tax treatment. To investigate this, MCF-7 cells were treated with BSO, a glutathione-synthesis inhibitor (Ali-Osman et al., 1996, Ford et al., 1991, O'Dwyer et al., 1992) as described in section 2.2.3. First, it was necessary to prove the efficacy of BSO in decreasing glutathione synthesis. Therefore, MCF-7 cells were treated with BSO and subsequently the intracellular concentration of glutathione compared to that of untreated cells was quantified using a $1\text{D-}^1\text{H}$ NMR spectrum. BSO was observed to efficiently decrease the concentration of glutathione in cells (Figure 3.9). Once established, we investigated whether treatment with BSO after Tax incubation would improve the killing effect. As shown in Figure 3.10, the treatment with BSO for 24 or 48 hours following Tax treatment did not show additive effects and did not significantly improve Tax killing effect, suggesting

that glutathione synthesis is not required for survival of cells directly post-Tax treatment.

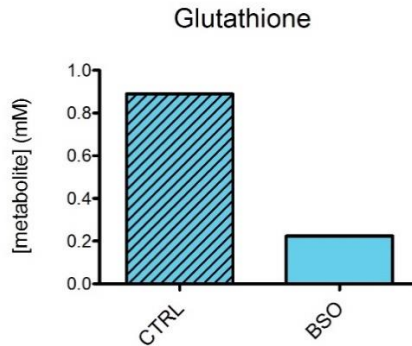


Figure 3.9. Glutathione-synthesis inhibition.

Histograms showing intracellular glutathione concentration (mM) in MCF-7 untreated (CTRL) cells and treated with BSO. Quantification obtained analysing the 1D-¹H NMR spectrum with Chenomx. BSO treatment inhibits glutathione synthesis causing a decrease in glutathione concentration compared to untreated cells. Values are normalized on total cell number.

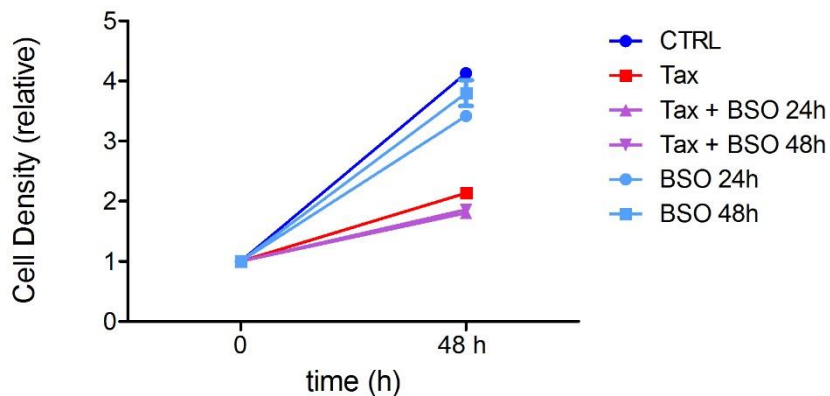


Figure 3.10. Additive effect of BSO and Tax on MCF-7 cells survival.

Graphs showing treated (Tax, Tax + BSO, BSO) and untreated (CTRL) MCF-7 cell density at 48 hours relative to the zero time point cell density. The addition of BSO after Tax treatment does not potentiate Tax killing effect. Values are mean of six replicates ± SEM.

3.3.7 Residual cell regrowth

The interest in characterizing the metabolic phenotype of the residual cells is mainly because of their potential for leading to tumour recurrence, which is the main cause of patient death. *Li et al.*, developed an *in vitro* recurrence model showing that residual breast cancer cells resume proliferation forming recurrence colonies (Li et al., 2014). The residual breast cancer cells analysed so far, taken at 48 hours post-treatment withdrawal, are not proliferating as evidenced by the time-course experiment, and this was true until the fifth day post-Tax removal (Figure 3.2). In order to unveil the time-point at which the residual cells in this model start to regrow, the same time-course experiment was carried out checking for regrowth beyond the fifth day, looking at the following time points: day 5, 7, 9, 11, 13 and 15 (respectively 120, 144, 168, 192, 216, 240 hours, Figure 3.11). It was not possible to obtain data for the control untreated cells after day 5 as they became confluent in the well of a 6-well plate. On the contrary, Tax-treated cells did not show increase in cell density between five and fifteen days post treatment (Figure 3.11). However, checking the cells under the microscope, it was possible to see small clones of cells starting to regrow. It was therefore clear that the SRB assay was not sensitive enough to capture the growth of few cells only. For this reason, the experiment was repeated for the same time points, performing only SRB staining instead of measuring the optical density in order to visualise the regrowth (Figure 3.12). In fact, between day 9 and day 15 small clones of regrowth are visible confirming the hypothesised ability of these residual cells to overcome the proliferation arrest leading to breast cancer cell recurrence.

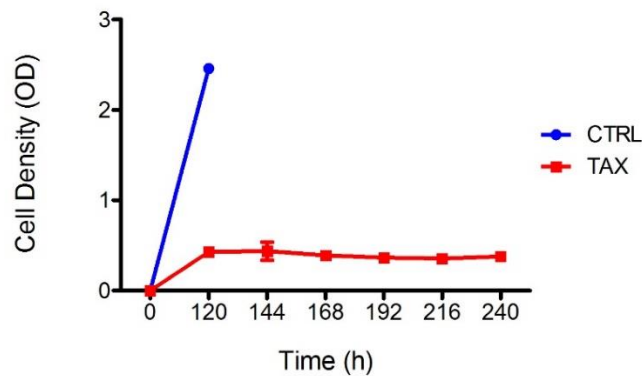


Figure 3.11. Residual cell regrowth time-course.

Curves showing SRB absorbance values for untreated (CTRL) and residual cells (TAX) 120, 144, 168, 192, 216 and 240 hours post-Tax treatment withdrawal. Values are mean of three replicates \pm SEM. Residual cells do not show increase in cell number for the whole length of the experiment.

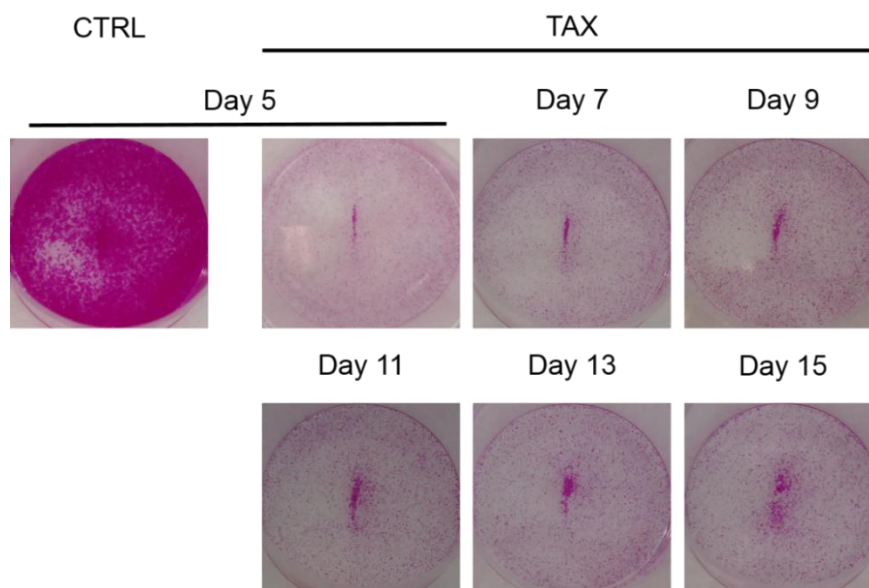


Figure 3.12. Residual cell regrowth staining.

Pictures showing SRB staining of untreated MCF-7 cells (CTRL) at day 5, and residual breast cancer cells (TAX) at day 5, 7, 9, 11, 13 and 15 post-Tax removal. From day 9 it is possible to visualize more cells stained by the SRB indicative of residual cell regrowth.

3.3.8 Clone 1 and 2 metabolic analysis

Once it was established that residual cells were able to escape docetaxel-mediated growth arrest and to restart growing, two clones that regrew were produced as described in 2.3.3, and maintained in culture in order to assess their metabolic phenotype. These cells were named respectively clone 1 and clone 2. Growth curves over four days were performed for the two clones and for the untreated MCF-7 cells as shown in Figure 3.13. These three population of cells had different doubling times between day 2 and day 4 (see 2.3.4), being 29.29 h for clone 2 and 30.6 h for untreated MCF-7, while clone 1 had a faster doubling time of 25.68 h. However, the main differences are visible in the lag phase of the growth curves, in fact clone 1 requires a longer time before starting the exponential growth, while clone 2 starts earlier compared to control MCF-7. These MCF-7 subclones therefore present altered growth after resuming docetaxel-induced cell cycle arrest. In order to understand if these clones derived from residual cells retain characteristics of the original untreated MCF-7 cells after they restart proliferating, metabolic analyses were performed on both clones. Firstly, investigation of the steady-state metabolic phenotype showed that essential amino acids, such as isoleucine, leucine, phenylalanine, tryptophan and valine were significantly more abundant in both clones than in untreated MCF-7 cells (Figure 3.14A), similar to what was seen in the residual cells. Among the non-essential amino acids, tyrosine was significantly more present in both clones, while glycine increase reached statistical significance only in clone 2 (Figure 3.14B). It is worth noting that the glycolysis-derived alanine and lactate were present at a similar level in all these cell types (Figure 3.14C). Due to this shift in amino acid metabolism and cell growth both in the residual cells and in the regrowth clones, we decided to investigate

mTOR activity in all these cells: a central kinase in the co-ordination of cell growth and metabolism.

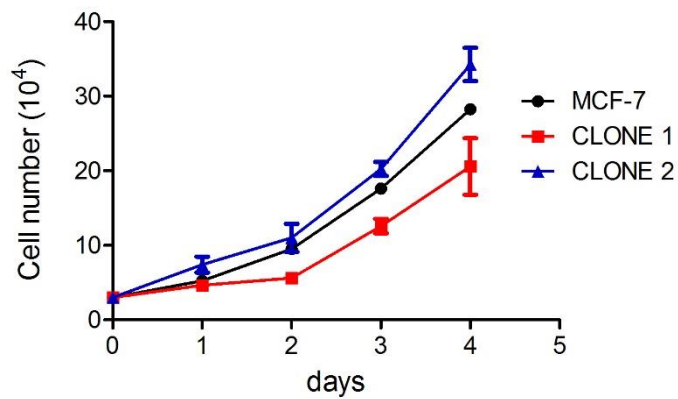


Figure 3.13. Growth curves.

MCF-7, clone 1 and clone 2 cells were seeded at 3×10^4 cell/well and number of cell was counted every day for four days. Results are shown as mean of three experiments \pm SEM. Both clones showed differences in the lag growth phase compare to the control MCF-7.

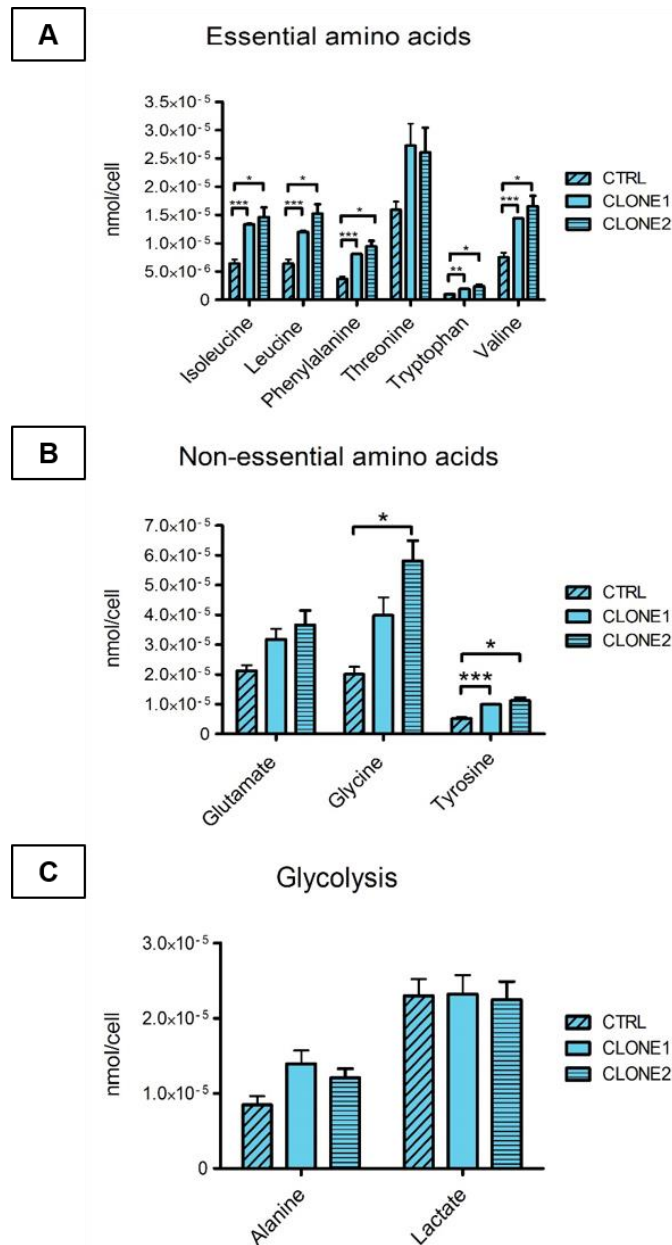


Figure 3.14. Clone 1 and clone 2 metabolic analysis.

Histograms representing the quantification (nmol/cell) of essential (A), non-essential (B) amino acids and glycolysis-derived metabolites (C) in untreated (CTRL) MCF-7 cells, clone 1 and clone 2 metabolic extracts, obtained analysing the 1D-¹H NMR spectra with Chenomx. Each value is normalised based on total cell number. Statistics is based on six replicates for CTRL, and three replicates for each clone. Values are presented as mean ± SEM (p<0.05). Most of the amino acids identified are more abundant in the regrowth clones.

3.3.9 mTOR activity in MCF-7, residual cells and regrowth clones

mTOR is a serine/threonine protein kinase known to be involved in processes such as cell growth, proliferation (Dowling et al., 2010) and cell metabolism, with particular involvement in the sensing and control of intracellular amino acids (Zheng et al., 2014, Efeyan et al., 2012). As results had shown the accumulation of essential and non-essential amino acids in both residual cells and outgrowing clones, it was important to define the mTOR status in these cells. mTOR activity can be assessed through the phosphorylation of a target protein, S6 kinase (S6K) (Wu et al., 2005). This was investigated using western blotting, which showed that mTOR activity decreased in the residual cells following Tax treatment (Figure 3.15). However, both clones present an increased amount of total S6K, while its phosphorylated form is present only in clone 1. Therefore, mTOR activity is not a prerogative for cell survival to docetaxel treatment.

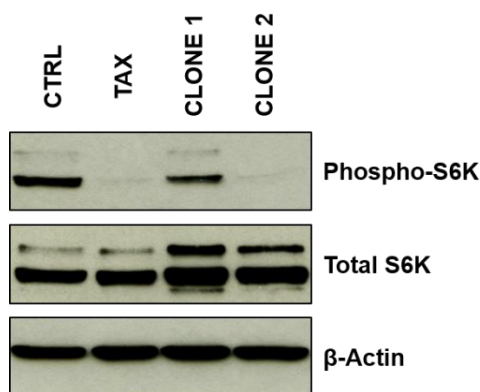


Figure 3.15. mTOR activity.

Image showing western blot bands for phospho-S6K, total S6K protein and β -actin obtained analysing untreated MCF-7 (CTRL), residual cells (TAX), clone 1 and clone 2 protein extracts via SDS-PAGE and western blot. The presence of phospho-S6K is indicative of mTOR activity, which is decreased in residual cells post Tax treatment and in clone 2 cells.

3.3.10 Clone 2 ¹³C-MFA

In the previous section, it emerged that, although restoring its proliferation ability, clone 2 maintains low mTOR activity despite the intracellular accumulation of essential amino acids (Figure 3.14A). In order to obtain more detailed information regarding its metabolic phenotype, clone 2 cells were incubated with [1,2-¹³C]glucose for six hours and metabolic flux analysis performed as previously described. The non-essential amino acids glycine and tyrosine, although more abundant in the regrowth clones than the untreated MCF-7, did not show ¹³C incorporation, therefore it is possible to exclude their *de novo* biosynthesis. This suggests that the increased concentrations are due to increased uptake of these amino acids through plasma membrane transport, or increased degradation of intracellular proteins. Due to the selective increase of amino acids observed (Figure 3.14), the former is most likely. The clone 2-derived metabolites that gained ¹³C enrichment are shown in Figure 3.16. Overall, the label incorporation into those intracellular metabolites detected was very similar between control MCF-7 cells and clone 2. The only metabolite showing statistically significant higher enrichment in clone 2 samples compared to untreated MCF-7 samples, was glutamate. In particular, there is a higher enrichment in [1,2-¹³C] and [2,3-¹³C]glutamate, suggestive of increased anabolic use of the TCA cycle. However, further work is necessary to confirm this phenotype.

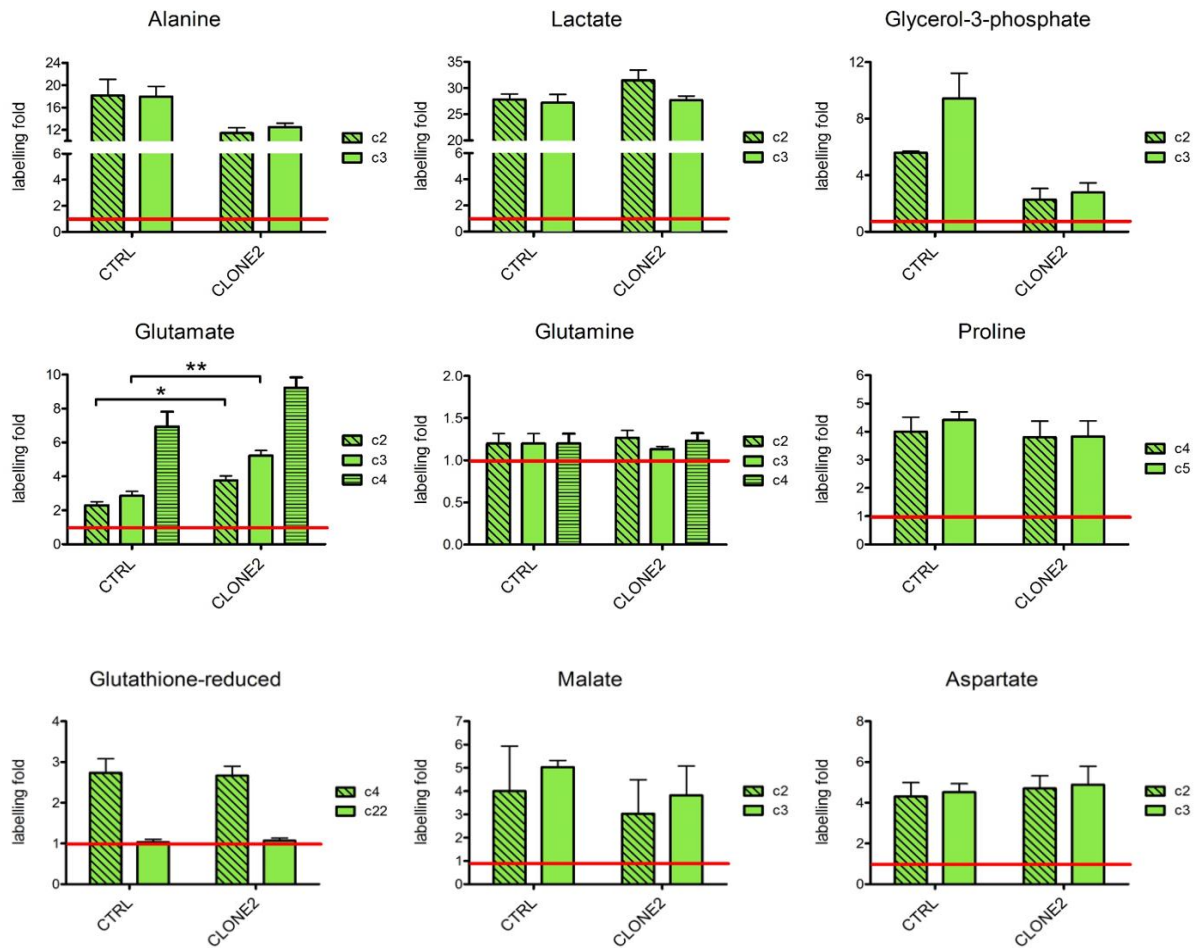


Figure 3.16. Clone 2 ¹³C-MFA.

Histograms showing relative ¹³C enrichment into specific metabolites extracted from clone 2 cells, compared to untreated MCF-7 cells (CTRL). The red line represents the ¹³C isotope natural abundance (here approximated with 1%). Analysis derived from ¹H-¹³C-HSQC NMR spectra; values are plotted as mean of three replicates ± SEM. Glutamate is the only one showing statistically significantly higher ¹³C enrichment for clone 2 (p<0.05).

3.4 DISCUSSION

Since its introduction in 1996, docetaxel has shown great efficacy against advanced and metastatic breast cancer (Cortes and Pazdur, 1995, Tankanow, 1998, Valero et al., 1995, Binder, 2013). In order to fully exploit its potential, it is fundamental to understand the mechanisms underlying incomplete remission and resistance to docetaxel treatment, which represent leading causes of cancer patient mortality (Chang et al., 2005, Creighton et al., 2009). In fact, it has been shown by *Creighton et al.* that residual breast cancer cells are likely to be the source of tumour relapse, presenting the characteristics of tumour-initiating cells (Creighton et al., 2009).

In recent years, the interconnected nature of the metabolic phenotype and genetic alterations in cancer have become clearer. One can hypothesise therefore that through the analysis of cellular metabolism, one obtains the best readout of the tumour metabolic phenotype. Given that, the aim of this thesis is to characterise the metabolic phenotype of the residual breast cancer cells: i.e. those that survived docetaxel treatment. This chapter focused on the *in vitro* experiments conducted on the MCF-7 breast cancer cell line, which maintains luminal A adenocarcinoma characteristics (Holliday and Speirs, 2011, Levenson and Jordan, 1997).

First of all, it was necessary to determine the concentration of docetaxel to be used for our purposes. We found that 10 nM was the optimal concentration for this cell line, therefore used for all the subsequent *in vitro* experiments. Moreover, in this thesis cells were treated for a short time only (4 hours) in order to avoid the induction of genomic or proteomic alterations that a long-term treatment could favour (Li et al., 2014), as well as to more accurately recapitulate the exposure of breast tumour cells in patients to this drug (compared with 24-48 hours incubations often used *in vitro*). Given that

solid tumour hypoxia is one of the main factors responsible for resistance and treatment failure (Ward et al., 2013, Milani and Harris, 2008, Zeng et al., 2015), MCF-7 cells were treated both under normoxic and hypoxic conditions. However, docetaxel killing efficacy did not show differences between the two conditions for this breast cancer cell line. These results are in contrast with some studies showing that the MCF-7 cells are more sensitive to Tax killing effects when cultured in hypoxic conditions (Strese et al., 2013) due to Tax-dependent inhibition of HIF1 α (Escuin et al., 2005).

It has been demonstrated in the literature that mitotic catastrophe is the main mechanism of cell death caused by Tax in breast cancer cell lines (Morse et al., 2005) following aberrant mitosis as a consequence of the anti-microtubule action of this drug. Interestingly, the morphological alterations observed in the MCF-7 residual cells show similarities with some of the features of human residual cancer such as enlarged nuclei and condensed chromatin (Viale, 2013). However, the time-course experiment shows that this taxane causes a stable cell growth arrest for several days post-treatment. The viable and non-proliferative state makes these residual cells comparable to the circulating and disseminated cancer cells found in patients, often responsible for metastatic breast cancer (Ignatiadis and Reinholz, 2011). In fact, if they do not undergo cell death, they could bypass cell cycle arrest leading to aberrant mitosis and aneuploidy (Bayet-Robert et al., 2010). They would also be likely to be entirely resistant to any further chemotherapeutic approaches that target cells in cycle, such as nucleotide mimetics and DNA damaging agents. It should be pointed out that the results of the time-course experiment were obtained through SRB assay, which is able to detect the cellular protein content, whereas DAPI or Ki67 staining would give information on the actual proliferative state of these cells. Characterizing the metabolic

phenotype of these residual cells is therefore vital in order to unveil the mechanisms that allow their survival to docetaxel treatment and design new therapies that target this.

Residual cells were obtained after treating MCF-7 cells with 10 nM Tax for 4 hours and leaving them to recover for 48 hours. This approach allows the study of metabolic effects in the cells that survived treatment that were not directly due to the drug. Subsequently, we performed an *in vitro* targeted metabolic analysis on these breast cancer residual cells, examining the polar fraction of metabolic extracts. Results are summarised and illustrated in Figure 3.17. Interestingly, the metabolic analysis evidenced intracellular accumulation of a certain class of metabolites in residual cells compared to the untreated MCF-7, including essential and non-essential amino acids, glycolysis-derived metabolites, phospholipid precursors and antioxidants. These are very intriguing results given that these residual cells are not proliferating, as evidenced by the time-course experiment. Furthermore, as cells are not able to synthesise essential amino acids (by definition), their accumulation in the residual cells could only result from increased uptake from the media or higher intracellular protein breakdown. However, the increase in non-essential amino acids and central carbon metabolites could also derive from higher cellular biosynthesis, besides extracellular uptake and intracellular macromolecules degradation. It is worth noticing that the concentrations of all the amino acids identified were strongly affected, resulting in highly significant p values. One possible explanation is the involvement of a process called macropinocytosis, a means by which cells uptake nutrients from the extracellular environment; in this way, proteins can be internalized from the media and degraded intracellularly to obtain free amino acids (Commisso et al., 2013).

Some of these metabolites, such as glutathione, lactate, alanine, threonine and glycerophosphocholine, have previously been shown to decrease in response to docetaxel treatment (Bayet-Robert et al., 2010). Thus, their increased levels in residual cells resemble treatment failure and potential malignancy of the survived cells.

The analysis of spent media and pathway tracing could help to better understand the origin of these metabolites' accumulation. Surprisingly, metabolic analysis of the media did not identify differences in the extracellular uptake of amino acids between the two conditions. This suggests that the residual cells intracellular accumulation of essential amino acids cannot be explained by increased extracellular uptake but it is more likely due to intracellular protein breakdown, although this would need to be further verified. Less straightforward is the explanation for tyrosine, as this is a semi-essential amino acid, being synthesised only from the intracellular oxidation of the essential amino acid phenylalanine. The increased intracellular phenylalanine concentration therefore allows accumulation of tyrosine in the residual cells. One could also infer that tyrosine is then consumed intracellularly in the residual cells, given that the secretion of both amino acids in the media does not show differences with control cells. The increase in non-essential amino acids and central carbon metabolite steady state could be also explained by a higher *de novo* biosynthesis by the cells. We wished to test this hypothesis through the use of stable isotope tracer analysis. Hence, cells were fed with a labelled metabolic precursor, [1,2-¹³C]glucose, and residual and untreated cell metabolites were analysed after a 6 hours flux. As would be expected, glucose was metabolised by the MCF-7 cells and downstream metabolites showed ¹³C enrichment. A difference in production rate was identified only for glycerol-3-phosphate, glutamine, and glutamate C(3). It is noteworthy that, even though glutamine was normally

provided in the culture media, residual breast cancer cells needed to further produce this amino acid from glutamate. The importance of glutamine as an alternative carbon source for cancer cells is becoming increasingly clear (Gaglio et al., 2011, Alberghina and Gaglio, 2014, DeBerardinis et al., 2007), it would therefore be appealing to investigate further the role of this amino acid in the breast cancer residual cell metabolism. It is important to underline that the ^{13}C -MFA results show the relative quantification of the ^{13}C enrichment, comparing it to the natural abundance of the same molecule. If the absolute quantification of these metabolites is taken into account, the higher intracellular abundance of alanine, lactate, glutamate and glutathione determines the presence of a bigger ^{13}C labelled pool of these metabolites produced by the residual cells. In particular, the increased aerobic production of lactate suggests the induction of the Warburg effect, which may have a pivotal role in the residual cell survival. In fact, LDH-A has previously been shown to be a useful target to overcome resistance to paclitaxel in breast cancer cells (Zhou et al., 2010). It is therefore possible to infer that the breast cancer cells that survived docetaxel treatment, which are in growth arrest at the time of the experiment, are significantly more metabolically active than the control MCF-7. This is also supported by the label incorporation observed in glutamate C(3), which indicates multiple TCA cycle rounds. These features could be explained by a therapy-induced senescent phenotype (Ewald et al., 2010, Collado and Serrano, 2010), which has been shown to demonstrate exploitable metabolic alterations (Dorr et al., 2013). Interestingly, a considerable fraction of labelled glutamate appears to be used in glutathione production, as suggested from the labelling enrichment in glutathione C(4), subsequently catabolised to pyroglutamate (van der Werf and Meister, 1975). Although the relative enrichment is similar between

control and treated cells, the metabolic analysis evidenced the presence of a bigger glutathione pool in the residual cells. Glutathione is an important cellular antioxidant, particularly useful to cancer cells to fight the high ROS production in order to survive despite the oxidative stress (Arrick and Nathan, 1984, Meister, 1983, Sullivan and Chandel, 2014). Moreover, it has been previously shown that increased expression of glutathione-related genes correlates with resistance to docetaxel in patients (Iwao-Koizumi et al., 2005). Whereas a gene expression analysis conducted by *Korde et al.*, highlighted the increased expression of genes implied in reactive oxygen species metabolism in patients resistant to docetaxel and capecitabine treatment (Korde et al., 2010). Hence, it is possible to speculate that the production of this antioxidant molecule mediates the escape from Tax killing by the residual cells (Arrick and Nathan, 1984, Cazenave et al., 1989). To test this, docetaxel treatment was followed by BSO treatment to induce glutathione depletion via synthesis inhibition, and verify if this results in higher breast cancer cells killing (Ford et al., 1991, O'Dwyer et al., 1992, Ali-Osman et al., 1996). However, there was no additive effect between the two drugs suggesting that glutathione synthesis is not a key process in residual cells survival after docetaxel treatment. As BSO was applied only after removing docetaxel, it must be considered that glutathione synthesis could be triggered early at the beginning of the treatment, being therefore able to accumulate prior to BSO administration. In this case, a co-treatment with the two drugs could provide a better outcome.

To complete the characterization of the metabolic phenotype of residual and untreated MCF-7 breast cancer cells, the conditioned media was also used for ^{13}C -MFA following the 6 hours flux experiment. Among the metabolites shown to be excreted in Figure 3.5, alanine and lactate proved to be produced from glucose due to ^{13}C isotope

incorporation. Again, although the relative enrichment is similar between the two conditions, when the higher concentration of these metabolites was taken into account, the pool of labelled lactate and alanine is consequently bigger in the residual cells conditioned media, although statistical significance is reached only for alanine. The secretion of lactate is known to contribute to the acidification of the extracellular microenvironment, facilitating tumour cell spreading and metastasis (Hirschhaeuser et al., 2011). This feature could support the idea that the residual cells are potentially more malignant than the primary tumour. The non-essential amino acid alanine presents a higher intracellular and extracellular concentration in the residual cells providing a further source of pyruvate, on top of being possibly employed in protein synthesis.

Overall, these breast cancer residual cells present a hypermetabolic phenotype, the aim of which is not supporting continued cell proliferation. This feature is in accordance with few recent studies showing that the metastatic capacity is developed in breast cancer in parallel with a decreased proliferation ability (Waldman et al., 2013, Jerby et al., 2012), a phenomenon known as “go or grow” (Giese et al., 1996). In this scenario, residual cells would carry on anabolic processes to support the production of key metabolites such as lactate, exemplified with the Warburg effect (Koppenol et al., 2011), and amino acids aimed at the biosynthesis of antioxidant molecules such as glutathione.

Residual cells represent a threat to cancer patient survival given their ability to resume proliferation and to support cancer relapse (Li et al., 2014, Creighton et al., 2009). It was therefore intriguing to determine whether the residual breast cancer cells used in the present study were able to restart cell growth. In fact, this study was able to show

that those cells that survived treatment were able to escape the induced senescent phenotype and resume proliferation around 9 days post-docetaxel withdrawal. At this point, it was interesting to characterise the metabolic phenotype of these cells responsible of tumour recurrence, in order to possibly identify features that could be targeted in a therapeutic approach. Two clones of regrowth were therefore established, named clone 1 and clone 2, and underwent metabolic analysis as previously described. Interestingly, the metabolic analysis underlined again the importance of essential amino acids, being more abundant in the regrowth clones, while a possible marker of malignancy such as lactate was the same as the untreated MCF-7. These results could be interpreted again through the “go or grow” behaviour: after resuming proliferation, the cells must use their transformed metabolism to build biomass to sustain cell growth. More information regarding this second aspect can be obtained through ^{13}C -MFA.

Most of the results presented so far highlighted an intracellular accumulation of essential and non-essential amino acids, therefore it would be interesting to understand to which extent they are fundamental for the survival of residual cells investigating the pathways which are known to be responsive to amino acids availability. The PI3K/Akt/mTOR pathway is known to respond to nutrient availability and growth factors, therefore controlling cell survival and proliferation (Paplomata and O'Regan, 2014); moreover, it has been shown to be involved in breast cancer resistance to therapy (Paplomata and O'Regan, 2013). In particular, mTOR is a serine/threonine protein kinase that acts phosphorylating and activating the p70-S6K ribosomal protein to stimulate initiation of translation (Wu et al., 2005). mTOR activity is regulated, among others, by the presence of amino acids (Efeyan et al., 2012). The

inhibition of mTOR in conditions of energetic demand has been shown to stimulate autophagy activation, which restores the intracellular amino acid levels which would in turn activate mTOR to sustain proliferation (Efeyan et al., 2012). This could well explain the metabolic phenotype observed by our analysis. In fact, the non-proliferative residual cells present a decreased mTOR activity compared to the control cells (Figure 3.15), which could be due to cellular stress conditions (Laplante and Sabatini, 2012) following docetaxel treatment. The induction of the autophagic process would then lead to the intracellular accumulation of amino acids seen in the residual cells. Furthermore, the feedback control over the mTOR complex could reactivate the protein kinase resulting in the recovery of residual cell proliferation as it happened for the regrowth clones. However, this is not true for both clones given that clone 2 does not show S6K activation by mTOR. This result is particularly intriguing since clone 2 cells, besides being able to proliferate, are characterized by an accumulation of essential amino acids as evidenced by the metabolic analysis, even though they do not recover mTOR activity. To further elucidate clone 2 metabolic phenotype, the pathways used in central catabolic and anabolic processes were mapped out performing ^{13}C -MFA. The [1,2- ^{13}C]glucose substrate was observed to be metabolised using the same pathways as control MCF-7 cells, meaning that these clones of tumour recurrence held characteristics of the primary tumour from which they derived. However, clone 2 cells present a higher production of [1,2- ^{13}C] and [2,3- ^{13}C] isotopomers of glutamate, derived from multiple TCA cycles and PC activity respectively. Recently, breast cancer has been shown to overexpress PC, and in particular its expression level positively correlates with malignant behaviour, such as higher invasiveness and metastatic potential (Phannasil et al., 2015). Therefore, we could infer that regrowth clone 2

presents a more malignant phenotype compared to control MCF-7 and residual breast cancer cells.

In conclusion, some of the breast cancer cells treated with the anti-microtubule agent docetaxel are able to survive, although entering a cell-cycle arrest condition. Nevertheless, the survived cells, defined as residual, exhibit a hypermetabolic phenotype, mainly characterized by amino acid accumulation, and higher ^{13}C enrichment in central carbon derived metabolites, that altogether offer the metabolic advantage for survival and tumour repopulation. As future studies, it would be interesting to investigate the treatment sensitivity of the recurrent clones of breast cancer originated from the docetaxel residual cells, either using the same treatment strategy, or exploring new therapeutic approaches, targeting for example the amino acids metabolism. However, any parallelism between this *in vitro* model and the recurrent tumours in humans should be carefully drawn, given the absence of communication between cells grown in monolayers and the tumour microenvironment typically surrounding human solid tumours. For these reasons, we wished to adopt a pre-clinical model for our metabolic investigations, as will be described in the next chapters.

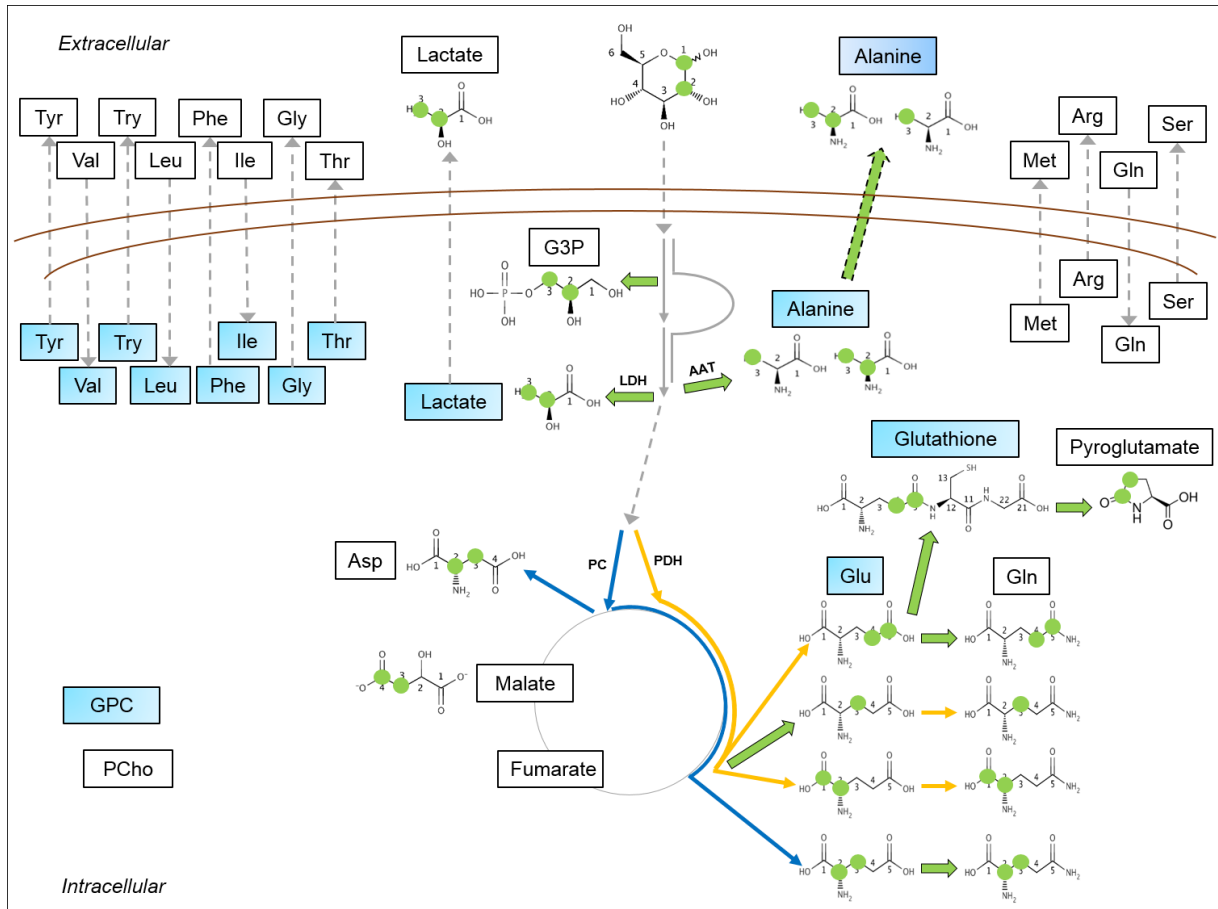


Figure 3.17. *In vitro* metabolic phenotype of residual breast cancer cells.

Residual breast cancer cells present intracellular accumulation of essential and non-essential amino acids, central carbon metabolism metabolites, lipid precursors and anti-oxidant molecules, and extracellular accumulation of alanine, while in growth arrest, compared to untreated MCF-7. Administration of [1,2-¹³C]glucose allowed tracing of the main pathways such as glycolysis, pentose phosphate pathway, TCA cycle and reaction branching from those. Residual cells increased the rate of production of glycerol-3-phosphate (G3P), lactate, alanine, glutamine, glutathione and pyroglutamate. They also underwent multiple TCA cycle increasing the production of specifically the [3-¹³C]glutamate isotopomer. Metabolites are in boxes, while enzymes are without. Light and dark blue boxes indicate increased intracellular and extracellular metabolite concentration respectively. Green cue ball indicates the ¹³C atom. Green arrows indicate increased production rate, grey dotted lines transport across membranes and continuous lines pathways. Abbreviations: AAT, alanine

aminotransferase; Arg, arginine; Asp, aspartate; Gln, glutamine; Glu, glutamate; Gly, glycine; GPC, glycerophosphocholine; Ile, isoleucine; LDH, lactate dehydrogenase; Leu, leucine; Met, methionine; PC, pyruvate carboxylase; PCho, phosphorylcholine; PDH, pyruvate dehydrogenase; Phe, phenylalanine; Ser, serine; Thr, threonine; Try, tryptophan; Tyr, tyrosine; Val, valine.

CHAPTER 4

***IN VIVO* ^{13}C -MFA: METHOD
DEVELOPMENT**

4.1 INTRODUCTION

A significant goal of cancer research is to improve treatments and to increase patient's survival. Therefore, it is fundamental to be able to translate laboratory findings to cancer patients. While *in vitro* studies allow the best control of experimental conditions, they are not able to recapitulate the complex hostile environment that surrounds solid tumours *in vivo*. In particular, hypoxia is understood to strongly influence tumour progression and resistance to therapy (Allinen et al., 2004, Carito et al., 2012, Ward et al., 2013). For this reason, this study was implemented with an *in vivo* animal model, where the real tissue complexity and three-dimensionality is comparable to that of humans. The *in vivo* system used in this thesis is the transgenic mouse model of breast cancer, the MMTV-PyMT. The oncoprotein Middle T antigen is expressed specifically in the mammary epithelium, therefore limiting the development of genetic modifications to the tissue of interest (Guy et al., 1992). Moreover, the spontaneous tumourigenesis does not require the introduction of exogenous human cells, which would require the presence of immunocompromised mice. The mammary tumour developed by this model recapitulates well complexity (including the interaction with the stromal compartment) and stages of progression of human breast cancers (Lin et al., 2003) sharing morphological and molecular similarities with the luminal human subtype (Robles and Varticovski, 2008, Lim et al., 2010). For these reasons, this pre-clinical model represents a good parallel with the MCF-7 cell line (Herschkowitz et al., 2007, Lim et al., 2010), on top of being closer to humans than other mouse models. Interestingly, these tumours present a high inter-animal expression homogeneity that gives consistency to the model (Herschkowitz et al., 2007). In order to properly assess the metabolic phenotype of the mouse mammary tumours, it was necessary to optimise

the ¹³C-MFA technique for the model used in this thesis. Working on metabolism *in vivo*, great emphasis is put on the choice of the correct approach for substrate administration, so that the metabolism is not altered and at the same time, minimal stress possible is caused to the animal. The parenteral routes of administration involve two main approaches such as injection (mainly sub-cutaneous, intraperitoneal and intravenous routes), and infusions (Shimizu, 2004, Turner et al., 2011). In fact, a number of studies have employed ¹³C-labelled tracers to map metabolic pathways *in vivo*, in some cases performing an infusion of labelled substrate into the tail or jugular veins under total anaesthesia (Marin-Valencia et al., 2012, Bandsma et al., 2004, van Dijk et al., 2003, Meissner et al., 2011), and a bolus injection in other cases (Fan et al., 2011, Yuneva et al., 2012, Hassel and Brathe, 2000, Lane et al., 2009, Beger et al., 2009). However, it is necessary to consider that anaesthesia influences metabolism (Brown et al., 2005), and it was therefore chosen to avoid anaesthesia for this study. As for the injection approach, i.v. and i.p. routes both allow a rapid absorption of the tracer into the blood flow (Shimizu, 2004) ensuring the tracer delivery to the mammary tissue in a feasible time frame. This chapter illustrates the optimisation of the technique, first comparing i.p. and i.v. route of injection, then establishing the labelling time point which will allow subsequent investigations following [1,2-¹³C]glucose administration to the animal.

4.2 INJECTION METHOD

Substrates can be administered to the laboratory animal via multiple sites. In order to avoid anaesthesia, a bolus injection was the preferred method in this study. Among the different routes of injection possible, we chose to compare the i.p. and the i.v. routes. Tumour bearing mice were injected with natural abundance glucose via i.v., i.p., or did not receive any injection; subsequently, mice were sacrificed 20 minutes post injection, the tumour excised, the polar metabolites extracted and subjected to 1D-¹H NMR spectroscopy. In this way, metabolites were identified and quantified, in order to compare them among the different conditions, to determine the best injection method. This analysis led to the quantification of six metabolites for each condition, either linked to or independent from glucose metabolism (Figure 4.1). Overall, the concentrations after i.p. or i.v. did not change significantly from the control situation of mice which did not receive any injection. However, for most of the metabolites besides lactate, the i.v. approach shows a median skewed towards smaller concentration values than i.p. and control, suggesting metabolic perturbations induced as a response to this route of injection. Moreover, except for leucine, the dispersion of all the metabolite concentration values after i.v. injection is characterised by a bigger standard deviation than the i.p. (Table 4.1) evidencing a higher biological variability due to the i.v. approach. Therefore, the injection of glucose via the i.p. route *in vivo* appears to maintain a metabolic condition closer to the control tumour taken from mice that did not receive an injection, than the i.v., also ensuring higher reproducibility.

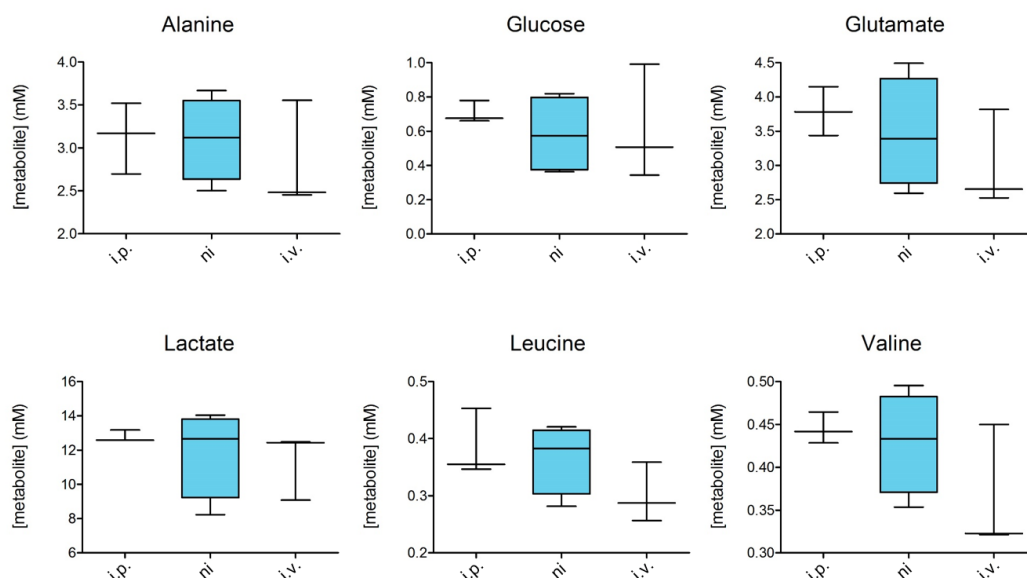


Figure 4.1. Comparison of injection sites.

Whiskers showing concentration (mM) of metabolite in the mouse mammary tumour metabolic extracts obtained analysing the 1D-¹H NMR spectra after unlabelled glucose intravenous (i.v.) or intraperitoneal (i.p.) bolus injection, compared to mice that did not receive any injection (ni). The median value is derived from three replicates for i.p. and i.v., and four replicates for ni. I.p. injection shows less variability than the i.v. and does not differ significantly from the control situation (ni).

Metabolite	SD	
	i.p.	i.v.
Alanine	0.4125	0.6267
Glucose	0.06449	0.3368
Glutamate	0.3555	0.7113
Lactate	0.3422	1.946
Leucine	0.05922	0.05248
Valine	0.01827	0.07393

Table 4.1 Metabolite concentration variability across replicates.

List of intra-tumoural metabolites assigned and standard deviation (SD) of the concentrations after i.p. and i.v. approach. All the metabolites besides leucine show a higher variability following i.v. injection compared to i.p.

4.3 LABELLING TIME POINT

In order to be able to unravel the metabolic phenotype of the mammary tumour developed by this mouse model, ¹³C-MFA was applied to the *in vivo* model. The previous results indicated an intraperitoneal bolus injection of glucose as the optimal approach of those studied. As stable isotope-labelled metabolites will be used dynamically depending on their availability to the tumour tissue, the point at which the tissue is sampled is likely to determine the sensitivity and resolution of downstream analyses. To investigate this, tumour-bearing mice were injected i.p. with a solution containing 100 nmoles of [1,2-¹³C]glucose and sacrificed 10, 20, 30 or 45 minutes after injection, before excision of the tumour. The amount of labelled glucose in the mammary tumour was assessed over time through quantification of the percentage of [1,2-¹³C]glucose isotopomer performing multiplet analysis on the improved 2D ¹H-¹³C-HSQC spectra (see 2.6.3) and comparing it across the different time points (Figure 4.2). The highest labelled glucose enrichment in the mammary tumour was reached 10 minutes post injection. After this time, the amount of labelled glucose present decreased until very little was left in the tumour 45 minutes post injection (Figure 4.2), presumably due to glucose being metabolised by the mammary tumour, although we cannot rule out the contribution of alterations in the availability of glucose in the peripheral plasma over time. The 30-minute time-point showed the highest reproducibility with over 10% of [1,2-¹³C]glucose remaining in the tissue (Figure 4.2), and was therefore chosen as the best time point for our purposes.

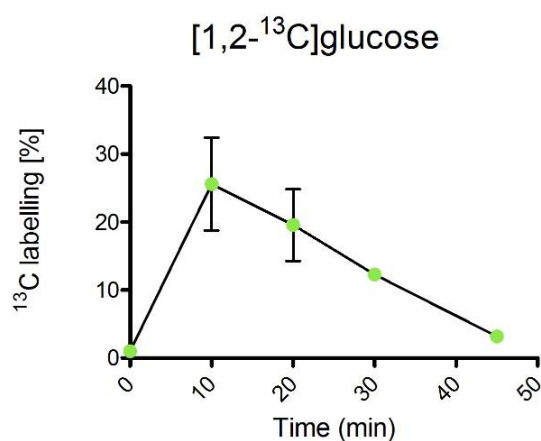


Figure 4.2. ^{13}C -glucose time-course in the mouse mammary tumour.

[1,2- ^{13}C]glucose percentage was calculated from the improved ^1H - ^{13}C -HSQC spectra obtained from mice sacrificed 10, 20, 30 or 45 minutes post injection. Plotted data are mean \pm SEM of 4 replicates for 10 and 30 minutes, and three replicates for 20 and 45 minutes. Maximum labelled glucose uptake into the mammary tumour is reached 10 minutes post injection, after which the enrichment progressively decreases reaching its minimum at 45 minutes. 30 minutes shows very little inter-animal variability, and represents a good compromise between the labelled glucose peak and the total consumption of it.

4.4 DISCUSSION

A number of studies demonstrated the importance of the tumour microenvironment for cancer survival, growth and resistance to therapy *in vivo* (Allinen et al., 2004, Carito et al., 2012, Ward et al., 2013). The bi-dimensionality of the *in vitro* samples does not account for the real complexity of the tumour-environment system *in vivo*. For this reason, it is necessary to move a step towards the human tumours, and this can be achieved using animal models. In particular, in this thesis the MMTV-PyMT transgenic mouse model of breast cancer was used. This model spontaneously develops mammary tumours that resemble the human disease in many respects (Lin et al., 2003, Lim et al., 2010).

The relevance of metabolic investigations to characterize tumour's phenotype had been previously stressed (see 1.3.1). Moreover, the ¹³C-MFA approach represents a powerful tool not only for *in vitro* systems, but also for animal models and human patients (Maher et al., 2012), as it uses a stable isotope and therefore avoids the safety issues found with the ¹⁸F or ¹¹C radioisotopes, also used in the clinic (Ho et al., 2014, Territo et al., 2015). However, *in vivo* studies using ¹³C-MFA are still in their infancy, and therefore standardisation of the methodological approach has not yet been done. Hence, this chapter illustrated the optimisation of the most suitable method to inject ¹³C-labelled substrates in our *in vivo* model in order to achieve quantifiable incorporation of glucose into the tumour tissue.

While many studies performed infusion of tracers, for our purposes it was necessary to avoid anaesthesia, which has been shown to alter metabolism (Kashiwagi et al., 2015, Schallner et al., 2014, Ayala et al., 2010, Brown et al., 2005). In order to determine the most appropriate mode of delivery for the study, we analysed the effect

of a bolus of glucose on a number of intra-tumoural metabolite concentrations, administered either through the intravenous or intraperitoneal routes. Although no significant differences in concentrations were found between the two methods compared to control mice, the cohort that had received glucose via the i.v. route exhibited higher variability between replicates (Table 4.1). There is also a higher risk to the animal after i.v. injection due to both the technical demands of the method (e.g. accidental perivascular injection especially in small animals, septicaemia, embolism) (Turner et al., 2011), and the physiological effects of a bolus of glucose (given at a concentration of 1M). Previous studies identified the i.p. route as a valid alternative to the i.v. showing a slower but comparable distribution of the tracer into the blood stream first, and into the organs after (Wong et al., 2011). Moreover, i.p. requires a less invasive and stressful handling of the mouse, while the i.v. injection requires the animal to spend a longer time in the restraint tube causing stress to the mouse (Shimizu, 2004). Overall, the i.p. injection was therefore found to be a more suitable.

The calculation of the ¹³C-enrichment in the *in vitro* system required the production of two identical samples in parallel, one provided with ¹³C-labelled glucose and the other with unlabelled glucose, in order to calculate the ¹³C-enrichment compared to natural abundance. This method is however not ideal for *in vivo* applications as the variability between subjects leads to poor reproducibility. Therefore, it was not feasible to use the mouse injected with unlabelled glucose as a control for the calculation of the ¹³C-enrichment. A different approach that has been developed by Dr. Christian Ludwig was used in this study, in which the relative ¹³C-enrichment into metabolites can be worked out using just the information of each NMR signal's structure (multiplet analysis, see 1.3.2 and 2.6.3) in the spectra derived from ¹³C-injected mice.

The bolus-injection approach does not result in or rely on isotopic steady-state labelling of the tissue or animal, which means that transient label enrichment in the intracellular metabolite pool was quantified instead (Noh et al., 2007, Wiechert and Noh, 2013). By excising the tumour at different time points after the injection, it is possible to construct a time-course of labelled glucose accumulation inside the mammary tumour. The highest enrichment was detectable 10 minutes after the injection, followed by a decrease in the percentage of labelled glucose inside the tumour, presumably due to its catabolism into downstream metabolites, although possible alterations in the availability of glucose in the peripheral plasma over time must also be considered. The decrease continued until almost no labelled tracer was left in the tissue 45 minutes post injection. In order to allow the build-up of enough downstream labelled metabolites 30 minutes was chosen as the best time point to perform downstream metabolic analysis of the mammary tumour. The combination of the use of this time point and improved ^1H - ^{13}C -HSQC spectra permitted an enhanced sensitivity over conventional NMR approaches and allowed good resolution of multiplet patterns.

The development of this method was carried out on the assumption that the distribution of the labelled tracer into the mammary tissue would be homogenous. However, as mentioned in the introduction, it is already well known that solid tumours are characterised by hypoxic areas (Allinen et al., 2004, Vaupel and Mayer, 2007) where the blood supply is absent or very limited. This aspect could indeed influence the diffusion of labelled glucose into the tumour, creating areas where the labelled glucose is absent which would lead to wrong conclusions and a high variability among different tumours and different areas of the same tumour. In this case, the choice of the area of

interest should not be determined randomly, but it could be taken following the imaging of the labelled glucose distribution into the mammary tumour through PET.

CHAPTER 5

RESIDUAL MAMMARY TUMOUR METABOLIC PHENOTYPE AFTER DOCETAXEL TREATMENT *IN VIVO*

5.1 INTRODUCTION

The pivotal role of residual tumours in affecting cancer patient survival has already been addressed in the previous chapters. Moreover, the contribution of the tumour microenvironment for the fate of the cancerous mass (Allinen et al., 2004, Carito et al., 2012, Ward et al., 2013, Iyengar et al., 2005) makes it necessary to study residual tumours in models that better resemble the human disease than the simplified *in vitro* experimental settings.

Pre-clinical models represent a good compromise between *in vitro* and clinical studies (Lim et al., 2010). In particular, the MMTV-PyMT transgenic mouse model of breast cancer mimics human patient's disease and progression to the aggressive, metastatic tumour well (Lin et al., 2003) and has therefore been chosen in this thesis as the *in vivo* model to study residual mammary tumours following docetaxel treatment. The mice used for this work underwent a docetaxel treatment schedule to mimic patient treatment, i.e. multiple cycles of chemotherapy with several days recovery between each cycle (Korde et al., 2010), after which residual tumours were available for investigations. Previous *in vivo* studies investigating docetaxel treatment of mammary tumours have concentrated on elucidating possible mechanisms of resistance (Tan et al., 2012), treatment efficacy (Morse et al., 2007), as well as gene expression pattern characterisation of residual tumours (Franci et al., 2013, Chang et al., 2005). Cancer cells remaining after treatment have been shown as a potential source of tumour relapse, exhibiting tumour-initiating features (Creighton et al., 2009). Moreover, they were shown to switch to a mesenchymal phenotype, expressing markers such as vimentin and metalloproteinase-2, increasing motility and invasive potential (Thiery and Sleeman, 2006), phenotype which is also thought to be more chemotherapy

resistant (Kajiyama et al., 2007). Other studies looked at biomarkers of tumour sensitivity or resistance to docetaxel in breast cancer patients, highlighting clear differences between the two categories, especially in the expression of genes controlling key processes such as cell cycle, DNA repair mechanisms and microtubule depolymerisation (Korde et al., 2010, Chang et al., 2003). Altogether, these lines of evidence support the malignant potential of the residual cancer, reinforcing the need for further investigation on the underlying mechanisms responsible. To our knowledge, there are no studies conducted in the MMTV-PyMT model looking at the metabolic phenotype of residual tumours, therefore this chapter will illustrate all our metabolic investigations on the residual mouse mammary tumours after docetaxel treatment.

5.2 TUMOUR VOLUMES

Solid cancer treatment efficacy can be evaluated based on the reduction of tumour mass (Eisenhauer et al., 2009). Therefore, MMTV-PyMT tumour-bearing female mice were treated starting at 9 weeks of age with docetaxel (35 mg/kg) and tumour volumes were measured one week after the last dose of chemotherapy comparing them to control saline-injected mice (placebo). Tax-treated mammary tumours showed a highly significant reduction in volume, compared to control (Figure 5.1, $p=0.0009$). However, the reduction was not 100% but rather an incomplete response of mammary tumours to docetaxel in this experimental model leading to the survival of a small group of cancer cells, here termed residual tumour. This phenotype is highly similar to that observed in breast cancer patients. Moreover, the assessment of tumour dimensions resulted in a clear separation into two groups for the untreated mice (Figure 5.1) which could represent the existence of subclasses of these mouse mammary tumours.

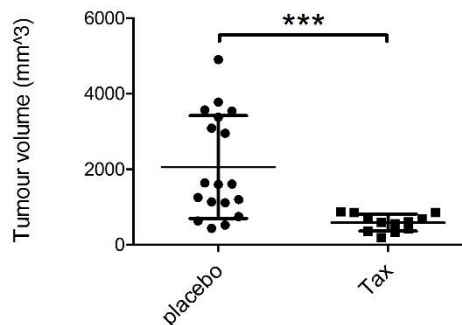


Figure 5.1. Tumour shrinkage after docetaxel treatment.

MMTV-PyMT tumour-bearing female mice dosed with 35 mg/kg docetaxel (Tax) compared to untreated (placebo). Mammary tumours were measured using digital callipers a week after the last dose of treatment and showed a highly significant reduction in tumour volume (mm³) post Tax, compared to untreated tumours ($p<0.001$). The scatter dot-plot shows mean \pm SD obtained from 18 replicates for placebo and 12 replicates for Tax.

5.3 GENE EXPRESSION ANALYSIS

Gene expression patterns vary within a tumour depending on the microenvironment and acquisition of additional genetic mutations (Martinez et al., 2015, Cooper et al., 2012, Gandellini et al., 2015). Chemotherapy and radiotherapy treatments are known to elicit changes in gene expression – either as part of the cell death or a survival response (Chang et al., 2003, Scherf et al., 2000). As the surviving cells after chemotherapy are likely to have survived due to upregulation of a specific set of survival pathways, analysis of the gene expression of these residual cells could provide some evidence of how they evade docetaxel-mediated cell death.

In order to delineate the gene expression profile in the MMTV-PyMT mouse model, RNA was extracted from residual (TAX) and untreated (placebo) mammary tumours and RNA sequencing performed as described in section 2.5.1. The differential analysis between the two conditions evidenced only six genes differentially expressed with statistical significance ($p < 0.05$) as listed in Table 5.1 and shown in Figure 5.2. Among those, five showed higher expression in the residual tumours, and only one, the RIKEN cDNA 2310057J18 gene, showed a decreased expression after treatment (Figure 5.2). Two of these genes have an unknown biological function, the RIKEN cDNA 2310057J18 gene and Fer-1-like 4, while three of them present involvement with skeletal muscle tissue (Ankyrin repeat domain 23, Cardiomyopathy associated 5, Xin actin-binding repeat containing 1) (Miller et al., 2003, Sarparanta, 2008, Hawke et al., 2007). Only one of them, the Mucin 4 (Muc4) gene, expresses a protein localised in epithelial cells (Rakha et al., 2005). The expression level of some of these genes, the Ankyrin repeat domain 23 and the Xin actin-binding repeat containing 1 in particular, is very low in the placebo-treated tumours (Figure 5.2). Overall, this is a very interesting

result, as it suggests that after treatment, the residual cells maintain an expression profile highly similar to that of the untreated tumours, and therefore treatment itself does not induce significant permanent alterations in gene expression. However, changes in metabolism can occur in the absence of gene expression changes, as pathway use can alter without the need for changes in enzyme expression. We therefore wished to investigate whether any changes in metabolism were elicited by docetaxel treatment in the cells that survived, despite the lack of transcriptional changes.

Gene name	Log2FoldChange	PValue*
Ankyrin repeat domain 23	-1.61868	0.02598
RIKEN cDNA 2310057J18 gene	1.09026	0.01070
Cardiomyopathy associated 5	-1.75184	0.00952
Fer-1-like 4	-1.44800	0.00952
Mucin 4	-1.56930	0.00952
Xin actin-binding repeat containing 1	-2.66203	0.00952

Table 5.1. Residual tumour gene expression analysis.

List of genes differentially expressed between residual and placebo tumours with statistically significant P values, ordered from the smallest statistical power to the highest. *=Benjamini & Hochberg adjusted p-value.

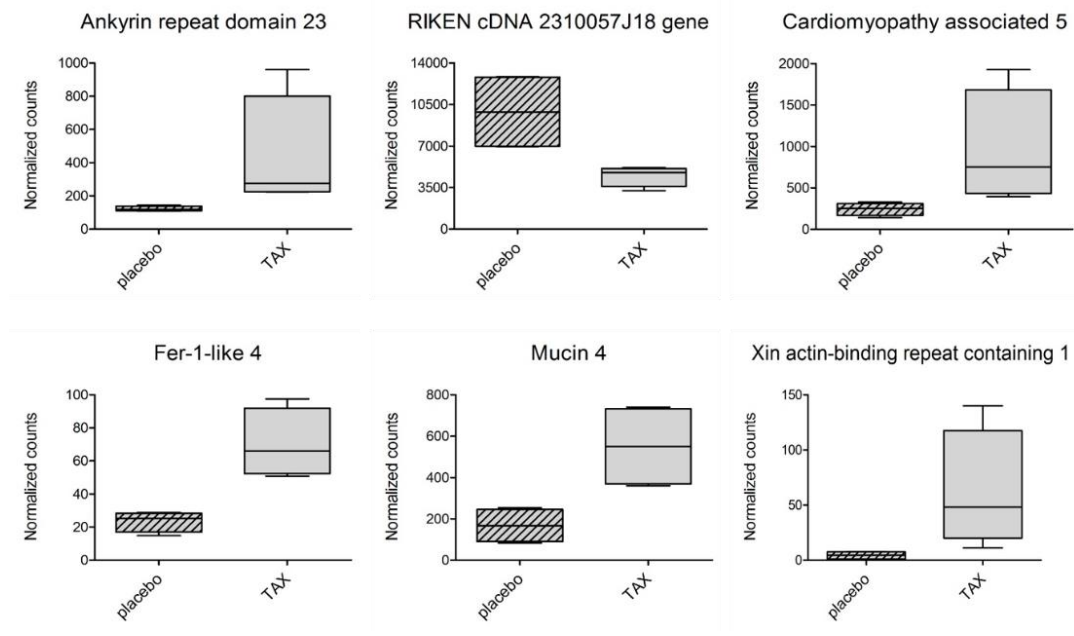


Figure 5.2. Residual mammary tumour differential gene expression.

Box-and-Whiskers showing the expression level of significantly ($p < 0.05$) up or down-regulated genes in residual tumours (TAX) compared to placebo tumours obtained after RNA sequencing. The line in the middle of the box represents the median, calculated from four replicates each condition.

5.4 RESIDUAL TUMOUR METABOLIC ANALYSIS

Any alteration of the cellular physiology is likely to be mirrored by changes in the composition and amount of cellular metabolites. In order to characterise the metabolic phenotype of the MMTV-PyMT-derived residual mammary tumours compared to the control group (placebo), tumours were harvested one week after the last dose of treatment and polar metabolites extracted (see 2.5.2). 1D-¹H NMR spectra were then acquired and used for metabolite identification and quantification as described in 2.6.3. This analysis led to the assignments of 14 metabolites in each spectrum, most of which were essential and non-essential amino acids (Figure 5.3A-B), glycolysis-derived metabolites (Figure 5.3C) and choline-derived metabolites (Figure 5.3D). Most of them could also be identified in the previous analysis of *in vitro* grown cells. However, comparing each metabolite's concentration in the residual tumours (TAX) with that in the untreated tumours (placebo), no significant differences emerged between the two conditions (Figure 5.3), contrary to our *in vitro* observations. Although these results could be understood as an unchanged tumour metabolism after treatment, a fine *in vivo* control of metabolites concentration that would quickly compensate for alterations should be taken into account. Moreover, the maintenance of the total metabolite pool could still be possible even in presence of alteration in the usage or production of metabolites. In order to test this hypothesis, and unravel the metabolic pathways involved, we performed stable isotope labelled tracer studies.

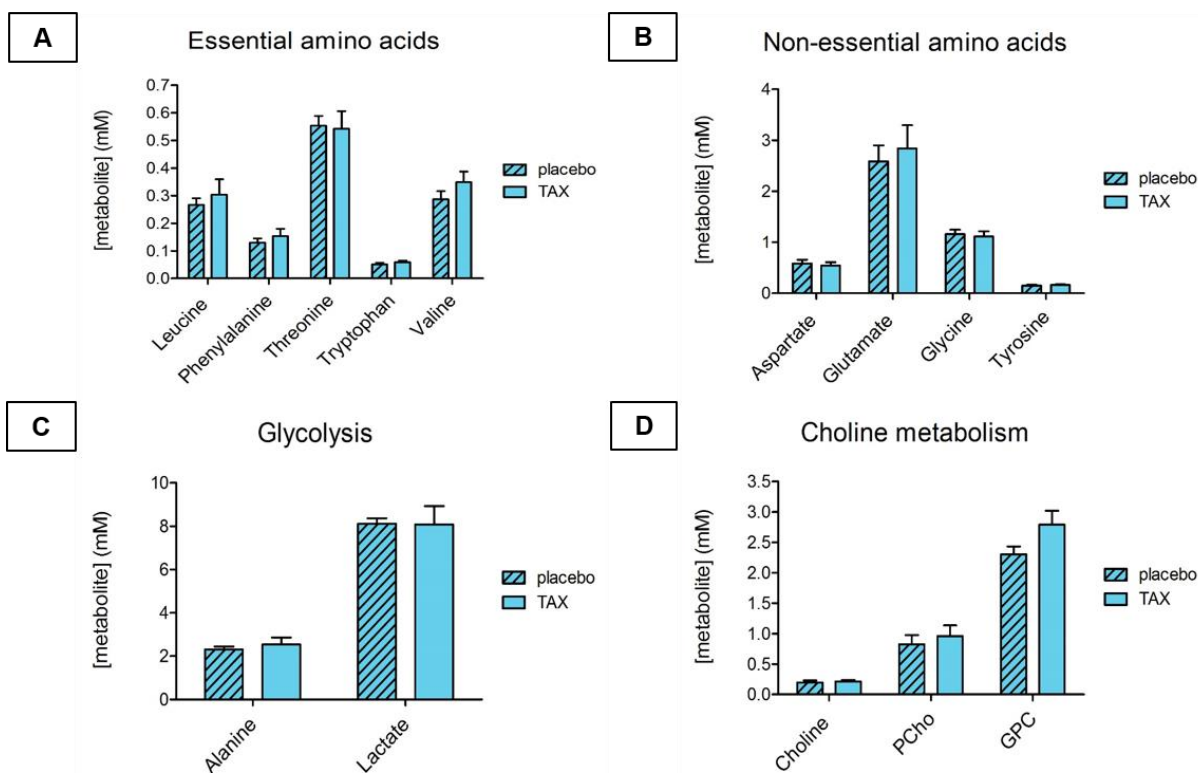


Figure 5.3. Mammary tumour-derived metabolite quantification.

Histograms representing the quantification of metabolites (in mM) within residual (TAX) and untreated (placebo) mammary tumours metabolic extracts, obtained analysing the 1D-proton NMR spectra. Concentrations are normalised per mg of tissue extracted. Results are shown as mean \pm SEM derived from four replicates for placebo and three replicates for TAX. No significant differences are identified in (A) essential, (B) non-essential amino acids, (C) glycolysis-derived and (D) choline-derived metabolites comparing residual and placebo tumours. Abbreviations: GPC, glycerophosphocholine; PCho, phosphorylcholine.

5.5 RESIDUAL TUMOUR ^{13}C -MFA BY NMR

5.5.1 Determining labelling time point

30 minutes was previously defined as the best time point to sample the mouse mammary tumour after $[1,2-^{13}\text{C}]$ glucose i.p. injection (Figure 4.2). However, following docetaxel treatment tumour volume is drastically reduced (Figure 5.1) affecting the amount of glucose consumed in that time-frame by the residual tumour compared to the untreated one. Assuming a lower consumption given by the smaller number of cancer cells in the residual tumours, a longer time point was tested for those mice. In fact, at 45 minutes post injection, residual tumours (TAX) showed an intra-tumour $[1,2-^{13}\text{C}]$ glucose availability similar to the placebo tumours at the 30 minutes time-point (Figure 5.4). These two time-points were therefore used for all the subsequent analyses in order to permit a fair comparison of metabolism between the two tumours.

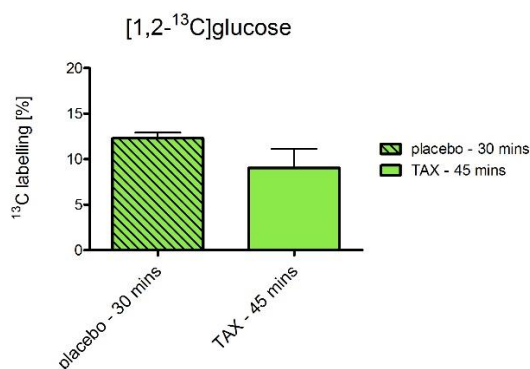


Figure 5.4. $[1,2-^{13}\text{C}]$ glucose enrichment in the mouse mammary tumour.

Histograms show the percentage of the $[1,2-^{13}\text{C}]$ glucose isotopomer in the residual (TAX) or control (placebo) tumour 45 or 30 minutes after labelled glucose injection, respectively. The percentages were calculated via multiplet analysis in the $^1\text{H}-^{13}\text{C}$ -HSQC spectra and are shown as mean \pm SEM of 4 replicates for placebo and three replicates for TAX. A longer time-point (45 minutes) is necessary for the residual tumour to reach a labelled glucose enrichment similar to the placebo tumour at 30 minutes post-injection.

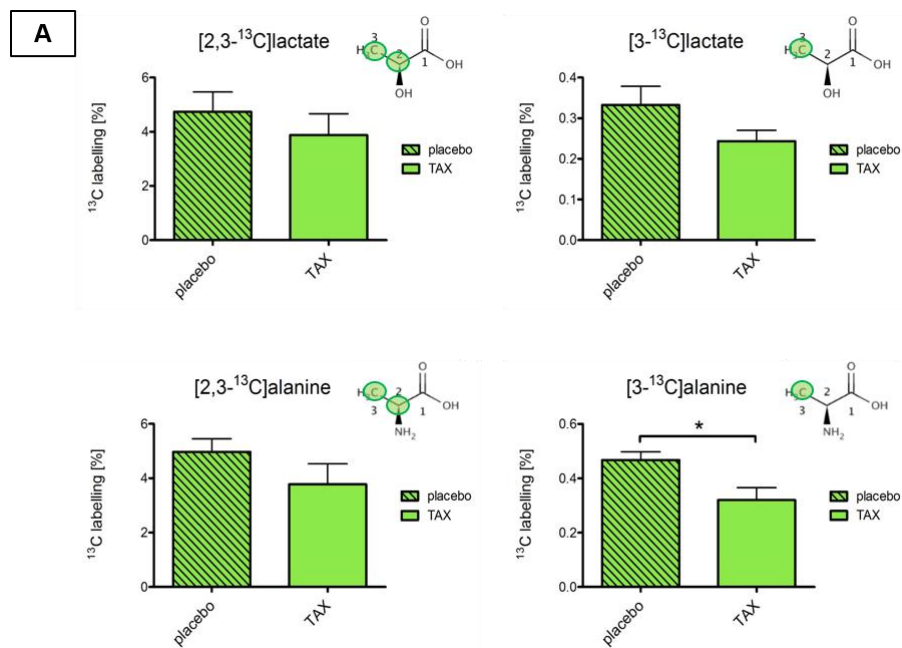
5.5.2 Comparing ^{13}C -MFA between residual and control tumours

Tracer based metabolic analysis using ^{13}C -labelled metabolic precursors (^{13}C -MFA) is a powerful tool to analyse metabolic mechanisms of phenotypic change, and adds complementary information over the analysis of metabolite concentrations. The additional information from fluxes allows for the assignment of the use of individual pathways.

Before harvesting the mammary tumours at the appropriate time point (described above in Figure 5.4), treated and untreated mice were injected i.p. with [1,2- ^{13}C]glucose. Metabolites were extracted from residual and placebo-treated (control) mammary tumours for subsequent NMR spectroscopy analysis using HSQC spectra (see 2.6.2, 2.6.3), acquired with NUS to have sufficient resolution in the incremented dimension to see ^{13}C - ^{13}C splittings in order to uniquely determine the isotopomer. The analysis of the percentage of the multiplet component for each labelled carbon in the identified metabolites allowed the simulation of the isotopomers present in the mixture (see 2.6.3). In this way, it was possible to trace the transition of the labelled carbons into different metabolites and to map the pathways by which the labelled glucose substrate was metabolised in the mouse mammary tumour tissue. Moreover, the relative abundance of each isotopomer was compared to uncover differences between Tax-treated residual and placebo-treated tumours. ^{13}C incorporation was observed into metabolites characteristic of glucose use through glycolysis, such as lactate and alanine (Figure 5.5A). Although there are no significant differences in the percentage of [2,3- ^{13}C]lactate and [2,3- ^{13}C]alanine isotopomers observed in residual (TAX) and untreated (placebo) tumours, the contribution of the oxidative branch of the PPP to the production of these two metabolites (recognised from the ^{13}C incorporation into C3-

only; see Figure 1.4D), appeared decreased in the residual tumours (Figure 5.5A). However, only the percentage of [3-¹³C]alanine isotopomer was significantly reduced in the residual tumours ($p=0.0367$). ¹³C-labelled pyruvate (itself not detected in HSQC spectra) was observed to have entered the TCA cycle, as evidenced by the label incorporation into intermediates such as succinate and malate (Figure 5.5B), demonstrating active oxidative mitochondrial metabolism in both conditions. Being a symmetric molecule, succinate isotopomers are identical, therefore we conventionally identified them as [1,2-¹³C] or [3,4-¹³C] isotopomers, consequently resulting in the production of [1,2-¹³C] or [3,4-¹³C] malate (Figure 5.5B). These isotopomers were slightly less abundant in the residual tumours, although with low statistical significance. Some TCA cycle intermediates were also observed to be used as precursors for the production of other metabolites such as glutamate, glutamine and aspartate (Figure 5.5B). The isotopomers predominantly present were [4,5-¹³C]glutamate, [4,5-¹³C]glutamine, [1,2-¹³C] and [3,4-¹³C]aspartate (Figure 5.5B) produced in the first round of a cycle in which glycolysis-derived [2,3-¹³C]pyruvate is oxidised to acetyl CoA by the PDH enzyme before entering the TCA cycle. A second round of the cycle from labelled oxaloacetate resulted in the production of [1,2-¹³C]glutamate and [3-¹³C]glutamate (Figure 5.5B); these molecules were then converted to [1,2-¹³C]glutamine and [3-¹³C]glutamine respectively (Figure 5.5B). The [1,2-¹³C]glutamine isotopomer is a larger proportion of the total glutamine pool in the untreated tumours compared to the treated tumours, although the difference did not reach significance. PDH-mediated conversion of pyruvate to acetyl CoA is not the only entry point of pyruvate into the TCA cycle. In fact, [2,3-¹³C]glutamate, [2,3-¹³C]glutamine and [2,3-¹³C]aspartate isotopomers were produced following the carboxylation of [2,3-

^{13}C]pyruvate by the PC enzyme to form oxaloacetate (see Figure 3.7). However, its contribution appeared similar between residual and untreated tumours.



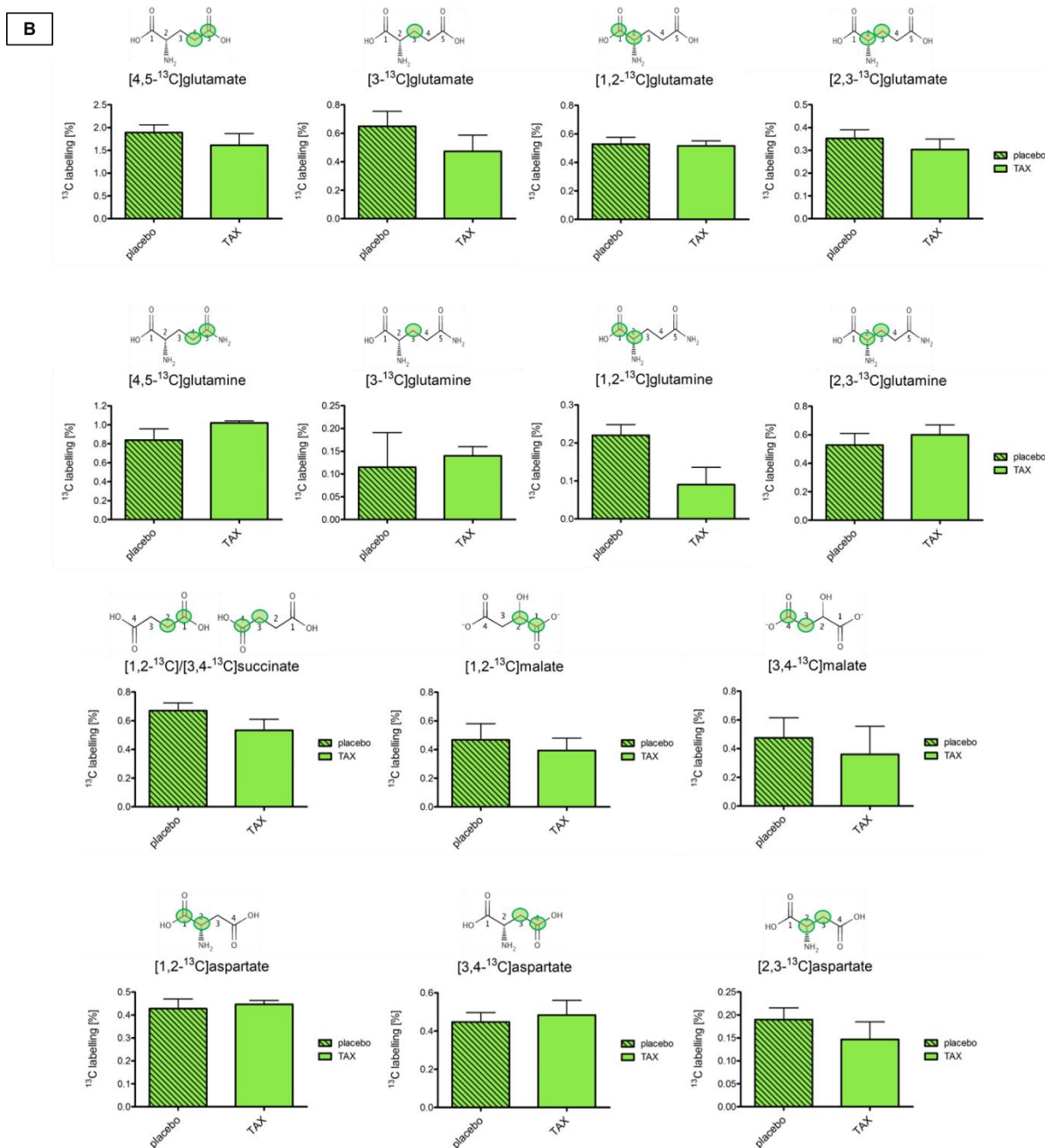


Figure 5.5. Isotopomers derived from $[1,2-^{13}\text{C}]$ glucose metabolism by the mouse mammary tumour.

Histograms representing the relative abundance of each isotopomer derived from the catabolism of the $[1,2-^{13}\text{C}]$ glucose substrate by the residual (TAX) and control (placebo) mammary tumours. Comparing the percentage of (A) glycolysis-derived metabolite and (B) TCA cycle-derived metabolite isotopomers, only $[3-^{13}\text{C}]$ alanine was significantly less produced in the residual tumours. Data are shown as mean \pm SEM of 4 replicates for placebo and three replicates for TAX.

5.6 MIDA by GC-MS

Mass spectrometry represents another analytical technique used to quantify the abundance of the different isotopomers in a metabolite pool after labelled substrate consumption. Moreover, this technique offers higher sensitivity than NMR spectroscopy, allowing the detection of very low abundance metabolites that could have been missed by the NMR spectroscopy-based metabolic analysis. Residual and control tumour-derived metabolites were analysed applying a GC-MS method (see 2.5.4) optimised in particular for the detection of TCA cycle intermediates, on top of the more common glycolysis-derived metabolites. Subsequently, a mass isotopomer distribution analysis (MIDA) was performed for each metabolite assigned. The different mass isotopomers are identified by the $m+n$ nomenclature, where n is the number of ^{13}C -labelled atoms present in the molecule. However, it is not possible to deduct the exact position of the labelled atom using the MS data only. The metabolism of the [1,2- ^{13}C]glucose through glycolysis led to incorporation of two ^{13}C atoms into pyruvate which was then rapidly converted to lactate and alanine, as evidenced by the very small fraction of $m+2$ pyruvate in contrast with a fairly high amount of $m+2$ alanine and lactate (Figure 5.6A). No differences were evidenced in this pathway for placebo and residual tumours, confirming the NMR analysis. The contribution of the oxidative PPP branch however, resulting in the production of $m+1$ pyruvate, was significantly higher in the residual tumours ($p=0.0322$, Figure 5.6A), but did not correspond to increased $m+1$ lactate and alanine, suggesting its consumption through the TCA cycle. In fact, Krebs cycle activity in these samples was confirmed by the identification of labelled citrate and malate (Figure 5.6B), in particular the single labelled malate species was slightly more abundant in the residual tumours. This was true also for the TCA cycle-

derived m+1 aspartate and glutamate (Figure 5.6B), however none of these differences was of statistical significance. The m+2 isotopomer of pyruvate is the main nutrient source of the TCA cycle as confirmed by the production of m+2 citrate, malate, aspartate and glutamate (Figure 5.6B). Unfortunately, this analysis was conducted on four replicates for placebo and only two replicates for Tax-treated mice, therefore we did not have a sufficient number of replicates to reach a good statistical power.

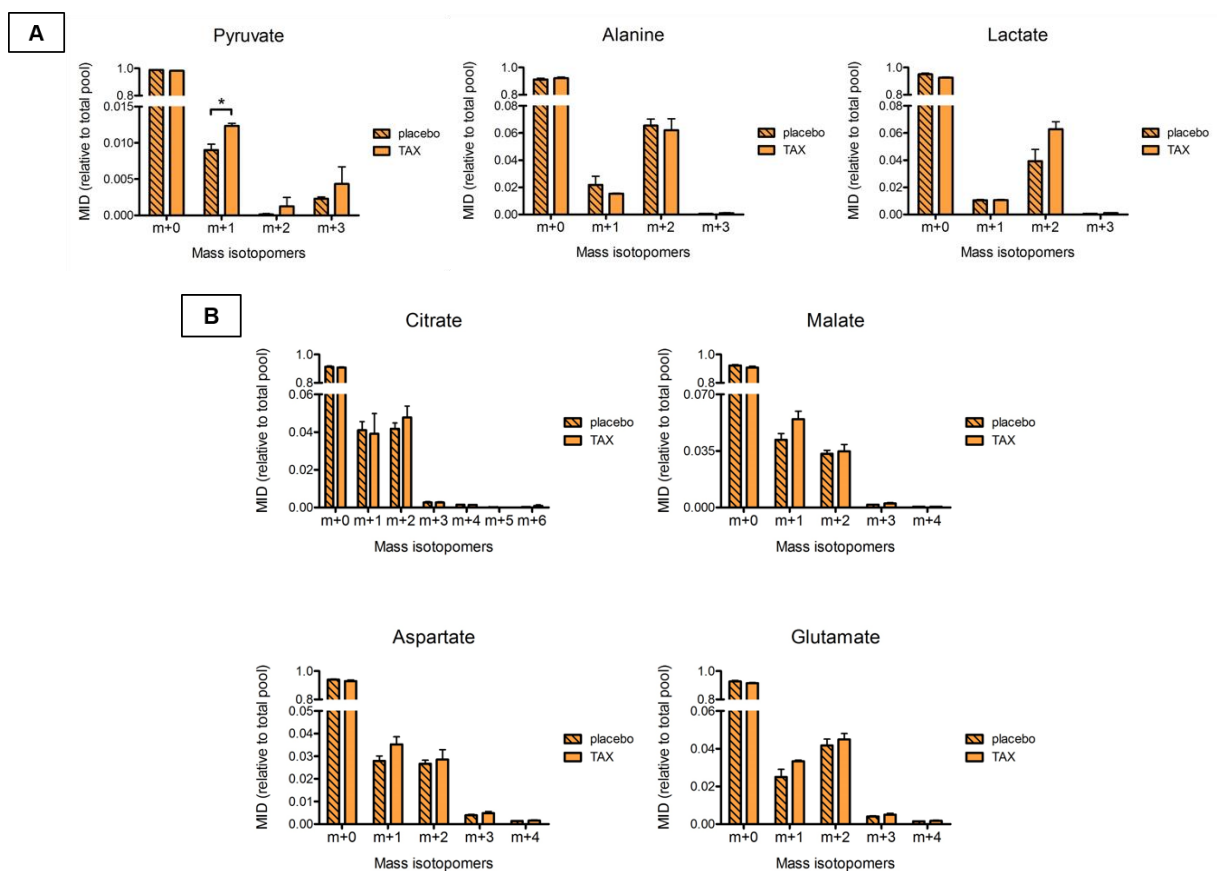


Figure 5.6. MIDA of [1,2-¹³C]glucose-derived mammary tumour metabolites.

Mammary tumour metabolites derived from [1,2-¹³C]glucose- injected treated (TAX) and control (placebo) mice were analysed by GC-MS (data acquired in collaboration with Marta Cascante at the University of Barcelona). Histograms showing the distribution and relative abundance of the different mass isotopomers (MID) relative to the total pool of A) glycolysis-derived and B) TCA cycle-derived metabolites. Data are shown as mean ± SEM of four replicates for placebo and two replicates for TAX.

5.7 DISCUSSION

The MMTV-PyMT mice have been used in this thesis to model the *in vivo* development of residual mammary tumours following the incomplete response of the tumours to the anti-microtubule agent docetaxel. The schedule used for these *in vivo* experiments consisted in two cycles of docetaxel treatment of tumour-bearing female mice starting at 9 weeks of age: at this age, mammary tumours, corresponding to early carcinoma stage (Lin et al., 2003), are palpable. The analysis of the residual mammary tumours instead, started one week after the last treatment. This approach allowed tumour cells to recover from the drug having enough time to metabolise and systemically eliminate the chemotherapy. Hence, as for the *in vitro* study, it was possible to investigate the residual mammary tumour phenotype excluding the short-term docetaxel-induced alterations. All results were compared to the untreated tumours derived from placebo-injected mice.

Firstly, tumour volumes were measured, which were significantly different between control and residual tumours, with docetaxel treatment causing large reductions in tumour size. It is important to note that the measurements were taken at the experimental endpoint, when the untreated tumour had developed a significant mass. Therefore, this result is interpreted as a reduced tumour volume due to treatment. In order to gain a better understanding of the metabolic changes occurring in the tumours in response to treatment, samples could be taken daily from the beginning of the treatment until the end of the experiment. At 9 weeks of age, the tumours are small and do not appear to increase in size during docetaxel treatment. This could mean the presence of a mixture of tumour cells, where a small fraction is dying, another fraction might be growing and other cells might be in growth arrest keeping the volume of the

mammary tumour quite constant. The presence of cells in growth arrest is in accordance to docetaxel anti-mitotic mode of action (Bayet-Robert et al., 2010) and also confirms what was observed in the *in vitro* results. Similarly, it would be appealing to determine when and if these cells were able to resume proliferation leading to cancer relapse. Moreover, two clear clusters of mammary tumours were observed in the placebo-treated mice, which may indicate the presence of different phenotypes, supporting the intra-tumoural heterogeneity typical of breast cancer (Skibinski and Kuperwasser, 2015, Martelotto et al., 2014). It would be interesting to investigate whether these two groups resulted in different sensitivity and response to the drug.

Cancer treatment could induce transcriptional changes, as well as intrinsic pre-existing genetic alterations (due to the presence of the transgene) could determine sensitivity or resistance to chemotherapy, and both situations could be at the heart of the metabolic reprogramming observed in these tumours. We therefore wished to perform gene expression analysis through sequencing of the residual and control tumour-derived mRNA. This analysis yielded only six genes significantly differentially expressed between residual and control tumours, possibly suggesting the need for a bigger number of samples of each condition given the high variability among different animals. Interestingly, these six genes were not previously linked to docetaxel residual mammary tumours. The only gene showing decreased expression in residual tumours was the RIKEN cDNA 2310057J18 gene whose biological function is still unknown. Among the genes predominantly expressed in the residual tumours, one has unknown biological function (Fer-1-like 4 gene), while the other four genes have been extensively described, although not in the context of cancer. The Ankyrin repeat domain 23 is part of the MARPs family (muscle ankyrin repeat proteins) mediating

interaction with titins in striated muscles (Miller et al., 2003). It is also known as DARP (diabetes-related ankyrin repeat protein), showing involvement with energy metabolism being more expressed in muscle (cardiac and skeletal) of insulin-resistant mice (Ikeda et al., 2003). The G2SBC database lists this gene as expressed in the mammary gland and in breast tumour, although there is no histological evidence of this. The Cardiomyopathy associated 5 gene expresses a protein also known as myospryn, localised in skeletal and cardiac muscles only (Sarparanta, 2008). It has been shown to be involved in the biogenesis of lysosome-related organelle complex, in protein kinase A signalling and titin-binding (Sarparanta, 2008) as well as the previous gene, playing an important role in muscle integrity maintenance. More recently, it has been shown to interact with and negatively regulate calcineurin activity, repressing muscle regeneration after injury (Kielbasa et al., 2011). The Xin actin-binding repeat containing 1 adapter protein is localised at cell-cell junctions of striated muscles and is involved in muscle regeneration and actin cytoskeleton remodelling (Hawke et al., 2007). Interestingly, all of the three above-described genes' present involvement with skeletal muscles and response to injuries. Given that they are significantly more expressed in the residual tumours, this might unveil an injury-like response to docetaxel treatment.

The fifth gene with higher expression in the residual cells is Muc4, which is the only one previously shown to be expressed in breast cancer (Workman et al., 2009, Rakha et al., 2005) and in particular overexpressed in metastatic breast cancer (Workman et al., 2009). It belongs to the mucin family (Rakha et al., 2005) among which the Mucin 1 gene expresses the well-known recurrent breast cancer serum biomarker CA 15-3 (Lee et al., 2013). It is already well known how much ErbBs activation contribute to

tumour development, in particular ErbB2 activation induces loss of cell-cell adhesion during early steps of tumour formation (Carraway et al., 2005). Muc4 has been identified as the ErbB2 intra-membrane ligand (Carraway et al., 2002) able to potentiate ErbB2-ErbB3 activation, therefore favouring tumour progression (Kozloski et al., 2010). However, our gene expression analysis did not evidence ErbB2 differential expression, therefore the Muc4 ErbB2-independent activity is more likely, as well as its anti-adhesion properties (Komatsu et al., 1997). This is further supported by its anti-apoptotic activity which inhibits the apoptosis response to cell detachment (Komatsu et al., 2001). Moreover, Muc4 overexpression has been shown to be responsible of immune-mediated tumour cell killing inhibition (Komatsu et al., 1999). Muc4 has been previously shown to be involved in chemoresistance in pancreatic cancer (Bafna et al., 2009), in melanoma cells (for paclitaxel, doxorubicin and vinblastine) (Hu et al., 2003) and in resistance to ER and HER2- targeted therapies in breast cancer (Chen et al., 2012). However, it is not known to be involved in resistance to docetaxel. Exploiting all the properties listed above, Muc4 mediates tumour progression, cell migration, invasiveness and resistance, therefore its higher expression in the residual tumours compared to the placebo-treated tumours could point to a more aggressive and malignant phenotype of these cells that survived docetaxel treatment.

Despite the interesting speculations about the six differentially expressed genes, it is worth noting that they are very few compared to what would be expected from such analysis. In fact, similar studies performing gene expression analysis were able to identify a higher number of pathways upregulated in residual tumours, among which the Jak/Stat pathway and a number of histone methyltransferases (Franci et al., 2013),

as well as enrichment in claudin-low and tumour-initiating features (Creighton et al., 2009). Interestingly, many of the features present in the residual tumour were not maintained in the relapsed one, which in turn showed a phenotype more similar to the primary tumour (Franci et al., 2013). This observation might support the hypothesis that the time point we used for the analysis of the residual mammary tumour was too late (one week after the last dose of treatment), leaving sufficient time to the tumour to potentially go back to a phenotype more similar to the primary tumour. This would explain the very few differences emerged between placebo and residual mammary tumours.

Although few studies investigated docetaxel influence on gene expression in breast cancer (Chang et al., 2005, Creighton et al., 2009, Korde et al., 2010), no previous work has characterised the metabolic phenotype of the residual breast cancers after docetaxel treatment. To address this question, a targeted metabolic analysis was performed to compare metabolite concentrations between residual and untreated mammary tumours. The metabolites identified in these samples can be classified in three main groups, such as essential and non-essential amino acids, glycolysis-derived and choline-metabolism related metabolites. Interestingly, unlike the cells, the mouse-derived metabolite quantification did not evidence any difference between Tax-treated and placebo mice. This could be explained by a higher *in vivo* turn-over of metabolites to keep their total pool at a steady-state level. For this reason, a more detailed analysis of metabolic mechanisms, using stable-isotope labelled tracers was employed to unveil differences on the dynamic of metabolite production or consumption. Moreover, the choline-derived metabolite's results are surprising: in fact, PCho has been previously shown to decrease after docetaxel treatment *in vivo* (Morse

et al., 2007), therefore used as a marker of treatment response. The maintenance of the cancer typical PCho signature in the residual tumours can therefore be a further confirmation of the incomplete response to docetaxel in these cancer cells. However, the apparent disparity in results could also be a product of the system and time point used for analysis. The study by Morse *et al.*, used sub-cutaneous xenografts of human breast cancer cell lines into immunocompromised mice – these tumours neither have the appropriate stroma, vasculature nor a chemotherapy-elicited immune response. In addition, the study was performed on tumour 2 and 4 days post-treatment, when the tumours are likely still responding directly to the toxic insult. Our data suggest that after this initial phase, the tumours return to a more ‘normal’ metabolism, rather than maintaining a chemotherapy-induced phenotype.

Through injecting Tax- and placebo- treated mice with the [1,2-¹³C]glucose tracer, it has been possible to map metabolic pathways involved in the *in vivo* glucose substrate consumption by the mammary tumour tissue and to perform relative quantification of isotopomer abundance through MIDA and ¹³C-MFA using GC-MS and NMR spectroscopy respectively. These results are summarised in Figure 5.7. Analysis of the transition of the [1,2-¹³C]glucose-derived ¹³C atoms into downstream metabolites allowed the tracing of glycolysis, PPP and the TCA cycle. Moreover, the isotopomer patterns obtained through NMR analysis suggested the presence of three distinct pools of metabolites, that derived from the PDH activity (i.e. [4,5-¹³C]glutamate, [3,4-¹³C]aspartate), PC activity (i.e. [2,3-¹³C]glutamate, [2,3-¹³C]aspartate), and that of the carbons that flowed through the oxPPP (i.e. [3-¹³C]alanine, [3-¹³C]lactate). The lower relative enrichment into the residual tumour derived- alanine and lactate might indicate either a reduced activity of the glycolytic pathway, or a different fate for the glycolysis-

derived pyruvate. However, the only isotopomer showing significantly reduced relative abundance was [3-¹³C]alanine, suggesting a reduced activity of the AAT enzyme in the residual mammary tumours using this analytical method. However, the fact that steady-state alanine concentrations did not change (Figure 5.3C), suggests that if activity of AAT is reduced, an alternative source of alanine must be available – either exogenous or from endogenous protein degradation (i.e. autophagy).

GC-MS is a more sensitive technique than NMR spectroscopy and this allows the identification of low abundance metabolites such as pyruvate and some TCA cycle intermediates. Using this technique, one can only get information regarding the number of labelled atoms in a molecule, but not about the position. Therefore, *a priori* knowledge about metabolic pathways is necessary to be able to hypothesise the correct isotopomer. In contrast, the precise position of ¹³C incorporation can be worked out using NMR spectroscopy, making these two techniques complementary to obtain the most complete information on ¹³C atom incorporation into metabolites. In fact, using NMR spectroscopy we were able to assume the production of glycolysis-derived [2,3-¹³C]pyruvate from the labelling pattern of the metabolites downstream of it. Use of GC-MS instead allowed its detection, confirming the presence of the m+2 isotopomer. Moreover, the single labelled pyruvate (m+1) was also detected, being significantly more abundant in the residual tumours, underlying a higher contribution of the oxidative PPP branch (Figure 1.4D). An upregulation of this pathway may be linked to a higher need for antioxidant molecules in these Tax-treated residual tumours, given that NADPH is a central factor for glutathione production (Cantor and Sabatini, 2012, Dang, 2012). Moreover, increased glutathione synthesis was already observed for the *in vitro* model used in this thesis (Figure 3.17). Interestingly, the excess of m+1

pyruvate did not lead to neither single labelled lactate nor alanine accumulation in residual tumours, being the latter significantly less produced as seen from the lower abundance of the [3-¹³C]alanine isotopomer (Figure 5.5A). m+1 pyruvate could instead be consumed in the TCA cycle, as confirmed by the presence of single labelled malate, aspartate and glutamate, which tended to be more abundant in the residual tumours, in accordance with the m+1 pyruvate results. However, it should be noted that only two replicates were analysed for the Tax-treated mice, therefore they are not enough to run a statistical test.

Residual tumour cells in patients have been demonstrated to be dormant for a long time, even years, before leading to cancer recurrence and in most cases patient mortality. It would be therefore interesting to investigate the recurrence capacity of the residual mammary tumours in the mouse model used for this thesis. The use of pre-clinical models of residual tumours is fundamental to investigate all the biological aspects responsible for their survival to therapy and to ideally find a target to underpin their survival in order to prevent their progression to untreatable tumour relapse.

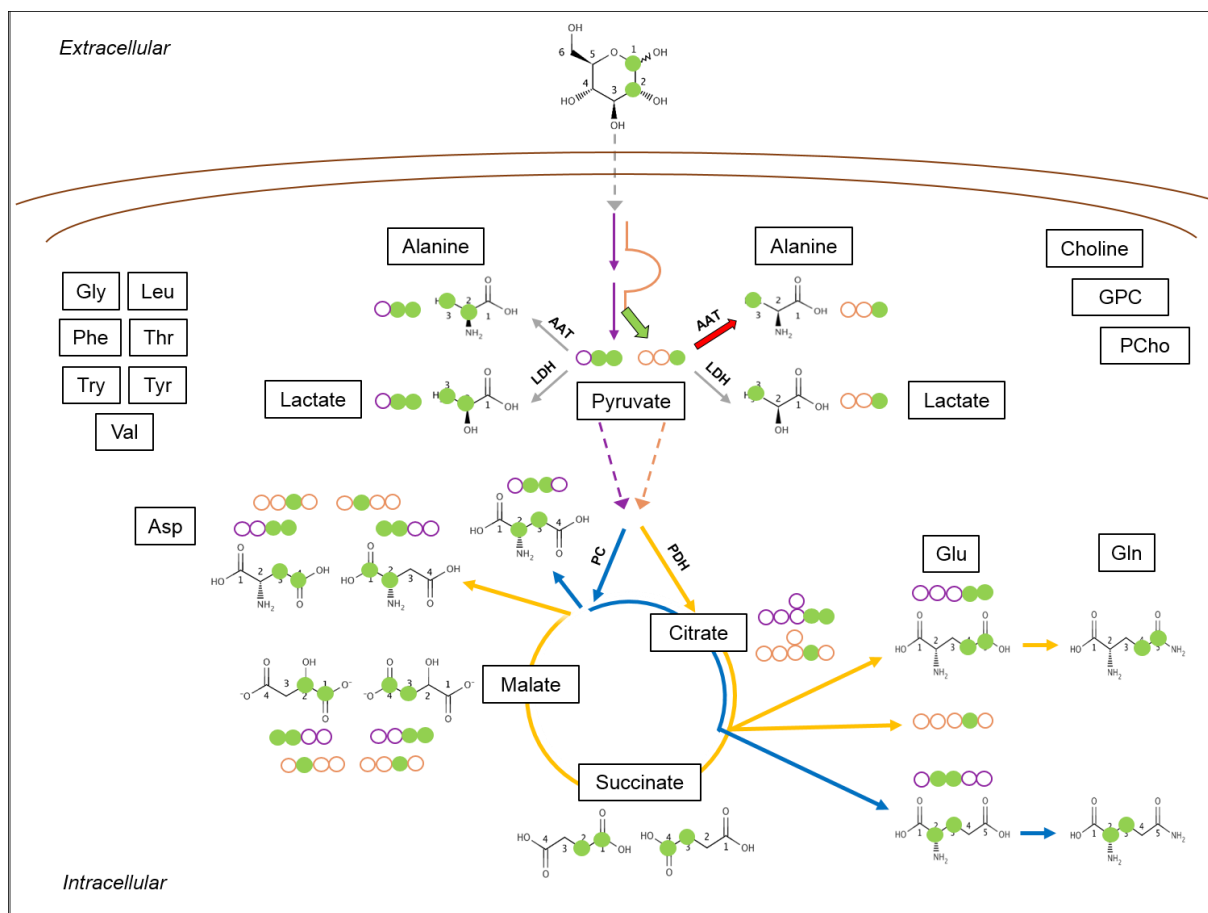


Figure 5.7. *In vivo* metabolic phenotype of residual mammary tumours.

Residual and untreated mouse mammary tumours did not show significant differences in terms of intracellular metabolite concentration. [1,2- ^{13}C]glucose was injected to trace pathway usage in the mammary tumour via GC-MS and NMR spectroscopy. The complementary use of these two techniques led to the identification of distinct pools of metabolite, such as the one produced by simple glycolysis (dark-purple), by flowing through the oxidative branch of the pentose phosphate pathway (oxPPP, orange), as well as the one derived from pyruvate dehydrogenase (PDH, yellow) or from pyruvate carboxylase (PC, blue) activity. Moreover, the relative quantification of isotopomer abundances suggested increased contribution of the oxPPP (resulting in higher abundance of $m+1$ pyruvate) and decreased alanine aminotransferase (AAT) activity (resulting in lower percentage of [3- ^{13}C]alanine) in the residual mammary tumours. For simplification purposes, metabolites produced in the second round of the TCA cycle are not represented. Metabolites are in boxes, while enzymes are without. The metabolite's structure is shown when identified using NMR spectroscopy, while cue ball structure indicates GC-MS-derived analysis. Green cue ball indicates the ^{13}C atom. Green arrow highlights increased and red arrow decreased production rate in the residual tumours.

Dotted lines stand for transport across membranes and continuous lines for pathways.
Abbreviations: Asp, aspartate; Gln, glutamine; Glu, glutamate; Gly, glycine; GPC, glycerophosphocholine; LDH, lactate dehydrogenase; Leu, leucine; PCho, phosphorylcholine; Phe, phenylalanine; Thr, threonine; Try, tryptophan; Tyr, tyrosine; Val, valine.

CHAPTER 6

GENERAL DISCUSSION

6.1 DISCUSSION

Major efforts in breast cancer research have been focused on early diagnosis and prevention. However, survival of patients with breast cancer is hampered by the presence of primary or secondary resistance to treatments in the primary or relapsed tumour, and metastatic tumours are still incurable (Gucalp et al., 2014). We therefore sought to contribute to the field investigating on how to possibly improve the treatment of late stage breast cancer.

In general, cancer research is moving more and more towards a personalised medicine that is designed to ensure higher treatment efficacy and reduced side-effects thanks to the use of specific biomarkers (Kalia, 2015). Recent studies have suggested that breast cancer may be one of the most heterogeneous tumour types (Skibinski and Kuperwasser, 2015), composed of many different subtypes identified using immunohistochemical markers, gene expression profiles (Perou et al., 2000, Sorlie et al., 2001), and more recently genomic (Curtis et al., 2012), genome-wide-association (Fachal and Dunning, 2015) and metabolomic studies (Claudino et al., 2007, Denkert et al., 2012). These subtypes are known to result in very different clinical outcomes and responses to therapies, requiring a new strategy in order to identify targeted drugs and provide the personalised medicine that has been promised.

The presence of biomarkers such as ER, PR, and HER2 have guided the choice of specific promising breast cancer treatments using immune (Wong and Hurvitz, 2014) and hormonal therapy (Abdulkareem and Zurmi, 2012). However, although specific, these drugs are often effective only in 50% of the patients, highlighting the need of further research on the subject. When tumours are resistant to these specific treatments, or are identified to be at a late stage of progression, systemic

chemotherapy is applied where possible. To date, the best efficacy has been observed using taxane-based therapies (docetaxel), often in combination with anthracyclines (Alken and Kelly, 2013). In order to improve outcomes, efforts have been made in predicting tumour response to systemic therapies, for example by identifying patterns of gene expression correlated with resistance to docetaxel in breast cancer patients (Chang et al., 2003, Iwao-Koizumi et al., 2005). However, the single biggest threat to breast cancer patient survival is the incomplete response to drugs, which leaves the patient with residual disease that is often resistant to therapies and therefore the main cause of death (Ignatiadis and Reinholz, 2011, Dieci et al., 2013).

Much of the field of cancer research has in recent years become interested in metabolism, as it has been known to be transformed in cancer for almost 100 years. This transformation is thought to be due to a number of both endogenous factors (e.g. genetic lesions in metabolic enzymes), or exogenous stimuli including adaptation to a hostile microenvironment (e.g. via biomass accumulation and redox control) (Koppenol et al., 2011, Cantor and Sabatini, 2012, Dang, 2012). The metabolome (the sum of all the metabolites present in a cell) represents the biological compartment downstream of the genome, transcriptome and proteome, that receives and interprets their inputs to dynamically respond to internal and environmental perturbations with the necessary functional and phenotypic changes. It therefore can be said to represent the most comprehensive readout of a cellular phenotype (Fiehn, 2001).

In particular, breast cancer is known to undergo metabolic reprogramming, and the main alterations have been recently reviewed (Mishra and Ambs, 2015). Metabolic profiling of breast cancers can therefore be used to identify metabolic biomarkers and to differentiate between tumour subtypes (Denkert et al., 2012). Interestingly, the

breast tumour subtypes that were defined by a metabolic signature did not necessarily correspond to the well-known molecular subtypes, suggesting that the metabolic phenotyping could provide an overarching means by which treatment response and patient outcome are predicted (Mishra and Ambs, 2015).

Importantly, this also questions whether the understanding of all the genetic subtypes is really necessary: as an example, enhanced cell proliferation could be instigated through a number of genetic lesions, but all of them have the end product of increasing nucleotide synthesis.

Bearing all this in mind, the overall aim of this thesis was to investigate whether after docetaxel treatment, the metabolic phenotype of residual breast cancer presented key metabolic alterations that could be specifically exploited to restore sensitivity and induce residual tumour killing.

It is important to make clear that the targeting cancer metabolism is not a new approach, but has been pursued since Warburg's discovery of altered cancer metabolism in the early 20th Century (Tennant et al., 2010). However, until now metabolic drugs did not show great efficacy in clinical trials mainly due to off-target side effects or very high toxicity (Jones and Schulze, 2012). For example, the anti-diabetic drug metformin is being tested in breast cancer after promising *in vitro* results, but results *in vivo* were not clear due to a lack of consistency between studies (Hatoum and McGowan, 2015). This may support the idea that a thorough analysis of metabolism and a deep understanding of all the connections in the metabolic network are fundamental in order to pinpoint the key pathways that could specifically be targeted. In order to precisely define the metabolic phenotype of a biological system, the more classical approach of metabolite identification and quantification needs to be

complemented with information about metabolic pathway usage that can be derived from metabolic fluxes.

Briefly, this thesis used the MCF-7 breast cancer cell line and the MMTV-PyMT mouse model of breast cancer to establish an *in vitro* and *in vivo* model of residual breast cancer. Metabolite quantification via NMR spectroscopy, gene expression analysis (*in vivo*), and [1,2-¹³C]glucose based ¹³C-MFA via NMR spectroscopy and GC-MS (only *in vivo*) have allowed to characterise the *in vitro* and *in vivo* metabolic phenotype of residual breast tumour after docetaxel treatment. The definition of ¹³C-MFA has been used throughout the whole thesis, however we limited our analysis to the experimental side of it, mainly performing pathway tracing and relatively quantifying labelling enrichment into metabolites. The analysis of all the metabolic fluxes in a network would need the use of algorithms and computational approaches that could connect all the information about intracellular and extracellular metabolites concentration and flux kinetics of some detected reactions, in order to create a model that could predict all fluxes (Wiechert, 2001, Sauer, 2006).

Interestingly, the residual cells *in vitro* were characterised by a docetaxel-induced growth arrest, during which cells were metabolically active resulting in increased glycolysis, accumulation of amino acids and increased antioxidant production.

The growth arrest induced *in vitro* may resemble the initial quiescent state of human residual tumours during which their detection is particularly challenging (Ignatiadis and Reinholz, 2011). However, they can restart to grow and result in tumour relapse, which is usually characterised by altered morphology and sensitivity to drugs, probably due to the selection of a more malignant phenotype which survived the treatment of the

primary tumour (Ignatiadis and Reinholz, 2011, Creighton et al., 2009). Our *in vitro* model recapitulated this as after a period of 'senescence' the residual cells resumed proliferation and we were able to characterise the phenotype of the regrowth clones. Despite what has been suggested in the literature, these cells demonstrated a phenotype similar to that of the untreated breast cancer cells, except for some intracellular amino acid accumulation, and it would therefore be interesting to evaluate if these clones also retained sensitivity to docetaxel. We cannot however rule out alterations in metabolic pathways that could not be specifically studied by our analytical method (e.g. glutamine and lipid metabolism).

The apparent discrepancy between what was expected from our interpretation of clinical observations and what we observed in our *in vitro* breast cancer model could be explained by the clear limitations of *in vitro* systems, where a two-dimensional layer of cancer cells cannot properly account for the complexity of the three-dimensional tumours *in vivo*. In fact, human tumours are highly interconnected with the microenvironment, the stromal component and the immune system (Fiaschi and Chiarugi, 2012).

In order to address our scientific questions in a model that would more closely resemble the human disease, the MMTV-PyMT transgenic mouse model of breast cancer was used.

The gene expression analysis of the residual mouse mammary tumours linked the upregulation of Muc4 with resistance to docetaxel treatment, pointing to a malignant phenotype of the residual tumours given its involvement in favouring cancer progression and metastasis (Komatsu et al., 2001, Workman et al., 2009). Interestingly, the amino acid and anti-oxidant accumulation detected in the *in vitro*

model was not evidenced *in vivo*, which may confirm the limitations of *in vitro* models. At the same time, the absence of clear separation between docetaxel-treated and untreated mammary tumour metabolism, as well as high similarities in gene expression, made us question whether the approach used was able to reveal existing differences. In fact, residual tumours left to grow for a further week after the last dose of treatment, are more likely to go back to the phenotype of the primary tumour, while residual tumours investigated straight after treatment may present an altered phenotype. However, it is also entirely possible that due to the interactions between the tumour cells and their environment in the *in vivo* model, we were not able to observe the amino acid and anti-oxidant accumulation as they could have been exchanged with this other compartment. Another explanation could refer to the intra-tumoural heterogeneity observed in breast cancer (Sun and Yu, 2015, Martelotto et al., 2014). If the same tumour mass is composed of cells with very different metabolism, the way the tumour is sampled becomes fundamental. Testing a small portion of the whole tumour might therefore have biased the analysis towards the phenotype of only that small group of cells. A better approach could consist in testing few samples from different areas of the same tumour.

Given the non-hazardous nature of the ^{13}C isotope (compared to the radioactive ^{14}C isotope), the application of the ^{13}C -MFA *in vivo* has been explored with promising results both in cancer patients (Maher et al., 2012, Fan et al., 2009) and in pre-clinical models (Fan et al., 2011, Binsl et al., 2010, Malloy et al., 1990). However, standardisation for these studies is still missing. Consequently, the first challenge to perform *in vivo* ^{13}C -MFA was the optimisation of the [1,2- ^{13}C]glucose substrate administration to the mouse. One of the main aspects to be considered was that,

following a systemic distribution of glucose via the blood flow, it will be metabolised by other organs, e.g. the liver, which would then release labelled metabolites in the blood stream that could be subsequently used in the tissue of interest misrepresenting the pathway usage by the tumour. However, in our model, dynamic labelling information was collected (Wiechert and Noh, 2013) at a specific time-point after the i.p. injection of the [1,2-¹³C]glucose, rather than performing a long time infusion to reach an isotopic steady-state. The short time frame used in this approach therefore reduces the risk of contamination with labelled metabolites derived from organs other than the mammary tumour itself. The complementary use of NMR spectroscopy and GC-MS allowed the acquisition of more precise and detailed information on pathway usage to better uncover the alterations in the residual mammary tumours. In fact, an increased flux through the oxPPP was observed in the residual tumours, which may underlie a response to a post-therapy increase in ROS counteracted via NADPH-based glutathione production. Moreover, this phenotype would confirm the residual tumour response to oxidative stress already pointed out in the analysis of the *in vitro* residual breast cancer cells.

6.2 CONCLUSIONS AND FUTURE WORKS

In conclusion, the objectives stated at the beginning of this thesis were fulfilled:

- *In vitro* and *in vivo* models of residual breast cancer after docetaxel treatment were successfully established,
- Polar metabolites were quantified *in vitro* and *in vivo* using NMR spectroscopy
- Pathways used in the metabolism of glucose were traced and relatively quantified applying ^{13}C -MFA to a breast cancer cell line
- A method for the *in vivo* administration of ^{13}C -labelled glucose to a mouse model was developed,
- Residual mouse mammary tumour phenotype was characterised using gene expression analysis and ^{13}C -MFA of pathways involved in ^{13}C -labelled glucose metabolism,
- *In vitro* residual breast cancer cells successfully resumed growth and formed clones of recurrent tumour.

As future work, it would be interesting to target the hypermetabolic phenotype seen in the *in vitro* settings, to investigate whether this is a condition fundamental to mediate breast cancer cell survival to docetaxel. In particular, assuming that catabolic processes such as autophagy and micropinocytosis are responsible for the intracellular accumulation of essential amino acids, inhibitors of these mechanisms could be used, such as chloroquine, bafilomycin (Duffy et al., 2015) and 5-(N-ethyl-Nisopropyl) amiloride (EIPA, tested only *in vitro*) (Commisso et al., 2013). Moreover, it would be interesting to test the ability of *in vivo* residual mammary tumour to cause tumour recurrence, and eventually to test its sensitivity to docetaxel. Investigations of other

aspects of breast cancer metabolism should also be carried out, i.e. lipid metabolism, in order to identify targetable metabolic alterations.

Tumour relapse and metastasis are common events that occur in many types of cancer, and their result is poor prognosis mainly due to insensitivity to previously effective chemotherapies. Metabolic reprogramming is also a hallmark found in all cancers studied thus far, therefore the characterisation of the metabolic phenotype to unravel specific metabolic targets in previously incurable residual cancers, is not only limited to the use of docetaxel and not limited to breast cancer, but could be applied to any type of tumour.

REFERENCES

- Abdulkareem, IH & Zurmi, IB 2012. Review of hormonal treatment of breast cancer. *Nigerian journal of clinical practice*, 15, 9-14.
- Agarwal, G, Ramakant, P, Forgach, ER, Rendon, JC, Chaparro, JM, Basurto, CS & Margaritoni, M 2009. Breast cancer care in developing countries. *World journal of surgery*, 33, 2069-76.
- Ahmed, Z, Zeeshan, S, Huber, C, Hensel, M, Schomburg, D, Munch, R, Eisenreich, W & Dandekar, T 2013. Software LS-MIDA for efficient mass isotopomer distribution analysis in metabolic modelling. *BMC bioinformatics*, 14, 218.
- Ahren, B, Winzell, MS & Pacini, G 2008. The augmenting effect on insulin secretion by oral versus intravenous glucose is exaggerated by high-fat diet in mice. *The Journal of endocrinology*, 197, 181-7.
- Alberghina, L & Gaglio, D 2014. Redox control of glutamine utilization in cancer. *Cell death & disease*, 5, e1561.
- Ali-Osman, F, Antoun, G, Wang, H, Rajagopal, S & Gagucas, E 1996. Buthionine sulfoximine induction of gamma-L-glutamyl-L-cysteine synthetase gene expression, kinetics of glutathione depletion and resynthesis, and modulation of carmustine-induced DNA-DNA cross-linking and cytotoxicity in human glioma cells. *Molecular pharmacology*, 49, 1012-20.
- Alken, S & Kelly, CM 2013. Benefit risk assessment and update on the use of docetaxel in the management of breast cancer. *Cancer management and research*, 5, 357-65.
- Allinen, M, Beroukhim, R, Cai, L, Brennan, C, Lahti-Domenici, J, Huang, H, Porter, D, Hu, M, Chin, L, Richardson, A, Schnitt, S, Sellers, WR & Polyak, K 2004. Molecular characterization of the tumor microenvironment in breast cancer. *Cancer cell*, 6, 17-32.
- Allred, DC, Clark, GM, Molina, R, Tandon, AK, Schnitt, SJ, Gilchrist, KW, Osborne, CK, Tormey, DC & Mcguire, WL 1992. Overexpression of HER-2/neu and its relationship with other prognostic factors change during the progression of in situ to invasive breast cancer. *Human pathology*, 23, 974-9.
- Anders, S, Pyl, PT & Huber, W 2014. HTSeq-a Python framework to work with high-throughput sequencing data. *Bioinformatics (Oxford, England)*.
- Andrikopoulos, S, Blair, AR, Deluca, N, Fam, BC & Proietto, J 2008. Evaluating the glucose tolerance test in mice. *American journal of physiology. Endocrinology and metabolism*, 295, E1323-32.

Arioli, V & Rossi, E 1970. Errors related to different techniques of intraperitoneal injection in mice. *Applied microbiology*, 19, 704-5.

Arrick, BA & Nathan, CF 1984. Glutathione metabolism as a determinant of therapeutic efficacy: a review. *Cancer research*, 44, 4224-32.

Atcc. *Animal cell culture guide* [Online]. Available: https://www.atcc.org/~media/PDFs/Culture%20Guides/AnimCellCulture_Guide.ashx [2015].

Ayala, JE, Samuel, VT, Morton, GJ, Obici, S, Croniger, CM, Shulman, GI, Wasserman, DH & Mcguinness, OP 2010. Standard operating procedures for describing and performing metabolic tests of glucose homeostasis in mice. *Disease models & mechanisms*, 3, 525-34.

Bacus, SS, Kiguchi, K, Chin, D, King, CR & Huberman, E 1990. Differentiation of cultured human breast cancer cells (AU-565 and MCF-7) associated with loss of cell surface HER-2/neu antigen. *Molecular carcinogenesis*, 3, 350-62.

Bafna, S, Kaur, S, Momi, N & Batra, SK 2009. Pancreatic cancer cells resistance to gemcitabine: the role of MUC4 mucin. *British journal of cancer*, 101, 1155-61.

Bai, RZ, Wu, Y, Liu, Q, Xie, K, Wei, YQ, Wang, YS, Liu, K, Luo, Y, Su, JM, Hu, B, Liu, JY, Li, Q, Niu, T, Zhao, ZW & Yang, L 2009. Suppression of lung cancer in murine model: treated by combination of recombinant human endostatin adenovirus with low-dose cisplatin. *Journal of experimental & clinical cancer research : CR*, 28, 31.

Bandsma, RH, Grefhorst, A, Van Dijk, TH, Van Der Sluijs, FH, Hammer, A, Reijngoud, DJ & Kuipers, F 2004. Enhanced glucose cycling and suppressed de novo synthesis of glucose-6-phosphate result in a net unchanged hepatic glucose output in ob/ob mice. *Diabetologia*, 47, 2022-31.

Barnard, ME, Boeke, CE & Tamimi, RM 2015. Established breast cancer risk factors and risk of intrinsic tumor subtypes. *Biochimica et biophysica acta*, 1856, 73-85.

Baselga, J, Cortes, J, Kim, SB, Im, SA, Hegg, R, Im, YH, Roman, L, Pedrini, JL, Pienkowski, T, Knott, A, Clark, E, Benyunes, MC, Ross, G & Swain, SM 2012. Pertuzumab plus trastuzumab plus docetaxel for metastatic breast cancer. *The New England journal of medicine*, 366, 109-19.

Bayet-Robert, M, Morvan, D, Chollet, P & Barthomeuf, C 2010. Pharmacometabolomics of docetaxel-treated human MCF7 breast cancer cells provides evidence of varying cellular responses at high and low doses. *Breast cancer research and treatment*, 120, 613-26.

- Bayley, JP & Devilee, P 2010. Warburg tumours and the mechanisms of mitochondrial tumour suppressor genes. Barking up the right tree? *Curr Opin Genet Dev*, 20, 324-9.
- Baysal, BE, Ferrell, RE, Willett-Brozick, JE, Lawrence, EC, Myssiorek, D, Bosch, A, Van Der Mey, A, Taschner, PE, Rubinstein, WS, Myers, EN, Richard, CW, 3rd, Cornelisse, CJ, Devilee, P & Devlin, B 2000. Mutations in SDHD, a mitochondrial complex II gene, in hereditary paraganglioma. *Science (New York, N.Y.)*, 287, 848-51.
- Beger, R, Hansen, D, Schnackenberg, L, Cross, B, Fatollahi, J, Lagunero, FT, Sarnyai, Z & Boros, L 2009. Single valproic acid treatment inhibits glycogen and RNA ribose turnover while disrupting glucose-derived cholesterol synthesis in liver as revealed by the [U-13C6]-d-glucose tracer in mice. *Metabolomics*, 5, 336-45.
- Bergers, G & Benjamin, LE 2003. Tumorigenesis and the angiogenic switch. *Nature reviews. Cancer*, 3, 401-10.
- Berwick, DC, Hers, I, Heesom, KJ, Moule, SK & Tavaré, JM 2002. The identification of ATP-citrate lyase as a protein kinase B (Akt) substrate in primary adipocytes. *The Journal of biological chemistry*, 277, 33895-900.
- Binder, S 2013. Evolution of taxanes in the treatment of metastatic breast cancer. *Clinical journal of oncology nursing*, 17 Suppl, 9-14.
- Binsl, TW, Alders, DJ, Heringa, J, Groeneveld, AB & Van Beek, JH 2010. Computational quantification of metabolic fluxes from a single isotope snapshot: application to an animal biopsy. *Bioinformatics (Oxford, England)*, 26, 653-60.
- Bockamp, E, Maringer, M, Spangenberg, C, Fees, S, Fraser, S, Eshkind, L, Oesch, F & Zabel, B 2002. Of mice and models: improved animal models for biomedical research. *Physiological genomics*, 11, 115-32.
- Boren, J, Cascante, M, Marin, S, Comin-Anduix, B, Centelles, JJ, Lim, S, Bassilian, S, Ahmed, S, Lee, WN & Boros, LG 2001. Gleevec (STI571) influences metabolic enzyme activities and glucose carbon flow toward nucleic acid and fatty acid synthesis in myeloid tumor cells. *The Journal of biological chemistry*, 276, 37747-53.
- Bossuyt, V, Provenzano, E, Symmans, WF, Boughey, JC, Coles, C, Curigliano, G, Dixon, JM, Esserman, LJ, Fastner, G, Kuehn, T, Peintinger, F, Von Minckwitz, G, White, J, Yang, W, Badve, S, Denkert, C, Macgrogan, G, Penault-Llorca, F, Viale, G & Cameron, D 2015. Recommendations for standardized pathological characterization of residual disease for neoadjuvant clinical trials of breast cancer by the BIG-NABCG collaboration. *Annals of oncology : official journal of the European Society for Medical Oncology / ESMO*, 26, 1280-91.

Breccia, M, Molica, M & Alimena, G 2014. How tyrosine kinase inhibitors impair metabolism and endocrine system function: a systematic updated review. *Leukemia research*, 38, 1392-8.

Broeders, M, Moss, S, Nystrom, L, Njor, S, Jonsson, H, Paap, E, Massat, N, Duffy, S, Lynge, E & Paci, E 2012. The impact of mammographic screening on breast cancer mortality in Europe: a review of observational studies. *Journal of medical screening*, 19 Suppl 1, 14-25.

Brooks, SC, Locke, ER & Soule, HD 1973. Estrogen receptor in a human cell line (MCF-7) from breast carcinoma. *The Journal of biological chemistry*, 248, 6251-3.

Brown, ET, Umino, Y, Loi, T, Solessio, E & Barlow, R 2005. Anesthesia can cause sustained hyperglycemia in C57/BL6J mice. *Visual neuroscience*, 22, 615-8.

Burdall, SE, Hanby, AM, Lansdown, MR & Speirs, V 2003. Breast cancer cell lines: friend or foe? *Breast cancer research : BCR*, 5, 89-95.

Cancer Genome Atlas Network 2012. Comprehensive molecular portraits of human breast tumours. *Nature*, 490, 61-70.

Cancer Research Uk. *Breast cancer statistics* [Online]. Available: <http://www.cancerresearchuk.org/health-professional/cancer-statistics/statistics-by-cancer-type/breast-cancer#heading-Zero> [Accessed October 2015].

Cancer Research Uk. *Cancer Statistics for the UK* [Online]. Available: <http://www.cancerresearchuk.org/health-professional/cancer-statistics#heading-Three> [Accessed June 2015].

Cancer Research Uk. *Docetaxel* [Online]. Available: <http://www.cancerresearchuk.org/about-cancer/cancers-in-general/treatment/cancer-drugs/docetaxel> [Accessed April 2016].

Cantor, JR & Sabatini, DM 2012. Cancer cell metabolism: one hallmark, many faces. *Cancer discovery*, 2, 881-98.

Cardaci, S, Zheng, L, Mackay, G, Van Den Broek, NJ, Mackenzie, ED, Nixon, C, Stevenson, D, Tumanov, S, Bulusu, V, Kamphorst, JJ, Vazquez, A, Fleming, S, Schiavi, F, Kalna, G, Blyth, K, Strathdee, D & Gottlieb, E 2015. Pyruvate carboxylation enables growth of SDH-deficient cells by supporting aspartate biosynthesis. *Nature cell biology*, 17, 1317-26.

Carito, V, Bonuccelli, G, Martinez-Outschoorn, UE, Whitaker-Menezes, D, Caroleo, MC, Cione, E, Howell, A, Pestell, RG, Lisanti, MP & Sotgia, F 2012. Metabolic remodeling of the tumor microenvironment: migration stimulating factor (MSF)

reprograms myofibroblasts toward lactate production, fueling anabolic tumor growth. *Cell cycle (Georgetown, Tex.)*, 11, 3403-14.

Carling, D, Zammit, VA & Hardie, DG 1987. A common bicyclic protein kinase cascade inactivates the regulatory enzymes of fatty acid and cholesterol biosynthesis. *FEBS letters*, 223, 217-22.

Carraway, KL, Perez, A, Idris, N, Jepson, S, Arango, M, Komatsu, M, Haq, B, Price-Schiavi, SA, Zhang, J & Carraway, CA 2002. Muc4/sialomucin complex, the intramembrane ErbB2 ligand, in cancer and epithelia: to protect and to survive. *Progress in nucleic acid research and molecular biology*, 71, 149-85.

Carraway, KL, Ramsauer, VP & Carraway, CA 2005. Glycoprotein contributions to mammary gland and mammary tumor structure and function: roles of adherens junctions, ErbBs and membrane MUCs. *Journal of cellular biochemistry*, 96, 914-26.

Castellino, S, O'mara, M, Koch, K, Borts, DJ, Bowers, GD & Maclauchlin, C 2012. Human metabolism of lapatinib, a dual kinase inhibitor: implications for hepatotoxicity. *Drug metabolism and disposition: the biological fate of chemicals*, 40, 139-50.

Cazenave, LA, Moscow, JA, Myers, CE & Cowan, KH 1989. Glutathione S-transferase and drug resistance. *Cancer treatment and research*, 48, 171-87.

Chang, JC, Wooten, EC, Tsimelzon, A, Hilsenbeck, SG, Gutierrez, MC, Elledge, R, Mohsin, S, Osborne, CK, Chamness, GC, Allred, DC & O'connell, P 2003. Gene expression profiling for the prediction of therapeutic response to docetaxel in patients with breast cancer. *Lancet*, 362, 362-9.

Chang, JC, Wooten, EC, Tsimelzon, A, Hilsenbeck, SG, Gutierrez, MC, Tham, YL, Kalidas, M, Elledge, R, Mohsin, S, Osborne, CK, Chamness, GC, Allred, DC, Lewis, MT, Wong, H & O'connell, P 2005. Patterns of resistance and incomplete response to docetaxel by gene expression profiling in breast cancer patients. *Journal of clinical oncology : official journal of the American Society of Clinical Oncology*, 23, 1169-77.

Chen, AC, Migliaccio, I, Rimawi, M, Lopez-Tarruella, S, Creighton, CJ, Massarweh, S, Huang, C, Wang, YC, Batra, SK, Gutierrez, MC, Osborne, CK & Schiff, R 2012. Upregulation of mucin4 in ER-positive/HER2-overexpressing breast cancer xenografts with acquired resistance to endocrine and HER2-targeted therapies. *Breast cancer research and treatment*, 134, 583-93.

Cheng, N, Chytil, A, Shyr, Y, Joly, A & Moses, HL 2008. Transforming growth factor-beta signaling-deficient fibroblasts enhance hepatocyte growth factor signaling in mammary carcinoma cells to promote scattering and invasion. *Molecular cancer research : MCR*, 6, 1521-33.

Cheng, T, Sudderth, J, Yang, C, Mullen, AR, Jin, ES, Mates, JM & Deberardinis, RJ 2011. Pyruvate carboxylase is required for glutamine-independent growth of tumor cells. *Proceedings of the National Academy of Sciences of the United States of America*, 108, 8674-9.

Christofk, HR, Vander Heiden, MG, Harris, MH, Ramanathan, A, Gerszten, RE, Wei, R, Fleming, MD, Schreiber, SL & Cantley, LC 2008a. The M2 splice isoform of pyruvate kinase is important for cancer metabolism and tumour growth. *Nature*, 452, 230-3.

Christofk, HR, Vander Heiden, MG, Wu, N, Asara, JM & Cantley, LC 2008b. Pyruvate kinase M2 is a phosphotyrosine-binding protein. *Nature*, 452, 181-6.

Clarke, M, Collins, R, Darby, S, Davies, C, Elphinstone, P, Evans, V, Godwin, J, Gray, R, Hicks, C, James, S, Mackinnon, E, MCGale, P, Mchugh, T, Peto, R, Taylor, C & Wang, Y 2005. Effects of radiotherapy and of differences in the extent of surgery for early breast cancer on local recurrence and 15-year survival: an overview of the randomised trials. *Lancet*, 366, 2087-106.

Claudino, WM, Quattrone, A, Biganzoli, L, Pestrin, M, Bertini, I & Di Leo, A 2007. Metabolomics: available results, current research projects in breast cancer, and future applications. *Journal of clinical oncology : official journal of the American Society of Clinical Oncology*, 25, 2840-6.

Cleator, S, Heller, W & Coombes, RC 2007. Triple-negative breast cancer: therapeutic options. *The Lancet. Oncology*, 8, 235-44.

Collado, M & Serrano, M 2010. Senescence in tumours: evidence from mice and humans. *Nature reviews. Cancer*, 10, 51-7.

Commisso, C, Davidson, SM, Soydaner-Azeloglu, RG, Parker, SJ, Kamphorst, JJ, Hackett, S, Grabocka, E, Nofal, M, Drebin, JA, Thompson, CB, Rabinowitz, JD, Metallo, CM, Vander Heiden, MG & Bar-Sagi, D 2013. Macropinocytosis of protein is an amino acid supply route in Ras-transformed cells. *Nature*, 497, 633-7.

Cooper, LA, Gutman, DA, Chisolm, C, Appin, C, Kong, J, Rong, Y, Kurc, T, Van Meir, EG, Saltz, JH, Moreno, CS & Brat, DJ 2012. The tumor microenvironment strongly impacts master transcriptional regulators and gene expression class of glioblastoma. *The American journal of pathology*, 180, 2108-19.

Cortes, JE & Pazdur, R 1995. Docetaxel. *Journal of clinical oncology : official journal of the American Society of Clinical Oncology*, 13, 2643-55.

Creighton, CJ, Li, X, Landis, M, Dixon, JM, Neumeister, VM, Sjolund, A, Rimm, DL, Wong, H, Rodriguez, A, Herschkowitz, JI, Fan, C, Zhang, X, He, X, Pavlick, A, Gutierrez, MC, Renshaw, L, Larionov, AA, Faratian, D, Hilsenbeck, SG, Perou, CM,

Lewis, MT, Rosen, JM & Chang, JC 2009. Residual breast cancers after conventional therapy display mesenchymal as well as tumor-initiating features. *Proceedings of the National Academy of Sciences of the United States of America*, 106, 13820-5.

Crown, SB, Ahn, WS & Antoniewicz, MR 2012. Rational design of (1)(3)C-labeling experiments for metabolic flux analysis in mammalian cells. *BMC systems biology*, 6, 43.

Curtis, C, Shah, SP, Chin, SF, Turashvili, G, Rueda, OM, Dunning, MJ, Speed, D, Lynch, AG, Samarajiwa, S, Yuan, Y, Graf, S, Ha, G, Haffari, G, Bashashati, A, Russell, R, Mckinney, S, Langerod, A, Green, A, Provenzano, E, Wishart, G, Pinder, S, Watson, P, Markowitz, F, Murphy, L, Ellis, I, Purushotham, A, Borresen-Dale, AL, Brenton, JD, Tavaré, S, Caldas, C & Aparicio, S 2012. The genomic and transcriptomic architecture of 2,000 breast tumours reveals novel subgroups. *Nature*, 486, 346-52.

Dang, CV 2012. Links between metabolism and cancer. *Genes & development*, 26, 877-90.

Dang, L, White, DW, Gross, S, Bennett, BD, Bittinger, MA, Driggers, EM, Fantin, VR, Jang, HG, Jin, S, Keenan, MC, Marks, KM, Prins, RM, Ward, PS, Yen, KE, Liao, LM, Rabinowitz, JD, Cantley, LC, Thompson, CB, Vander Heiden, MG & Su, SM 2009. Cancer-associated IDH1 mutations produce 2-hydroxyglutarate. *Nature*, 462, 739-44.

Dankort, DL & Muller, WJ 2000. Signal transduction in mammary tumorigenesis: a transgenic perspective. *Oncogene*, 19, 1038-44.

David, CJ, Chen, M, Assanah, M, Canoll, P & Manley, JL 2010. HnRNP proteins controlled by c-Myc deregulate pyruvate kinase mRNA splicing in cancer. *Nature*, 463, 364-8.

De Saedeleer, CJ, Porporato, PE, Copetti, T, Perez-Escuredo, J, Payen, VL, Brisson, L, Feron, O & Sonveaux, P 2014. Glucose deprivation increases monocarboxylate transporter 1 (MCT1) expression and MCT1-dependent tumor cell migration. *Oncogene*, 33, 4060-8.

De Weger, VA, Beijnen, JH & Schellens, JH 2014. Cellular and clinical pharmacology of the taxanes docetaxel and paclitaxel--a review. *Anti-cancer drugs*, 25, 488-94.

Deberardinis, RJ & Cheng, T 2010. Q's next: the diverse functions of glutamine in metabolism, cell biology and cancer. *Oncogene*, 29, 313-24.

Deberardinis, RJ, Mancuso, A, Daikhin, E, Nissim, I, Yudkoff, M, Wehrli, S & Thompson, CB 2007. Beyond aerobic glycolysis: transformed cells can engage in glutamine metabolism that exceeds the requirement for protein and nucleotide

synthesis. *Proceedings of the National Academy of Sciences of the United States of America*, 104, 19345-50.

Degraffenried, LA, Friedrichs, WE, Russell, DH, Donzis, EJ, Middleton, AK, Silva, JM, Roth, RA & Hidalgo, M 2004. Inhibition of mTOR activity restores tamoxifen response in breast cancer cells with aberrant Akt Activity. *Clinical cancer research : an official journal of the American Association for Cancer Research*, 10, 8059-67.

Delaglio, F, Grzesiek, S, Vuister, GW, Zhu, G, Pfeifer, J & Bax, A 1995. NMRPipe: a multidimensional spectral processing system based on UNIX pipes. *Journal of biomolecular NMR*, 6, 277-93.

Denkert, C, Bucher, E, Hilvo, M, Salek, R, Oresic, M, Griffin, J, Brockmoller, S, Klauschen, F, Loibl, S, Barupal, DK, Budczies, J, Iljin, K, Nekljudova, V & Fiehn, O 2012. Metabolomics of human breast cancer: new approaches for tumor typing and biomarker discovery. *Genome medicine*, 4, 37.

Di Leo, A, Curigliano, G, Dieras, V, Malorni, L, Sotiriou, C, Swanton, C, Thompson, A, Tutt, A & Piccart, M 2015. New approaches for improving outcomes in breast cancer in Europe. *Breast (Edinburgh, Scotland)*, 24, 321-30.

Dieci, MV, Arnedos, M, Delaloge, S & Andre, F 2013. Quantification of residual risk of relapse in breast cancer patients optimally treated. *Breast (Edinburgh, Scotland)*, 22 Suppl 2, S92-5.

Dorr, JR, Yu, Y, Milanovic, M, Beuster, G, Zasada, C, Dabritz, JH, Lisec, J, Lenze, D, Gerhardt, A, Schleicher, K, Kratzat, S, Purfurst, B, Walenta, S, Mueller-Klieser, W, Graler, M, Hummel, M, Keller, U, Buck, AK, Dorken, B, Willmitzer, L, Reimann, M, Kempa, S, Lee, S & Schmitt, CA 2013. Synthetic lethal metabolic targeting of cellular senescence in cancer therapy. *Nature*, 501, 421-5.

Dowling, RJ, Topisirovic, I, Fonseca, BD & Sonenberg, N 2010. Dissecting the role of mTOR: lessons from mTOR inhibitors. *Biochimica et biophysica acta*, 1804, 433-9.

Draoui, N, Schicke, O, Seront, E, Bouzin, C, Sonveaux, P, Riant, O & Feron, O 2014. Antitumor activity of 7-aminocarboxycoumarin derivatives, a new class of potent inhibitors of lactate influx but not efflux. *Molecular cancer therapeutics*, 13, 1410-8.

Duffy, A, Le, J, Sausville, E & Emadi, A 2015. Autophagy modulation: a target for cancer treatment development. *Cancer chemotherapy and pharmacology*, 75, 439-47.

Dunn, WB, Broadhurst, DI, Atherton, HJ, Goodacre, R & Griffin, JL 2011. Systems level studies of mammalian metabolomes: the roles of mass spectrometry and nuclear magnetic resonance spectroscopy. *Chemical Society reviews*, 40, 387-426.

Efeyan, A, Zoncu, R & Sabatini, DM 2012. Amino acids and mTORC1: from lysosomes to disease. *Trends in molecular medicine*, 18, 524-33.

Eigenbrodt, E, Reinacher, M, Scheefers-Borchel, U, Scheefers, H & Friis, R 1992. Double role for pyruvate kinase type M2 in the expansion of phosphometabolite pools found in tumor cells. *Critical reviews in oncogenesis*, 3, 91-115.

Eisenhauer, EA, Therasse, P, Bogaerts, J, Schwartz, LH, Sargent, D, Ford, R, Dancey, J, Arbuck, S, Gwyther, S, Mooney, M, Rubinstein, L, Shankar, L, Dodd, L, Kaplan, R, Lacombe, D & Verweij, J 2009. New response evaluation criteria in solid tumours: revised RECIST guideline (version 1.1). *European journal of cancer (Oxford, England : 1990)*, 45, 228-47.

Elmore, JG, Armstrong, K, Lehman, CD & Fletcher, SW 2005. Screening for breast cancer. *Jama*, 293, 1245-56.

Elstrom, RL, Bauer, DE, Buzzai, M, Karnauskas, R, Harris, MH, Plas, DR, Zhuang, H, Cinalli, RM, Alavi, A, Rudin, CM & Thompson, CB 2004. Akt stimulates aerobic glycolysis in cancer cells. *Cancer Res*, 64, 3892-9.

Escuin, D, Kline, ER & Giannakakou, P 2005. Both microtubule-stabilizing and microtubule-destabilizing drugs inhibit hypoxia-inducible factor-1alpha accumulation and activity by disrupting microtubule function. *Cancer research*, 65, 9021-8.

Evan, GI & Littlewood, TD 1993. The role of c-myc in cell growth. *Curr Opin Genet Dev*, 3, 44-9.

Ewald, JA, Desotelle, JA, Wilding, G & Jarrard, DF 2010. Therapy-induced senescence in cancer. *Journal of the National Cancer Institute*, 102, 1536-46.

Fachal, L & Dunning, AM 2015. From candidate gene studies to GWAS and post-GWAS analyses in breast cancer. *Current opinion in genetics & development*, 30, 32-41.

Faivre, S, Kroemer, G & Raymond, E 2006. Current development of mTOR inhibitors as anticancer agents. *Nature reviews. Drug discovery*, 5, 671-88.

Fan, TW, Lane, AN, Higashi, RM, Farag, MA, Gao, H, Bousamra, M & Miller, DM 2009. Altered regulation of metabolic pathways in human lung cancer discerned by (13)C stable isotope-resolved metabolomics (SIRM). *Molecular cancer*, 8, 41.

Fan, TW, Lane, AN, Higashi, RM & Yan, J 2011. Stable isotope resolved metabolomics of lung cancer in a SCID mouse model. *Metabolomics*, 7, 257-69.

Fedele, P, Orlando, L, Schiavone, P, Calvani, N, Caliolo, C, Quaranta, A, Nacci, A & Cinieri, S 2015. Recent advances in the treatment of hormone receptor positive HER2

negative metastatic breast cancer. *Critical reviews in oncology/hematology*, 94, 291-301.

Feng, Z, Hu, W, De Stanchina, E, Teresky, AK, Jin, S, Lowe, S & Levine, AJ 2007. The regulation of AMPK beta1, TSC2, and PTEN expression by p53: stress, cell and tissue specificity, and the role of these gene products in modulating the IGF-1-AKT-mTOR pathways. *Cancer research*, 67, 3043-53.

Ferlay, J, Shin, HR, Bray, F, Forman, D, Mathers, C & Parkin, DM 2010. Estimates of worldwide burden of cancer in 2008: GLOBOCAN 2008. *Int J Cancer*, 127, 2893-917.

Ferroni, P, Riondino, S, Buonomo, O, Palmirotta, R, Guadagni, F & Roselli, M 2015. Type 2 Diabetes and Breast Cancer: The Interplay between Impaired Glucose Metabolism and Oxidant Stress. *Oxidative medicine and cellular longevity*, 2015, 183928.

Fiaschi, T & Chiarugi, P 2012. Oxidative stress, tumor microenvironment, and metabolic reprogramming: a diabolic liaison. *International journal of cell biology*, 2012, 762825.

Fiehn, O 2001. Combining genomics, metabolome analysis, and biochemical modelling to understand metabolic networks. *Comparative and functional genomics*, 2, 155-68.

Flier, JS, Mueckler, MM, Usher, P & Lodish, HF 1987. Elevated levels of glucose transport and transporter messenger RNA are induced by ras or src oncogenes. *Science*, 235, 1492-5.

Fluck, MM & Schaffhausen, BS 2009. Lessons in signaling and tumorigenesis from polyomavirus middle T antigen. *Microbiology and molecular biology reviews : MMBR*, 73, 542-63, Table of Contents.

Forbes, NS, Meadows, AL, Clark, DS & Blanch, HW 2006. Estradiol stimulates the biosynthetic pathways of breast cancer cells: detection by metabolic flux analysis. *Metabolic engineering*, 8, 639-52.

Ford, JM, Yang, JM & Hait, WN 1991. Effect of buthionine sulfoximine on toxicity of verapamil and doxorubicin to multidrug resistant cells and to mice. *Cancer research*, 51, 67-72.

Foulkes, WD, Stefansson, IM, Chappuis, PO, Begin, LR, Goffin, JR, Wong, N, Trudel, M & Akslen, LA 2003. Germline BRCA1 mutations and a basal epithelial phenotype in breast cancer. *Journal of the National Cancer Institute*, 95, 1482-5.

Franci, C, Zhou, J, Jiang, Z, Modrusan, Z, Good, Z, Jackson, E & Kouros-Mehr, H 2013. Biomarkers of residual disease, disseminated tumor cells, and metastases in the MMTV-PyMT breast cancer model. *PloS one*, 8, e58183.

Francis, PA, Regan, MM, Fleming, GF, Lang, I, Ciruelos, E, Bellet, M, Bonnefoi, HR, Climent, MA, Da Prada, GA, Burstein, HJ, Martino, S, Davidson, NE, Geyer, CE, Jr., Walley, BA, Coleman, R, Kerbrat, P, Buchholz, S, Ingle, JN, Winer, EP, Rabaglio-Poretti, M, Maibach, R, Ruepp, B, Giobbie-Hurder, A, Price, KN, Colleoni, M, Viale, G, Coates, AS, Goldhirsch, A & Gelber, RD 2015. Adjuvant ovarian suppression in premenopausal breast cancer. *The New England journal of medicine*, 372, 436-46.

Gaglio, D, Metallo, CM, Gameiro, PA, Hiller, K, Danna, LS, Balestrieri, C, Alberghina, L, Stephanopoulos, G & Chiaradonna, F 2011. Oncogenic K-Ras decouples glucose and glutamine metabolism to support cancer cell growth. *Molecular systems biology*, 7, 523.

Gandellini, P, Andriani, F, Merlino, G, D'aiuto, F, Roz, L & Callari, M 2015. Complexity in the tumour microenvironment: Cancer associated fibroblast gene expression patterns identify both common and unique features of tumour-stroma crosstalk across cancer types. *Seminars in cancer biology*.

Ghanbari, P, Mohseni, M, Tabasinezhad, M, Yousefi, B, Saei, AA, Sharifi, S, Rashidi, MR & Samadi, N 2014. Inhibition of survivin restores the sensitivity of breast cancer cells to docetaxel and vinblastine. *Applied biochemistry and biotechnology*, 174, 667-81.

Giese, A, Loo, MA, Tran, N, Haskett, D, Coons, SW & Berens, ME 1996. Dichotomy of astrocytoma migration and proliferation. *International journal of cancer. Journal international du cancer*, 67, 275-82.

Gimm, O, Armanios, M, Dziema, H, Neumann, HP & Eng, C 2000. Somatic and occult germ-line mutations in SDHD, a mitochondrial complex II gene, in nonfamilial pheochromocytoma. *Cancer research*, 60, 6822-5.

Giroix, MH, Nadi, AB, Sener, A, Portha, B & Malaisse, WJ 2002. Metabolism of D-[3-3H]glucose, D-[5-3H]glucose, D-[U-14C]glucose, D-[1-14C]glucose and D-[6-14C]glucose in pancreatic islets in an animal model of type-2 diabetes. *International journal of molecular medicine*, 9, 381-4.

Gottlieb, E & Tomlinson, IP 2005. Mitochondrial tumour suppressors: a genetic and biochemical update. *Nature reviews. Cancer*, 5, 857-66.

Green, A & Beer, P 2010. Somatic mutations of IDH1 and IDH2 in the leukemic transformation of myeloproliferative neoplasms. *N Engl J Med*, 362, 369-70.

Griffin, JL & Shockcor, JP 2004. Metabolic profiles of cancer cells. *Nature reviews. Cancer*, 4, 551-61.

Gross, MI, Demo, SD, Dennison, JB, Chen, L, Chernov-Rogan, T, Goyal, B, Janes, JR, Laidig, GJ, Lewis, ER, Li, J, Mackinnon, AL, Parlati, F, Rodriguez, ML, Shwonek, PJ, Sjogren, EB, Stanton, TF, Wang, T, Yang, J, Zhao, F & Bennett, MK 2014. Antitumor activity of the glutaminase inhibitor CB-839 in triple-negative breast cancer. *Molecular cancer therapeutics*, 13, 890-901.

Gucalp, A, Gupta, GP, Pilewskie, ML, Sutton, EJ & Norton, L 2014. Advances in managing breast cancer: a clinical update. *F1000prime reports*, 6, 66.

Gunsoy, NB, Garcia-Closas, M & Moss, SM 2014. Estimating breast cancer mortality reduction and overdiagnosis due to screening for different strategies in the United Kingdom. *British journal of cancer*, 110, 2412-9.

Günther, U, Chong, M, Volpari, T, Koczula, K, Atkins, K, Bunce, C & Khanim, F 2015. Metabolic Fluxes in Cancer Metabolism. In: Mazurek, S. & Shoshan, M. (eds.) *Tumor Cell Metabolism*. Springer Vienna.

Guy, CT, Cardiff, RD & Muller, WJ 1992. Induction of mammary tumors by expression of polyomavirus middle T oncogene: a transgenic mouse model for metastatic disease. *Molecular and cellular biology*, 12, 954-61.

Gwinn, DM, Shackelford, DB, Egan, DF, Mihaylova, MM, Mery, A, Vasquez, DS, Turk, BE & Shaw, RJ 2008. AMPK phosphorylation of raptor mediates a metabolic checkpoint. *Molecular cell*, 30, 214-26.

Hanahan, D & Weinberg, RA 2000. The hallmarks of cancer. *Cell*, 100, 57-70.

Hanahan, D & Weinberg, RA 2011. Hallmarks of cancer: the next generation. *Cell*, 144, 646-74.

Hare, JM, Fishman, JE, Gerstenblith, G, Difede Velazquez, DL, Zambrano, JP, Suncion, VY, Tracy, M, Ghersin, E, Johnston, PV, Brinker, JA, Breton, E, Davis-Sproul, J, Schulman, IH, Byrnes, J, Mendizabal, AM, Lowery, MH, Rouy, D, Altman, P, Wong Po Foo, C, Ruiz, P, Amador, A, Da Silva, J, Mcniece, IK, Heldman, AW, George, R & Lardo, A 2012. Comparison of allogeneic vs autologous bone marrow-derived mesenchymal stem cells delivered by transendocardial injection in patients with ischemic cardiomyopathy: the POSEIDON randomized trial. *Jama*, 308, 2369-79.

Harris, AL 2002. Hypoxia--a key regulatory factor in tumour growth. *Nature reviews. Cancer*, 2, 38-47.

Hassan, MS, Ansari, J, Spooner, D & Hussain, SA 2010. Chemotherapy for breast cancer (Review). *Oncology reports*, 24, 1121-31.

Hassel, B & Brathe, A 2000. Cerebral metabolism of lactate in vivo: evidence for neuronal pyruvate carboxylation. *Journal of cerebral blood flow and metabolism : official journal of the International Society of Cerebral Blood Flow and Metabolism*, 20, 327-36.

Hatoum, D & MCGowan, EM 2015. Recent advances in the use of metformin: can treating diabetes prevent breast cancer? *BioMed research international*, 2015, 548436.

Hawke, TJ, Atkinson, DJ, Kanatous, SB, Van Der Ven, PF, Goetsch, SC & Garry, DJ 2007. Xin, an actin binding protein, is expressed within muscle satellite cells and newly regenerated skeletal muscle fibers. *American journal of physiology. Cell physiology*, 293, C1636-44.

Health & Social Care Information Centre. *Breast Screening Programme, England - 2011-12* [Online]. Available: <http://www.hscic.gov.uk/catalogue/PUB10339> [Accessed June 2015].

Helczynska, K, Larsson, AM, Holmquist Mengelbier, L, Bridges, E, Fredlund, E, Borgquist, S, Landberg, G, Pahlman, S & Jirstrom, K 2008. Hypoxia-inducible factor-2alpha correlates to distant recurrence and poor outcome in invasive breast cancer. *Cancer research*, 68, 9212-20.

Helmlinger, G, Yuan, F, Dellian, M & Jain, RK 1997. Interstitial pH and pO₂ gradients in solid tumors in vivo: high-resolution measurements reveal a lack of correlation. *Nature medicine*, 3, 177-82.

Herbst, RS & Khuri, FR 2003. Mode of action of docetaxel - a basis for combination with novel anticancer agents. *Cancer treatment reviews*, 29, 407-15.

Herschkowitz, JI, Simin, K, Weigman, VJ, Mikaelian, I, Usary, J, Hu, Z, Rasmussen, KE, Jones, LP, Assefnia, S, Chandrasekharan, S, Backlund, MG, Yin, Y, Khramtsov, AI, Bastein, R, Quackenbush, J, Glazer, RI, Brown, PH, Green, JE, Kopelovich, L, Furth, PA, Palazzo, JP, Olopade, OI, Bernard, PS, Churchill, GA, Van Dyke, T & Perou, CM 2007. Identification of conserved gene expression features between murine mammary carcinoma models and human breast tumors. *Genome biology*, 8, R76.

Hiller, K & Metallo, CM 2013. Profiling metabolic networks to study cancer metabolism. *Current opinion in biotechnology*, 24, 60-8.

Hilvo, M, Denkert, C, Lehtinen, L, Muller, B, Brockmoller, S, Seppanen-Laakso, T, Budczies, J, Bucher, E, Yetukuri, L, Castillo, S, Berg, E, Nygren, H, Sysi-Aho, M, Griffin, JL, Fiehn, O, Loibl, S, Richter-Ehrenstein, C, Radke, C, Hyotylainen, T, Kallioniemi, O, Iljin, K & Oresic, M 2011. Novel theranostic opportunities offered by characterization of altered membrane lipid metabolism in breast cancer progression. *Cancer research*, 71, 3236-45.

Hirschhaeuser, F, Sattler, UG & Mueller-Klieser, W 2011. Lactate: a metabolic key player in cancer. *Cancer research*, 71, 6921-5.

Hitosugi, T, Zhou, L, Elf, S, Fan, J, Kang, HB, Seo, JH, Shan, C, Dai, Q, Zhang, L, Xie, J, Gu, TL, Jin, P, Aleckovic, M, Leroy, G, Kang, Y, Sudderth, JA, Deberardinis, RJ, Luan, CH, Chen, GZ, Muller, S, Shin, DM, Owonikoko, TK, Lonial, S, Arellano, ML, Khoury, HJ, Khuri, FR, Lee, BH, Ye, K, Boggon, TJ, Kang, S, He, C & Chen, J 2012. Phosphoglycerate mutase 1 coordinates glycolysis and biosynthesis to promote tumor growth. *Cancer cell*, 22, 585-600.

Ho, CL, Chen, S, Leung, YL, Cheng, T, Wong, KN, Cheung, SK, Liang, R & Chim, CS 2014. 11C-acetate PET/CT for metabolic characterization of multiple myeloma: a comparative study with 18F-FDG PET/CT. *Journal of nuclear medicine : official publication, Society of Nuclear Medicine*, 55, 749-52.

Hojjat-Farsangi, M 2014. Small-molecule inhibitors of the receptor tyrosine kinases: promising tools for targeted cancer therapies. *International journal of molecular sciences*, 15, 13768-801.

Holliday, DL & Speirs, V 2011. Choosing the right cell line for breast cancer research. *Breast cancer research : BCR*, 13, 215.

Holmquist-Mengelbier, L, Fredlund, E, Lofstedt, T, Noguera, R, Navarro, S, Nilsson, H, Pietras, A, Vallon-Christersson, J, Borg, A, Gradin, K, Poellinger, L & Pahlman, S 2006. Recruitment of HIF-1alpha and HIF-2alpha to common target genes is differentially regulated in neuroblastoma: HIF-2alpha promotes an aggressive phenotype. *Cancer cell*, 10, 413-23.

Hu, Q, Chen, WX, Zhong, SL, Zhang, JY, Ma, TF, Ji, H, Lv, MM, Tang, JH & Zhao, JH 2014. MicroRNA-452 contributes to the docetaxel resistance of breast cancer cells. *Tumour biology : the journal of the International Society for Oncodevelopmental Biology and Medicine*, 35, 6327-34.

Hu, W, Zhang, C, Wu, R, Sun, Y, Levine, A & Feng, Z 2010. Glutaminase 2, a novel p53 target gene regulating energy metabolism and antioxidant function. *Proceedings of the National Academy of Sciences of the United States of America*, 107, 7455-60.

Hu, YP, Haq, B, Carraway, KL, Savaraj, N & Lampidis, TJ 2003. Multidrug resistance correlates with overexpression of Muc4 but inversely with P-glycoprotein and multidrug resistance related protein in transfected human melanoma cells. *Biochemical pharmacology*, 65, 1419-25.

Hwang, TL & Shaka, AJ 1995. Water Suppression That Works. Excitation Sculpting Using Arbitrary Wave-Forms and Pulsed-Field Gradients. *Journal of Magnetic Resonance, Series A*, 112, 275-9.

Ignatiadis, M & Reinholz, M 2011. Minimal residual disease and circulating tumor cells in breast cancer. *Breast cancer research : BCR*, 13, 222.

Ikeda, K, Emoto, N, Matsuo, M & Yokoyama, M 2003. Molecular identification and characterization of a novel nuclear protein whose expression is up-regulated in insulin-resistant animals. *The Journal of biological chemistry*, 278, 3514-20.

Iwao-Koizumi, K, Matoba, R, Ueno, N, Kim, SJ, Ando, A, Miyoshi, Y, Maeda, E, Noguchi, S & Kato, K 2005. Prediction of docetaxel response in human breast cancer by gene expression profiling. *Journal of clinical oncology : official journal of the American Society of Clinical Oncology*, 23, 422-31.

Iyengar, P, Espina, V, Williams, TW, Lin, Y, Berry, D, Jelicks, LA, Lee, H, Temple, K, Graves, R, Pollard, J, Chopra, N, Russell, RG, Sasisekharan, R, Trock, BJ, Lippman, M, Calvert, VS, Petricoin, EF, 3rd, Liotta, L, Dadachova, E, Pestell, RG, Lisanti, MP, Bonaldo, P & Scherer, PE 2005. Adipocyte-derived collagen VI affects early mammary tumor progression in vivo, demonstrating a critical interaction in the tumor/stroma microenvironment. *The Journal of clinical investigation*, 115, 1163-76.

Jerby, L, Wolf, L, Denkert, C, Stein, GY, Hilvo, M, Oresic, M, Geiger, T & Ruppin, E 2012. Metabolic associations of reduced proliferation and oxidative stress in advanced breast cancer. *Cancer research*, 72, 5712-20.

Jerusalem, G, Bachelot, T, Barrios, C, Neven, P, Di Leo, A, Janni, W & De Boer, R 2015. A new era of improving progression-free survival with dual blockade in postmenopausal HR(+), HER2(-) advanced breast cancer. *Cancer treatment reviews*, 41, 94-104.

Jiang, BH, Agani, F, Passaniti, A & Semenza, GL 1997. V-SRC induces expression of hypoxia-inducible factor 1 (HIF-1) and transcription of genes encoding vascular endothelial growth factor and enolase 1: involvement of HIF-1 in tumor progression. *Cancer Res*, 57, 5328-35.

Jones, NP & Schulze, A 2012. Targeting cancer metabolism--aiming at a tumour's sweet-spot. *Drug discovery today*, 17, 232-41.

Justus, CR, Sanderlin, EJ & Yang, LV 2015. Molecular Connections between Cancer Cell Metabolism and the Tumor Microenvironment. *International journal of molecular sciences*, 16, 11055-86.

Kajiyama, H, Shibata, K, Terauchi, M, Yamashita, M, Ino, K, Nawa, A & Kikkawa, F 2007. Chemoresistance to paclitaxel induces epithelial-mesenchymal transition and enhances metastatic potential for epithelial ovarian carcinoma cells. *International journal of oncology*, 31, 277-83.

Kalia, M 2015. Biomarkers for personalized oncology: recent advances and future challenges. *Metabolism: clinical and experimental*, 64, S16-21.

Karantalis, V, Difede, DL, Gerstenblith, G, Pham, S, Symes, J, Zambrano, JP, Fishman, J, Pattany, P, Mcniece, I, Conte, J, Schulman, S, Wu, K, Shah, A, Breton, E, Davis-Sproul, J, Schwarz, R, Feigenbaum, G, Mushtaq, M, Suncion, VY, Lardo, AC, Borrello, I, Mendizabal, A, Karas, TZ, Byrnes, J, Lowery, M, Heldman, AW & Hare, JM 2014. Autologous mesenchymal stem cells produce concordant improvements in regional function, tissue perfusion, and fibrotic burden when administered to patients undergoing coronary artery bypass grafting: The Prospective Randomized Study of Mesenchymal Stem Cell Therapy in Patients Undergoing Cardiac Surgery (PROMETHEUS) trial. *Circulation research*, 114, 1302-10.

Kashiwagi, Y, Rokugawa, T, Yamada, T, Obata, A, Watabe, H, Yoshioka, Y & Abe, K 2015. Pharmacological MRI response to a selective dopamine transporter inhibitor, GBR12909, in awake and anesthetized rats. *Synapse (New York, N.Y.)*, 69, 203-12.

Keun, HC, Beckonert, O, Griffin, JL, Richter, C, Moskau, D, Lindon, JC & Nicholson, JK 2002. Cryogenic probe ¹³C NMR spectroscopy of urine for metabolomic studies. *Anal Chem*, 74, 4588-93.

Kielbasa, OM, Reynolds, JG, Wu, CL, Snyder, CM, Cho, MY, Weiler, H, Kandarian, S & Naya, FJ 2011. Myospryn is a calcineurin-interacting protein that negatively modulates slow-fiber-type transformation and skeletal muscle regeneration. *FASEB journal : official publication of the Federation of American Societies for Experimental Biology*, 25, 2276-86.

Kim, JW, Tchernyshyov, I, Semenza, GL & Dang, CV 2006. HIF-1-mediated expression of pyruvate dehydrogenase kinase: a metabolic switch required for cellular adaptation to hypoxia. *Cell metabolism*, 3, 177-85.

Kim, SB, Yoo, C, Ro, J, Im, SA, Im, YH, Kim, JH, Ahn, JH, Jung, KH, Song, HS, Kang, SY, Park, HS & Chung, HC 2014. Combination of docetaxel and TSU-68, an oral antiangiogenic agent, in patients with metastatic breast cancer previously treated with anthracycline: Randomized phase II multicenter trial. *Investigational new drugs*.

Komatsu, M, Carraway, CA, Fregien, NL & Carraway, KL 1997. Reversible disruption of cell-matrix and cell-cell interactions by overexpression of sialomucin complex. *The Journal of biological chemistry*, 272, 33245-54.

Komatsu, M, Jepson, S, Arango, ME, Carothers Carraway, CA & Carraway, KL 2001. Muc4/sialomucin complex, an intramembrane modulator of ErbB2/HER2/Neu, potentiates primary tumor growth and suppresses apoptosis in a xenotransplanted tumor. *Oncogene*, 20, 461-70.

Komatsu, M, Yee, L & Carraway, KL 1999. Overexpression of sialomucin complex, a rat homologue of MUC4, inhibits tumor killing by lymphokine-activated killer cells. *Cancer research*, 59, 2229-36.

Koppenol, WH, Bounds, PL & Dang, CV 2011. Otto Warburg's contributions to current concepts of cancer metabolism. *Nature reviews. Cancer*, 11, 325-37.

Koppenol Wh, BP, Dang Cv 2011. Otto Warburg's contributions to current concepts of cancer metabolism. *Nat Rev Cancer*, 11, 325-37.

Korde, LA, Lusa, L, Mcshane, L, Lebowitz, PF, Lukes, L, Camphausen, K, Parker, JS, Swain, SM, Hunter, K & Zujewski, JA 2010. Gene expression pathway analysis to predict response to neoadjuvant docetaxel and capecitabine for breast cancer. *Breast cancer research and treatment*, 119, 685-99.

Korhonen, T, Huhtala, H & Holli, K 2004. A comparison of the biological and clinical features of invasive lobular and ductal carcinomas of the breast. *Breast cancer research and treatment*, 85, 23-9.

Korkola, JE, Devries, S, Fridlyand, J, Hwang, ES, Estep, AL, Chen, YY, Chew, KL, Dairkee, SH, Jensen, RM & Waldman, FM 2003. Differentiation of lobular versus ductal breast carcinomas by expression microarray analysis. *Cancer research*, 63, 7167-75.

Kozloski, GA, Carraway, CA & Carraway, KL 2010. Mechanistic and signaling analysis of Muc4-ErbB2 signaling module: new insights into the mechanism of ligand-independent ErbB2 activity. *Journal of cellular physiology*, 224, 649-57.

Krieg, M, Haas, R, Brauch, H, Acker, T, Flamme, I & Plate, KH 2000. Up-regulation of hypoxia-inducible factors HIF-1alpha and HIF-2alpha under normoxic conditions in renal carcinoma cells by von Hippel-Lindau tumor suppressor gene loss of function. *Oncogene*, 19, 5435-43.

Kroemer, G, Marino, G & Levine, B 2010. Autophagy and the integrated stress response. *Molecular cell*, 40, 280-93.

Laemmli, UK 1970. Cleavage of structural proteins during the assembly of the head of bacteriophage T4. *Nature*, 227, 680-5.

Lane, AN, Fan, TW, Bousamra, M, 2nd, Higashi, RM, Yan, J & Miller, DM 2011. Stable isotope-resolved metabolomics (SIRM) in cancer research with clinical application to nonsmall cell lung cancer. *Omics : a journal of integrative biology*, 15, 173-82.

Lane, AN, Fan, TWM, Higashi, RM, Tan, J, Bousamra, M & Miller, DM 2009. Prospects for clinical cancer metabolomics using stable isotope tracers. *Experimental and Molecular Pathology*, 86, 165-73.

- Laplante, M & Sabatini, DM 2012. mTOR signaling in growth control and disease. *Cell*, 149, 274-93.
- Lee, JS, Park, S, Park, JM, Cho, JH, Kim, SI & Park, BW 2013. Elevated levels of serum tumor markers CA 15-3 and CEA are prognostic factors for diagnosis of metastatic breast cancers. *Breast cancer research and treatment*, 141, 477-84.
- Lee, P, Vousden, KH & Cheung, EC 2014. TIGAR, TIGAR, burning bright. *Cancer & metabolism*, 2, 1.
- Lee, WN, Guo, P, Lim, S, Bassilian, S, Lee, ST, Boren, J, Cascante, M, Go, VL & Boros, LG 2004. Metabolic sensitivity of pancreatic tumour cell apoptosis to glycogen phosphorylase inhibitor treatment. *British journal of cancer*, 91, 2094-100.
- Levenson, AS & Jordan, VC 1997. MCF-7: the first hormone-responsive breast cancer cell line. *Cancer research*, 57, 3071-8.
- Li, S, Kennedy, M, Payne, S, Kennedy, K, Seewaldt, VL, Pizzo, SV & Bachelder, RE 2014. Model of tumor dormancy/recurrence after short-term chemotherapy. *PLoS one*, 9, e98021.
- Liedtke, AJ, Renstrom, B & Nellis, SH 1992. Correlation between [5-3H]glucose and [U-14C]deoxyglucose as markers of glycolysis in reperfused myocardium. *Circulation research*, 71, 689-700.
- Lim, E, Wu, D, Pal, B, Bouras, T, Asselin-Labat, ML, Vaillant, F, Yagita, H, Lindeman, GJ, Smyth, GK & Visvader, JE 2010. Transcriptome analyses of mouse and human mammary cell subpopulations reveal multiple conserved genes and pathways. *Breast cancer research : BCR*, 12, R21.
- Lin, EY, Jones, JG, Li, P, Zhu, L, Whitney, KD, Muller, WJ & Pollard, JW 2003. Progression to malignancy in the polyoma middle T oncoprotein mouse breast cancer model provides a reliable model for human diseases. *The American journal of pathology*, 163, 2113-26.
- Lin, NU, Claus, E, Sohl, J, Razzak, AR, Arnaout, A & Winer, EP 2008. Sites of distant recurrence and clinical outcomes in patients with metastatic triple-negative breast cancer: high incidence of central nervous system metastases. *Cancer*, 113, 2638-45.
- Lin, NU, Vanderplas, A, Hughes, ME, Theriault, RL, Edge, SB, Wong, YN, Blayney, DW, Niland, JC, Winer, EP & Weeks, JC 2012a. Clinicopathologic features, patterns of recurrence, and survival among women with triple-negative breast cancer in the National Comprehensive Cancer Network. *Cancer*, 118, 5463-72.
- Lin, NU, Vanderplas, A, Hughes, ME, Theriault, RL, Edge, SB, Wong, YN, Blayney, DW, Niland, JC, Winer, EP & Weeks, JC 2012b. Clinicopathologic features, patterns

of recurrence, and survival among women with triple-negative breast cancer in the National Comprehensive Cancer Network. *Cancer*.

Liu, H, Scholz, C, Zang, C, Schefe, JH, Habbel, P, Regierer, AC, Schulz, CO, Possinger, K & Eucker, J 2012. Metformin and the mTOR inhibitor everolimus (RAD001) sensitize breast cancer cells to the cytotoxic effect of chemotherapeutic drugs in vitro. *Anticancer research*, 32, 1627-37.

Liu, J, Litt, L, Segal, MR, Kelly, MJ, Pelton, JG & Kim, M 2011. Metabolomics of oxidative stress in recent studies of endogenous and exogenously administered intermediate metabolites. *International journal of molecular sciences*, 12, 6469-501.

Liu, J, Zhang, C, Hu, W & Feng, Z 2015. Tumor suppressor p53 and its mutants in cancer metabolism. *Cancer letters*, 356, 197-203.

Liu, L, Cash, TP, Jones, RG, Keith, B, Thompson, CB & Simon, MC 2006. Hypoxia-induced energy stress regulates mRNA translation and cell growth. *Molecular cell*, 21, 521-31.

Liu, X, Ser, Z & Locasale, JW 2014. Development and quantitative evaluation of a high-resolution metabolomics technology. *Anal Chem*, 86, 2175-84.

Loboda, A, Jozkowicz, A & Dulak, J 2012. HIF-1 versus HIF-2--is one more important than the other? *Vascular pharmacology*, 56, 245-51.

Locasale, JW, Grassian, AR, Melman, T, Lyssiotis, CA, Mattaini, KR, Bass, AJ, Heffron, G, Metallo, CM, Muranen, T, Sharfi, H, Sasaki, AT, Anastasiou, D, Mullarky, E, Vokes, NI, Sasaki, M, Beroukhim, R, Stephanopoulos, G, Ligon, AH, Meyerson, M, Richardson, AL, Chin, L, Wagner, G, Asara, JM, Brugge, JS, Cantley, LC & Vander Heiden, MG 2011. Phosphoglycerate dehydrogenase diverts glycolytic flux and contributes to oncogenesis. *Nature genetics*, 43, 869-74.

Ludwig, C & Günther, UL 2011. MetaboLab--advanced NMR data processing and analysis for metabolomics. *BMC bioinformatics*, 12, 366.

Ludwig, C & Viant, MR 2010. Two-dimensional J-resolved NMR spectroscopy: review of a key methodology in the metabolomics toolbox. *Phytochem Anal*, 21, 22-32.

Luo, J, Virnig, B, Hendryx, M, Wen, S, Chelebowski, R, Chen, C, Rohan, T, Tinker, L, Wactawski-Wende, J, Lessin, L & Margolis, K 2014. Diabetes, diabetes treatment and breast cancer prognosis. *Breast cancer research and treatment*, 148, 153-62.

Ma, J, Guo, Y, Chen, S, Zhong, C, Xue, Y, Zhang, Y, Lai, X, Wei, Y, Yu, S, Zhang, J & Liu, W 2014. Metformin enhances tamoxifen-mediated tumor growth inhibition in ER-positive breast carcinoma. *BMC cancer*, 14, 172.

Maher, EA, Marin-Valencia, I, Bachoo, RM, Mashimo, T, Raisanen, J, Hatanpaa, KJ, Jindal, A, Jeffrey, FM, Choi, C, Madden, C, Mathews, D, Pascual, JM, Mickey, BE, Malloy, CR & Deberardinis, RJ 2012. Metabolism of [U-13 C]glucose in human brain tumors in vivo. *NMR in biomedicine*, 25, 1234-44.

Mahoney, MC, Bevers, T, Linos, E & Willett, WC 2008. Opportunities and strategies for breast cancer prevention through risk reduction. *CA: a cancer journal for clinicians*, 58, 347-71.

Malloy, CR, Sherry, AD & Jeffrey, FM 1990. Analysis of tricarboxylic acid cycle of the heart using 13C isotope isomers. *The American journal of physiology*, 259, H987-95.

Margenthaler, JA 2011. Optimizing conservative breast surgery. *Journal of surgical oncology*, 103, 306-12.

Marin-Valencia, I, Yang, C, Mashimo, T, Cho, S, Baek, H, Yang, XL, Rajagopalan, KN, Maddie, M, Vemireddy, V, Zhao, Z, Cai, L, Good, L, Tu, BP, Hatanpaa, KJ, Mickey, BE, Mates, JM, Pascual, JM, Maher, EA, Malloy, CR, Deberardinis, RJ & Bachoo, RM 2012. Analysis of tumor metabolism reveals mitochondrial glucose oxidation in genetically diverse human glioblastomas in the mouse brain in vivo. *Cell metabolism*, 15, 827-37.

Martelotto, LG, Ng, CK, Piscuoglio, S, Weigelt, B & Reis-Filho, JS 2014. Breast cancer intra-tumor heterogeneity. *Breast cancer research : BCR*, 16, 210.

Martinez, E, Yoshihara, K, Kim, H, Mills, GM, Trevino, V & Verhaak, RG 2015. Comparison of gene expression patterns across 12 tumor types identifies a cancer supercluster characterized by TP53 mutations and cell cycle defects. *Oncogene*, 34, 2732-40.

Marusyk, A & Polyak, K 2010. Tumor heterogeneity: causes and consequences. *Biochimica et biophysica acta*, 1805, 105-17.

Mastracci, TL, Tjan, S, Bane, AL, O'malley, FP & Andrulis, IL 2005. E-cadherin alterations in atypical lobular hyperplasia and lobular carcinoma in situ of the breast. *Modern pathology : an official journal of the United States and Canadian Academy of Pathology, Inc*, 18, 741-51.

Matoba, S, Kang, JG, Patino, WD, Wragg, A, Boehm, M, Gavrilova, O, Hurley, PJ, Bunz, F & Hwang, PM 2006. p53 regulates mitochondrial respiration. *Science (New York, N.Y.)*, 312, 1650-3.

Mazurek, S, Boschek, CB & Eigenbrodt, E 1997. The role of phosphometabolites in cell proliferation, energy metabolism, and tumor therapy. *Journal of bioenergetics and biomembranes*, 29, 315-30.

Meissner, M, Herrema, H, Van Dijk, TH, Gerding, A, Havinga, R, Boer, T, Muller, M, Reijngoud, DJ, Groen, AK & Kuipers, F 2011. Bile acid sequestration reduces plasma glucose levels in db/db mice by increasing its metabolic clearance rate. *PLoS one*, 6, e24564.

Meister, A 1983. Selective modification of glutathione metabolism. *Science (New York, N.Y.)*, 220, 472-7.

Melchor, L & Benitez, J 2013. The complex genetic landscape of familial breast cancer. *Human genetics*, 132, 845-63.

Menendez, JA & Lupu, R 2007. Fatty acid synthase and the lipogenic phenotype in cancer pathogenesis. *Nature reviews. Cancer*, 7, 763-77.

Metallo, CM, Gameiro, PA, Bell, EL, Mattaini, KR, Yang, J, Hiller, K, Jewell, CM, Johnson, ZR, Irvine, DJ, Guarente, L, Kelleher, JK, Vander Heiden, MG, Iliopoulos, O & Stephanopoulos, G 2012. Reductive glutamine metabolism by IDH1 mediates lipogenesis under hypoxia. *Nature*, 481, 380-4.

Metallo, CM & Vander Heiden, MG 2013. Understanding metabolic regulation and its influence on cell physiology. *Molecular cell*, 49, 388-98.

Metallo, CM, Walther, JL & Stephanopoulos, G 2009. Evaluation of ¹³C isotopic tracers for metabolic flux analysis in mammalian cells. *Journal of biotechnology*, 144, 167-74.

Miccheli, A, Tomassini, A, Puccetti, C, Valerio, M, Peluso, G, Tuccillo, F, Calvani, M, Manetti, C & Conti, F 2006. Metabolic profiling by ¹³C-NMR spectroscopy: [1,2-¹³C₂]glucose reveals a heterogeneous metabolism in human leukemia T cells. *Biochimie*, 88, 437-48.

Milani, M & Harris, AL 2008. Targeting tumour hypoxia in breast cancer. *European journal of cancer (Oxford, England : 1990)*, 44, 2766-73.

Miller, MK, Bang, ML, Witt, CC, Labeit, D, Trombitas, C, Watanabe, K, Granzier, H, Mcelhinny, AS, Gregorio, CC & Labeit, S 2003. The muscle ankyrin repeat proteins: CARP, ankrd2/Arpp and DARP as a family of titin filament-based stress response molecules. *Journal of molecular biology*, 333, 951-64.

Mishra, P & Ambs, S 2015. Metabolic Signatures of Human Breast Cancer. *Molecular & cellular oncology*, 2.

Morrish, F, Isern, N, Sadilek, M, Jeffrey, M & Hockenbery, DM 2009. c-Myc activates multiple metabolic networks to generate substrates for cell-cycle entry. *Oncogene*, 28, 2485-91.

Morse, DL, Gray, H, Payne, CM & Gillies, RJ 2005. Docetaxel induces cell death through mitotic catastrophe in human breast cancer cells. *Molecular cancer therapeutics*, 4, 1495-504.

Morse, DL, Raghunand, N, Sadarangani, P, Murthi, S, Job, C, Day, S, Howison, C & Gillies, RJ 2007. Response of choline metabolites to docetaxel therapy is quantified in vivo by localized (31)P MRS of human breast cancer xenografts and in vitro by high-resolution (31)P NMR spectroscopy of cell extracts. *Magnetic resonance in medicine : official journal of the Society of Magnetic Resonance in Medicine / Society of Magnetic Resonance in Medicine*, 58, 270-80.

Moulder, S & Hortobagyi, GN 2008. Advances in the treatment of breast cancer. *Clinical pharmacology and therapeutics*, 83, 26-36.

Mullen, AR, Wheaton, WW, Jin, ES, Chen, PH, Sullivan, LB, Cheng, T, Yang, Y, Linehan, WM, Chandel, NS & Deberardinis, RJ 2012. Reductive carboxylation supports growth in tumour cells with defective mitochondria. *Nature*, 481, 385-8.

Murase, K, Yanai, A, Saito, M, Imamura, M, Miyagawa, Y, Takatsuka, Y, Inoue, N, Ito, T, Hirota, S, Sasa, M, Katagiri, T, Fujimoto, Y, Hatada, T, Ichii, S, Nishizaki, T, Tomita, N & Miyoshi, Y 2014. Biological characteristics of luminal subtypes in pre- and postmenopausal estrogen receptor-positive and HER2-negative breast cancers. *Breast cancer (Tokyo, Japan)*, 21, 52-7.

Murray, S, Briasoulis, E, Linardou, H, Bafaloukos, D & Papadimitriou, C 2012. Taxane resistance in breast cancer: mechanisms, predictive biomarkers and circumvention strategies. *Cancer treatment reviews*, 38, 890-903.

Musolino, A, Michiara, M, Conti, GM, Boggiani, D, Zatelli, M, Palleschi, D, Bella, MA, Sgargi, P, Di Blasio, B & Ardizzoni, A 2012. Human epidermal growth factor receptor 2 status and interval breast cancer in a population-based cancer registry study. *Journal of clinical oncology : official journal of the American Society of Clinical Oncology*, 30, 2362-8.

Nishimura, K & Kimura, Y 1965. The metabolic pathway of glucose in brain tissue with special reference to the pentose phosphate pathway. II. Studies on the glucose oxidation pathway using glucose-14C. *The Japanese journal of experimental medicine*, 35, 359-70.

Noh, K, Gronke, K, Luo, B, Takors, R, Oldiges, M & Wiechert, W 2007. Metabolic flux analysis at ultra short time scale: isotopically non-stationary 13C labeling experiments. *Journal of biotechnology*, 129, 249-67.

Nwabo Kamdje, AH, Seke Etet, PF, Vecchio, L, Tagne, RS, Amvene, JM, Muller, JM, Krampera, M & Lukong, KE 2014. New targeted therapies for breast cancer: A focus

on tumor microenvironmental signals and chemoresistant breast cancers. *World journal of clinical cases*, 2, 769-86.

O'dwyer, PJ, Hamilton, TC, Young, RC, Lacreta, FP, Carp, N, Tew, KD, Padavic, K, Comis, RL & Ozols, RF 1992. Depletion of glutathione in normal and malignant human cells in vivo by buthionine sulfoximine: clinical and biochemical results. *Journal of the National Cancer Institute*, 84, 264-7.

Orekhov, VY & Jaravine, VA 2011. Analysis of non-uniformly sampled spectra with multi-dimensional decomposition. *Progress in nuclear magnetic resonance spectroscopy*, 59, 271-92.

Owens, KM, Kulawiec, M, Desouki, MM, Vanniarajan, A & Singh, KK 2011. Impaired OXPHOS complex III in breast cancer. *PloS one*, 6, e23846.

Packham, G & Cleveland, JL 1995. c-Myc and apoptosis. *Biochim Biophys Acta*, 1242, 11-28.

Pagani, O, Regan, MM, Walley, BA, Fleming, GF, Colleoni, M, Lang, I, Gomez, HL, Tondini, C, Burstein, HJ, Perez, EA, Ciruelos, E, Stearns, V, Bonnefoi, HR, Martino, S, Geyer, CE, Jr., Pinotti, G, Puglisi, F, Crivellari, D, Ruhstaller, T, Winer, EP, Rabaglio-Poretti, M, Maibach, R, Ruepp, B, Giobbie-Hurder, A, Price, KN, Bernhard, J, Luo, W, Ribi, K, Viale, G, Coates, AS, Gelber, RD, Goldhirsch, A & Francis, PA 2014. Adjuvant exemestane with ovarian suppression in premenopausal breast cancer. *The New England journal of medicine*, 371, 107-18.

Pan, Z & Raftery, D 2007. Comparing and combining NMR spectroscopy and mass spectrometry in metabolomics. *Anal Bioanal Chem*, 387, 525-7.

Papandreou, I, Lim, AL, Laderoute, K & Denko, NC 2008. Hypoxia signals autophagy in tumor cells via AMPK activity, independent of HIF-1, BNIP3, and BNIP3L. *Cell death and differentiation*, 15, 1572-81.

Paplomata, E & O'regan, R 2013. New and emerging treatments for estrogen receptor-positive breast cancer: focus on everolimus. *Therapeutics and clinical risk management*, 9, 27-36.

Paplomata, E & O'regan, R 2014. The PI3K/AKT/mTOR pathway in breast cancer: targets, trials and biomarkers. *Therapeutic advances in medical oncology*, 6, 154-66.

Park, SK, Dadak, AM, Haase, VH, Fontana, L, Giaccia, AJ & Johnson, RS 2003. Hypoxia-induced gene expression occurs solely through the action of hypoxia-inducible factor 1alpha (HIF-1alpha): role of cytoplasmic trapping of HIF-2alpha. *Molecular and cellular biology*, 23, 4959-71.

Perou, CM, Sorlie, T, Eisen, MB, Van De Rijn, M, Jeffrey, SS, Rees, CA, Pollack, JR, Ross, DT, Johnsen, H, Akslén, LA, Fluge, O, Pergamenschikov, A, Williams, C, Zhu, SX, Lonning, PE, Borresen-Dale, AL, Brown, PO & Botstein, D 2000. Molecular portraits of human breast tumours. *Nature*, 406, 747-52.

Phannasil, P, Thuwajit, C, Warnnissorn, M, Wallace, JC, Macdonald, MJ & Jitrapakdee, S 2015. Pyruvate Carboxylase Is Up-Regulated in Breast Cancer and Essential to Support Growth and Invasion of MDA-MB-231 Cells. *PLoS one*, 10, e0129848.

Phipps, AI, Malone, KE, Porter, PL, Daling, JR & Li, CI 2008. Reproductive and hormonal risk factors for postmenopausal luminal, HER-2-overexpressing, and triple-negative breast cancer. *Cancer*, 113, 1521-6.

Porter, P 2008. "Westernizing" women's risks? Breast cancer in lower-income countries. *N Engl J Med*, 358, 213-6.

Portugal, J, Mansilla, S & Bataller, M 2010. Mechanisms of drug-induced mitotic catastrophe in cancer cells. *Current pharmaceutical design*, 16, 69-78.

Possemato, R, Marks, KM, Shaul, YD, Pacold, ME, Kim, D, Birsoy, K, Sethumadhavan, S, Woo, HK, Jang, HG, Jha, AK, Chen, WW, Barrett, FG, Stransky, N, Tsun, ZY, Cowley, GS, Barretina, J, Kalaany, NY, Hsu, PP, Ottina, K, Chan, AM, Yuan, B, Garraway, LA, Root, DE, Mino-Kenudson, M, Brachtel, EF, Driggers, EM & Sabatini, DM 2011. Functional genomics reveal that the serine synthesis pathway is essential in breast cancer. *Nature*, 476, 346-50.

Prat, A & Perou, CM 2011. Deconstructing the molecular portraits of breast cancer. *Molecular oncology*, 5, 5-23.

Pratt, SE & Pollak, MN 1993. Estrogen and antiestrogen modulation of MCF7 human breast cancer cell proliferation is associated with specific alterations in accumulation of insulin-like growth factor-binding proteins in conditioned media. *Cancer research*, 53, 5193-8.

Putignani, L, Raffa, S, Pescosolido, R, Rizza, T, Del Chierico, F, Leone, L, Aimati, L, Signore, F, Carrozzo, R, Callea, F, Torrisi, MR & Grammatico, P 2012. Preliminary evidences on mitochondrial injury and impaired oxidative metabolism in breast cancer. *Mitochondrion*, 12, 363-9.

Rakha, EA, Boyce, RW, Abd El-Rehim, D, Kurien, T, Green, AR, Paish, EC, Robertson, JF & Ellis, IO 2005. Expression of mucins (MUC1, MUC2, MUC3, MUC4, MUC5AC and MUC6) and their prognostic significance in human breast cancer. *Modern pathology : an official journal of the United States and Canadian Academy of Pathology, Inc*, 18, 1295-304.

Richardson, AD, Yang, C, Osterman, A & Smith, JW 2008. Central carbon metabolism in the progression of mammary carcinoma. *Breast cancer research and treatment*, 110, 297-307.

Richmond, A & Su, Y 2008. Mouse xenograft models vs GEM models for human cancer therapeutics. *Disease models & mechanisms*, 1, 78-82.

Robey, IF, Stephen, RM, Brown, KS, Baggett, BK, Gatenby, RA & Gillies, RJ 2008. Regulation of the Warburg effect in early-passage breast cancer cells. *Neoplasia (New York, N. Y.)*, 10, 745-56.

Robles, AI & Varticovski, L 2008. Harnessing genetically engineered mouse models for preclinical testing. *Chem Biol Interact*, 171, 159-64.

Roy, A, Bhattacharyya, M, Ernsting, MJ, May, JP & Li, SD 2014. Recent progress in the development of polysaccharide conjugates of docetaxel and paclitaxel. *Wiley interdisciplinary reviews. Nanomedicine and nanobiotechnology*, 6, 349-68.

Salem, AF, Whitaker-Menezes, D, Lin, Z, Martinez-Outschoorn, UE, Tanowitz, HB, Al-Zoubi, MS, Howell, A, Pestell, RG, Sotgia, F & Lisanti, MP 2012. Two-compartment tumor metabolism: autophagy in the tumor microenvironment and oxidative mitochondrial metabolism (OXPHOS) in cancer cells. *Cell cycle (Georgetown, Tex.)*, 11, 2545-56.

Sandoo, A, Kitas, GD & Carmichael, AR 2015. Breast cancer therapy and cardiovascular risk: focus on trastuzumab. *Vascular health and risk management*, 11, 223-8.

Sanli, UA, Uslu, R, Karabulut, B, Sezgin, C, Saydam, G, Omay, SB & Goker, E 2002. Which dosing scheme is suitable for the taxanes? An in vitro model. *Archives of pharmacal research*, 25, 550-5.

Santarpia, L, Qi, Y, Stemke-Hale, K, Wang, B, Young, EJ, Booser, DJ, Holmes, FA, O'shaughnessy, J, Hellerstedt, B, Pippen, J, Vidaurre, T, Gomez, H, Valero, V, Hortobagyi, GN, Symmans, WF, Bottai, G, Di Leo, A, Gonzalez-Angulo, AM & Pusztai, L 2012. Mutation profiling identifies numerous rare drug targets and distinct mutation patterns in different clinical subtypes of breast cancers. *Breast cancer research and treatment*, 134, 333-43.

Sarparanta, J 2008. Biology of myospryn: what's known? *Journal of muscle research and cell motility*, 29, 177-80.

Sauer, U 2006. Metabolic networks in motion: ¹³C-based flux analysis. *Molecular systems biology*, 2, 62.

Schallner, N, Ulbrich, F, Engelstaedter, H, Biermann, J, Auwaerter, V, Loop, T & Goebel, U 2014. Isoflurane but not sevoflurane or desflurane aggravates injury to neurons in vitro and in vivo via p75NTR-NF-kB activation. *Anesthesia and analgesia*, 119, 1429-41.

Scherf, U, Ross, DT, Waltham, M, Smith, LH, Lee, JK, Tanabe, L, Kohn, KW, Reinhold, WC, Myers, TG, Andrews, DT, Scudiero, DA, Eisen, MB, Sausville, EA, Pommier, Y, Botstein, D, Brown, PO & Weinstein, JN 2000. A gene expression database for the molecular pharmacology of cancer. *Nature genetics*, 24, 236-44.

Schindl, M, Schoppmann, SF, Samonigg, H, Hausmaninger, H, Kwasny, W, Gnant, M, Jakesz, R, Kubista, E, Birner, P & Oberhuber, G 2002. Overexpression of hypoxia-inducible factor 1alpha is associated with an unfavorable prognosis in lymph node-positive breast cancer. *Clinical cancer research : an official journal of the American Association for Cancer Research*, 8, 1831-7.

Schulze, A & Harris, AL 2012. How cancer metabolism is tuned for proliferation and vulnerable to disruption. *Nature*, 491, 364-73.

Schwartzenberg-Bar-Yoseph, F, Armoni, M & Karnieli, E 2004. The tumor suppressor p53 down-regulates glucose transporters GLUT1 and GLUT4 gene expression. *Cancer research*, 64, 2627-33.

Scott, DA, Richardson, AD, Filipp, FV, Knutzen, CA, Chiang, GG, Ronai, ZA, Osterman, AL & Smith, JW 2011. Comparative metabolic flux profiling of melanoma cell lines: beyond the Warburg effect. *The Journal of biological chemistry*, 286, 42626-34.

Semenza, GL 2009. Regulation of cancer cell metabolism by hypoxia-inducible factor 1. *Seminars in cancer biology*, 19, 12-6.

Semenza, GL 2013. HIF-1 mediates metabolic responses to intratumoral hypoxia and oncogenic mutations. *The Journal of clinical investigation*, 123, 3664-71.

Sharp, TE, 3rd & George, JC 2014. Stem cell therapy and breast cancer treatment: review of stem cell research and potential therapeutic impact against cardiotoxicities due to breast cancer treatment. *Frontiers in oncology*, 4, 299.

Shen, L, Sun, X, Fu, Z, Yang, G, Li, J & Yao, L 2012. The fundamental role of the p53 pathway in tumor metabolism and its implication in tumor therapy. *Clinical cancer research : an official journal of the American Association for Cancer Research*, 18, 1561-7.

Shim, H, Dolde, C, Lewis, BC, Wu, CS, Dang, G, Jungmann, RA, Dalla-Favera, R & Dang, CV 1997. c-Myc transactivation of LDH-A: implications for tumor metabolism and growth. *Proc Natl Acad Sci U S A*, 94, 6658-63.

Shimizu, S 2004. Chapter 32 - Routes of Administration. *In: Bullock, P. H. J. H. G. (ed.) The Laboratory Mouse*. London: Academic Press.

Simstein, R, Burow, M, Parker, A, Weldon, C & Beckman, B 2003. Apoptosis, chemoresistance, and breast cancer: insights from the MCF-7 cell model system. *Experimental biology and medicine (Maywood, N.J.)*, 228, 995-1003.

Skibinski, A & Kuperwasser, C 2015. The origin of breast tumor heterogeneity. *Oncogene*.

Slamon, DJ, Clark, GM, Wong, SG, Levin, WJ, Ullrich, A & Mcguire, WL 1987. Human breast cancer: correlation of relapse and survival with amplification of the HER-2/neu oncogene. *Science (New York, N.Y.)*, 235, 177-82.

Smith, SA, Levante, TO, Meier, BH & Ernst, RR 1994. Computer Simulations in Magnetic Resonance. An Object-Oriented Programming Approach. *Journal of Magnetic Resonance, Series A*, 106, 75-105.

Soerjomataram, I, Louwman, MW, Ribot, JG, Roukema, JA & Coebergh, JW 2008. An overview of prognostic factors for long-term survivors of breast cancer. *Breast cancer research and treatment*, 107, 309-30.

Sonnenblick, A, Fumagalli, D, Sotiriou, C & Piccart, M 2014. Is the differentiation into molecular subtypes of breast cancer important for staging, local and systemic therapy, and follow up? *Cancer treatment reviews*, 40, 1089-95.

Sonveaux, P, Vegran, F, Schroeder, T, Wergin, MC, Verrax, J, Rabbani, ZN, De Saedeleer, CJ, Kennedy, KM, Diepart, C, Jordan, BF, Kelley, MJ, Gallez, B, Wahl, ML, Feron, O & Dewhirst, MW 2008. Targeting lactate-fueled respiration selectively kills hypoxic tumor cells in mice. *The Journal of clinical investigation*, 118, 3930-42.

Sorlie, T, Perou, CM, Tibshirani, R, Aas, T, Geisler, S, Johnsen, H, Hastie, T, Eisen, MB, Van De Rijn, M, Jeffrey, SS, Thorsen, T, Quist, H, Matese, JC, Brown, PO, Botstein, D, Lonning, PE & Borresen-Dale, AL 2001. Gene expression patterns of breast carcinomas distinguish tumor subclasses with clinical implications. *Proceedings of the National Academy of Sciences of the United States of America*, 98, 10869-74.

Strauss, LG 1997. Positron Emission Tomography: Current Role for Diagnosis and Therapy Monitoring in Oncology. *The oncologist*, 2, 381-8.

Strese, S, Fryknas, M, Larsson, R & Gullbo, J 2013. Effects of hypoxia on human cancer cell line chemosensitivity. *BMC cancer*, 13, 331.

- Sullivan, LB & Chandel, NS 2014. Mitochondrial reactive oxygen species and cancer. *Cancer & metabolism*, 2, 17.
- Sun, XX & Yu, Q 2015. Intra-tumor heterogeneity of cancer cells and its implications for cancer treatment. *Acta pharmacologica Sinica*, 36, 1219-27.
- Szyperski, T, Bailey, JE & Wüthrich, K 1996. Detecting and dissecting metabolic fluxes using biosynthetic fractional ¹³C labeling and two-dimensional NMR spectroscopy. *Trends in Biotechnology*, 14, 453-9.
- Szyperski, T, Glaser, RW, Hochuli, M, Fiaux, J, Sauer, U, Bailey, JE & Wuthrich, K 1999. Bioreaction network topology and metabolic flux ratio analysis by biosynthetic fractional ¹³C labeling and two-dimensional NMR spectroscopy. *Metabolic engineering*, 1, 189-97.
- Talks, KL, Turley, H, Gatter, KC, Maxwell, PH, Pugh, CW, Ratcliffe, PJ & Harris, AL 2000. The expression and distribution of the hypoxia-inducible factors HIF-1alpha and HIF-2alpha in normal human tissues, cancers, and tumor-associated macrophages. *The American journal of pathology*, 157, 411-21.
- Tan, MH, De, S, Bebek, G, Orloff, MS, Wesolowski, R, Downs-Kelly, E, Budd, GT, Stark, GR & Eng, C 2012. Specific kinesin expression profiles associated with taxane resistance in basal-like breast cancer. *Breast cancer research and treatment*, 131, 849-58.
- Tankanow, RM 1998. Docetaxel: a taxoid for the treatment of metastatic breast cancer. *American journal of health-system pharmacy : AJHP : official journal of the American Society of Health-System Pharmacists*, 55, 1777-91.
- Tennant, DA, Duran, RV, Boulahbel, H & Gottlieb, E 2009. Metabolic transformation in cancer. *Carcinogenesis*, 30, 1269-80.
- Tennant, DA, Duran, RV & Gottlieb, E 2010. Targeting metabolic transformation for cancer therapy. *Nature reviews. Cancer*, 10, 267-77.
- Territo, PR, Maluccio, M, Riley, AA, Mccarthy, BP, Fletcher, J, Tann, M, Saxena, R & Skill, NJ 2015. Evaluation of ¹¹C-acetate and ¹⁸F-FDG PET/CT in mouse multidrug resistance gene-2 deficient mouse model of hepatocellular carcinoma. *BMC medical imaging*, 15, 15.
- Thiery, JP & Sleeman, JP 2006. Complex networks orchestrate epithelial-mesenchymal transitions. *Nature reviews. Molecular cell biology*, 7, 131-42.
- Timmerman, LA, Holton, T, Yuneva, M, Louie, RJ, Padro, M, Daemen, A, Hu, M, Chan, DA, Ethier, SP, Van 'T Veer, LJ, Polyak, K, McCormick, F & Gray, JW 2013. Glutamine

sensitivity analysis identifies the xCT antiporter as a common triple-negative breast tumor therapeutic target. *Cancer cell*, 24, 450-65.

Tirkkonen, M, Johannsson, O, Agnarsson, BA, Olsson, H, Ingvarsson, S, Karhu, R, Tanner, M, Isola, J, Barkardottir, RB, Borg, A & Kallioniemi, OP 1997. Distinct somatic genetic changes associated with tumor progression in carriers of BRCA1 and BRCA2 germ-line mutations. *Cancer research*, 57, 1222-7.

Tlsty, TD 2001. Stromal cells can contribute oncogenic signals. *Seminars in cancer biology*, 11, 97-104.

Tomlinson, IP, Alam, NA, Rowan, AJ, Barclay, E, Jaeger, EE, Kelsell, D, Leigh, I, Gorman, P, Lamlum, H, Rahman, S, Roylance, RR, Olpin, S, Bevan, S, Barker, K, Hearle, N, Houlston, RS, Kiuru, M, Lehtonen, R, Karhu, A, Vilkki, S, Laiho, P, Eklund, C, Vierimaa, O, Aittomaki, K, Hietala, M, Sistonen, P, Paetau, A, Salovaara, R, Herva, R, Launonen, V & Aaltonen, LA 2002. Germline mutations in FH predispose to dominantly inherited uterine fibroids, skin leiomyomata and papillary renal cell cancer. *Nature genetics*, 30, 406-10.

Tsilidis, KK, Kasimis, JC, Lopez, DS, Ntzani, EE & Ioannidis, JP 2015. Type 2 diabetes and cancer: umbrella review of meta-analyses of observational studies. *BMJ (Clinical research ed.)*, 350, g7607.

Turner, PV, Brabb, T, Pekow, C & Vasbinder, MA 2011. Administration of Substances to Laboratory Animals: Routes of Administration and Factors to Consider. *Journal of the American Association for Laboratory Animal Science : JAALAS*, 50, 600-13.

Tutt, A, Robson, M, Garber, JE, Domchek, SM, Audeh, MW, Weitzel, JN, Friedlander, M, Arun, B, Loman, N, Schmutzler, RK, Wardley, A, Mitchell, G, Earl, H, Wickens, M & Carmichael, J 2010. Oral poly(ADP-ribose) polymerase inhibitor olaparib in patients with BRCA1 or BRCA2 mutations and advanced breast cancer: a proof-of-concept trial. *Lancet*, 376, 235-44.

Valero, V, Holmes, FA, Walters, RS, Theriault, RL, Esparza, L, Fraschini, G, Fonseca, GA, Bellet, RE, Buzdar, AU & Hortobagyi, GN 1995. Phase II trial of docetaxel: a new, highly effective antineoplastic agent in the management of patients with anthracycline-resistant metastatic breast cancer. *Journal of clinical oncology : official journal of the American Society of Clinical Oncology*, 13, 2886-94.

Van Cleef, A, Altintas, S, Huizing, M, Papadimitriou, K, Van Dam, P & Tjalma, W 2014. Current view on ductal carcinoma in situ and importance of the margin thresholds: A review. *Facts, views & vision in ObGyn*, 6, 210-8.

- Van Der Werf, P & Meister, A 1975. The metabolic formation and utilization of 5-oxo-L-proline (L-pyrroglutamate, L-pyrrolidone carboxylate). *Advances in enzymology and related areas of molecular biology*, 43, 519-56.
- Van Dijk, TH, Boer, TS, Havinga, R, Stellaard, F, Kuipers, F & Reijngoud, DJ 2003. Quantification of hepatic carbohydrate metabolism in conscious mice using serial blood and urine spots. *Analytical biochemistry*, 322, 1-13.
- Van Dyke, T & Jacks, T 2002. Cancer modeling in the modern era: progress and challenges. *Cell*, 108, 135-44.
- Vander Heiden, MG, Cantley, LC & Thompson, CB 2009. Understanding the Warburg effect: the metabolic requirements of cell proliferation. *Science (New York, N.Y.)*, 324, 1029-33.
- Vargo-Gogola, T & Rosen, JM 2007. Modelling breast cancer: one size does not fit all. *Nature reviews. Cancer*, 7, 659-72.
- Vaupel, P, Briest, S & Hockel, M 2002. Hypoxia in breast cancer: pathogenesis, characterization and biological/therapeutic implications. *Wiener medizinische Wochenschrift (1946)*, 152, 334-42.
- Vaupel, P & Mayer, A 2007. Hypoxia in cancer: significance and impact on clinical outcome. *Cancer metastasis reviews*, 26, 225-39.
- Venkitaraman, AR 2002. Cancer susceptibility and the functions of BRCA1 and BRCA2. *Cell*, 108, 171-82.
- Verma, S, Miles, D, Gianni, L, Krop, IE, Welslau, M, Baselga, J, Pegram, M, Oh, DY, Dieras, V, Guardino, E, Fang, L, Lu, MW, Olsen, S & Blackwell, K 2012. Trastuzumab emtansine for HER2-positive advanced breast cancer. *The New England journal of medicine*, 367, 1783-91.
- Viale, G 2013. Characterization and clinical impact of residual disease after neoadjuvant chemotherapy. *Breast (Edinburgh, Scotland)*, 22 Suppl 2, S88-91.
- Viant, MR 2003. Improved methods for the acquisition and interpretation of NMR metabolomic data. *Biochemical and biophysical research communications*, 310, 943-8.
- Vici, P, Pizzuti, L, Natoli, C, Gamucci, T, Di Lauro, L, Barba, M, Sergi, D, Botti, C, Michelotti, A, Moschetti, L, Mariani, L, Izzo, F, D'onofrio, L, Sperduti, I, Conti, F, Rossi, V, Cassano, A, Maugeri-Sacca, M, Mottolese, M & Marchetti, P 2015. Triple positive breast cancer: a distinct subtype? *Cancer treatment reviews*, 41, 69-76.

Vona-Davis, L & Rose, DP 2012. Type 2 diabetes and obesity metabolic interactions: common factors for breast cancer risk and novel approaches to prevention and therapy. *Current diabetes reviews*, 8, 116-30.

Vorkas, PA, Isaac, G, Anwar, MA, Davies, AH, Want, EJ, Nicholson, JK & Holmes, E 2015. Untargeted UPLC-MS profiling pipeline to expand tissue metabolome coverage: application to cardiovascular disease. *Anal Chem*, 87, 4184-93.

Waldman, YY, Geiger, T & Ruppin, E 2013. A genome-wide systematic analysis reveals different and predictive proliferation expression signatures of cancerous vs. non-cancerous cells. *PLoS genetics*, 9, e1003806.

Walther, JL, Metallo, CM, Zhang, J & Stephanopoulos, G 2012. Optimization of ¹³C isotopic tracers for metabolic flux analysis in mammalian cells. *Metab Eng*, 14, 162-71.

Warburg, O 1923. Metabolism of tumours. *Biochem. Z*, 142, 317-33.

Warburg, O, Wind, F & Negelein, E 1927. THE METABOLISM OF TUMORS IN THE BODY. *J Gen Physiol*, 8, 519-30.

Ward, C, Langdon, SP, Mullen, P, Harris, AL, Harrison, DJ, Supuran, CT & Kunkler, IH 2013. New strategies for targeting the hypoxic tumour microenvironment in breast cancer. *Cancer treatment reviews*, 39, 171-9.

Ward, PS & Thompson, CB 2012. Metabolic reprogramming: a cancer hallmark even warburg did not anticipate. *Cancer cell*, 21, 297-308.

Wasif, N, Maggard, MA, Ko, CY & Giuliano, AE 2010. Invasive lobular vs. ductal breast cancer: a stage-matched comparison of outcomes. *Annals of surgical oncology*, 17, 1862-9.

Wellings, SR & Jensen, HM 1973. On the origin and progression of ductal carcinoma in the human breast. *Journal of the National Cancer Institute*, 50, 1111-8.

Wider, G, Hosur, RV & Wüthrich, K 1983. Suppression of the solvent resonance in 2D NMR spectra of proteins in H₂O solution. *Journal of Magnetic Resonance (1969)*, 52, 130-5.

Wiechert, W 2001. ¹³C metabolic flux analysis. *Metabolic engineering*, 3, 195-206.

Wiechert, W & Noh, K 2013. Isotopically non-stationary metabolic flux analysis: complex yet highly informative. *Current opinion in biotechnology*, 24, 979-86.

Wiesener, MS, Jurgensen, JS, Rosenberger, C, Scholze, CK, Horstrup, JH, Warnecke, C, Mandriota, S, Bechmann, I, Frei, UA, Pugh, CW, Ratcliffe, PJ, Bachmann, S, Maxwell, PH & Eckardt, KU 2003. Widespread hypoxia-inducible expression of HIF-2alpha in distinct cell populations of different organs. *FASEB journal : official*

publication of the Federation of American Societies for Experimental Biology, 17, 271-3.

Wise, DR, Deberardinis, RJ, Mancuso, A, Sayed, N, Zhang, XY, Pfeiffer, HK, Nissim, I, Daikhin, E, Yudkoff, M, McMahon, SB & Thompson, CB 2008. Myc regulates a transcriptional program that stimulates mitochondrial glutaminolysis and leads to glutamine addiction. *Proceedings of the National Academy of Sciences of the United States of America*, 105, 18782-7.

Wise, DR, Ward, PS, Shay, JE, Cross, JR, Gruber, JJ, Sachdeva, UM, Platt, JM, Dematteo, RG, Simon, MC & Thompson, CB 2011. Hypoxia promotes isocitrate dehydrogenase-dependent carboxylation of alpha-ketoglutarate to citrate to support cell growth and viability. *Proceedings of the National Academy of Sciences of the United States of America*, 108, 19611-6.

Wong, DJ & Hurvitz, SA 2014. Recent advances in the development of anti-HER2 antibodies and antibody-drug conjugates. *Annals of translational medicine*, 2, 122.

Wong, KP, Sha, W, Zhang, X & Huang, SC 2011. Effects of administration route, dietary condition, and blood glucose level on kinetics and uptake of 18F-FDG in mice. *Journal of nuclear medicine : official publication, Society of Nuclear Medicine*, 52, 800-7.

Workman, HC, Miller, JK, Ingalla, EQ, Kaur, RP, Yamamoto, DI, Beckett, LA, Young, LJ, Cardiff, RD, Borowsky, AD, Carraway, KL, Sweeney, C & Carraway, KL, 3rd 2009. The membrane mucin MUC4 is elevated in breast tumor lymph node metastases relative to matched primary tumors and confers aggressive properties to breast cancer cells. *Breast cancer research : BCR*, 11, R70.

Wu, L, Birlle, DC & Tannock, IF 2005. Effects of the mammalian target of rapamycin inhibitor CCI-779 used alone or with chemotherapy on human prostate cancer cells and xenografts. *Cancer research*, 65, 2825-31.

Yalcin, B 2013. Overview on locally advanced breast cancer: defining, epidemiology, and overview on neoadjuvant therapy. *Experimental oncology*, 35, 250-2.

Yan, H, Parsons, DW, Jin, G, McLendon, R, Rasheed, BA, Yuan, W, Kos, I, Batinic-Haberle, I, Jones, S, Riggins, GJ, Friedman, H, Friedman, A, Reardon, D, Herndon, J, Kinzler, KW, Velculescu, VE, Vogelstein, B & Bigner, DD 2009. IDH1 and IDH2 mutations in gliomas. *N Engl J Med*, 360, 765-73.

Yang, L, Pang, Y & Moses, HL 2010. TGF-beta and immune cells: an important regulatory axis in the tumor microenvironment and progression. *Trends in immunology*, 31, 220-7.

Yang, TJ, Morrow, M, Modi, S, Zhang, Z, Krause, K, Siu, C, McCormick, B, Powell, SN & Ho, AY 2015. The Effect of Molecular Subtype and Residual Disease on Locoregional Recurrence in Breast Cancer Patients Treated with Neoadjuvant Chemotherapy and Postmastectomy Radiation. *Annals of surgical oncology*.

Yardley, DA, Noguchi, S, Pritchard, KI, Burris, HA, 3rd, Baselga, J, Gnant, M, Hortobagyi, GN, Campone, M, Pistilli, B, Piccart, M, Melichar, B, Petrakova, K, Arena, FP, Erdkamp, F, Harb, WA, Feng, W, Cahana, A, Taran, T, Lebewohl, D & Rugo, HS 2013. Everolimus plus exemestane in postmenopausal patients with HR(+) breast cancer: BOLERO-2 final progression-free survival analysis. *Advances in therapy*, 30, 870-84.

Yared, JA & Tkaczuk, KH 2012. Update on taxane development: new analogs and new formulations. *Drug design, development and therapy*, 6, 371-84.

Ye, J, Mancuso, A, Tong, X, Ward, PS, Fan, J, Rabinowitz, JD & Thompson, CB 2012. Pyruvate kinase M2 promotes de novo serine synthesis to sustain mTORC1 activity and cell proliferation. *Proceedings of the National Academy of Sciences of the United States of America*, 109, 6904-9.

Youlten, DR, Cramb, SM, Dunn, NA, Muller, JM, Pyke, CM & Baade, PD 2012. The descriptive epidemiology of female breast cancer: an international comparison of screening, incidence, survival and mortality. *Cancer epidemiology*, 36, 237-48.

Yuneva, MO, Fan, TW, Allen, TD, Higashi, RM, Ferraris, DV, Tsukamoto, T, Mates, JM, Alonso, FJ, Wang, C, Seo, Y, Chen, X & Bishop, JM 2012. The metabolic profile of tumors depends on both the responsible genetic lesion and tissue type. *Cell metabolism*, 15, 157-70.

Zardavas, D & Piccart, M 2015. Neoadjuvant therapy for breast cancer. *Annual review of medicine*, 66, 31-48.

Zeng, W, Liu, P, Pan, W, Singh, SR & Wei, Y 2015. Hypoxia and hypoxia inducible factors in tumor metabolism. *Cancer letters*, 356, 263-7.

Zhao, H, Langerod, A, Ji, Y, Nowels, KW, Nesland, JM, Tibshirani, R, Bukholm, IK, Karesen, R, Botstein, D, Borresen-Dale, AL & Jeffrey, SS 2004. Different gene expression patterns in invasive lobular and ductal carcinomas of the breast. *Molecular biology of the cell*, 15, 2523-36.

Zheng, W, Tayyari, F, Gowda, GA, Raftery, D, Mclamore, ES, Porterfield, DM, Donkin, SS, Bequette, B & Teegarden, D 2015. Altered glucose metabolism in Harvey-ras transformed MCF10A cells. *Molecular carcinogenesis*, 54, 111-20.

Zheng, X, Liang, Y, He, Q, Yao, R, Bao, W, Bao, L, Wang, Y & Wang, Z 2014. Current models of mammalian target of rapamycin complex 1 (mTORC1) activation by growth factors and amino acids. *International journal of molecular sciences*, 15, 20753-69.

Zhou, M, Zhao, Y, Ding, Y, Liu, H, Liu, Z, Fodstad, O, Riker, AI, Kamarajugadda, S, Lu, J, Owen, LB, Ledoux, SP & Tan, M 2010. Warburg effect in chemosensitivity: targeting lactate dehydrogenase-A re-sensitizes taxol-resistant cancer cells to taxol. *Molecular cancer*, 9, 33.

Zhu, X & Verma, S 2015. Targeted therapy in her2-positive metastatic breast cancer: a review of the literature. *Current oncology (Toronto, Ont.)*, 22, S19-28.